1972

# The application of impact dampers to continuous systems

Ranjit Kumar Roy



Department: Mechanical and Aerospace Engineering

# THE APPLICATION OF IMPACT DAMPERS TO CONTINUOUS SYSTEMS

by

RANJIT KUMAR ROY, 1947-

A

DISSERTATION

Presented to the Faculty of the Graduate School of the

UNIVERSITY OF MISSOURI-ROLLA

In Partial Fulfillment of the Requirements for the Degree

DOCTOR OF PHILOSOPHY

in

MECHANICAL ENGINEERING

1972



Clark R. Barber, Advisors J. Earl Foster

Floyd M. Cunningham S. J. Pagano

R. T. Johnson Harold Dean Keith

# ABSTRACT

A study has been made of the application of impact dampers to two types of continuous systems, a simply supported and a clamped beam. Previous efforts have included the effect of impact dampers on single degree of freedom and other systems with finite numbers of degrees of freedom.

Experimental models were tested in the laboratory and finite element computer programs were developed to calculate response. Results from calculations agree favorably with experimental tests. Further, results from the first few natural modes also compare reasonably with data published on systems with finite number of degrees of freedom.

Curves are presented which enable the user to apply impact dampers to these types of continuous systems. Curves show the amount of the isolation to be expected for values of significant system parameters.

# ACKNOWLEDGEMENTS

The author greatefully acknowledges the guidance and valuable assistance of his supervising professors, Dr. R.D. Rocke and Dr. J.E.Foster. The author wishes to express his gratitude to Dr. F.M.Cunningham and Dr. D.Cronin for their suggestions and encouragement in the conduct of the experimental effort. The author also wishes to thank the technicians of The Engineering Mechanics Department, members of the Ranco Electronics, Mr. Prakash Krishnaswamy, and Dr. P. Doraibabu for technical assistance.

The author would like to acknowledge the valuable assistance of Dr. Foster, in the final revision of the manuscript. Last but not the least is author's wife, who deserves special appreciation for her understanding, encouragement and assistance in preparing this report.

TABLE OF CONTENTS

Table of contents (continued)

# LIST OF ILLUSTRATIONS

List of illustrations (continued)

# NOMENCLATURE AND LIST OF SYMBOLS

| | | |
|---|---|---|
| $a$ | = | cross sectional area |
| $A_n$ | = | constant associated with the nth mode |
| $A_0$ | = | stress amplitude without the impact damper |
| $A_d$ | = | stress amplitude with the impact damper |
| $B_n$ | = | constant associated with the nth mode |
| $C_{int}$ | = | coefficient of internal damping |
| $C_{ext}$ | = | coefficient of external damping |
| $C_c$ | = | collision function |
| $D_{1n}, D_{2n}, \ldots$ | = | constants |
| $e$ | = | coefficient of restitution |
| $E_1, E_2, E_n$ | = | constants |
| $E$ | = | modulus of elasticity |
| $F_n$ | = | response amplitude due to the forcing function in the nth mode |
| $g$ | = | acceleration due to gravity, 32.2 ft/sec$^2$ |
| $h$ | = | amplitude of the base displacement |
| $H_n$ | = | mode participation factor |
| $I$ | = | cross sectional area moment of inertia |
| $\ell$ | = | length of a beam segment |
| $L$ | = | length of the beam |
| $m$ | = | generalized mass |
| $m$ | = | mass of the particle |
| $m_d$ | = | lumped mass with the damper container |
| $N$ | = | number of segments in the beam |

Nomenclature and list of symbols (continued)

| | | |
|---|---|---|
| $R$ | = | radius of curvature |
| $S$ | = | clearance for particle motion |
| $U_n$ | = | nth mode shape |
| $v$ | = | velocity of the particle |
| $Y_d$ | = | beam displacement at the node point where damper is attached |
| $\sigma$ | = | flexural stress |
| $\mu$ | = | ratio of the particle mass to the equivalent mass |
| $\delta$ | = | Delta function |
| $\xi$ | = | damping ratio |
| $\psi$ | = | phase angle |
| $\rho$ | = | mass density |
| $\omega$ | = | natural frequency in radians per second |
| $\omega_d$ | = | damped frequency in radians per second |
| $\Omega$ | = | frequency of the base excitation |
| $[\ ]$ | = | matrix of dimensions $r \times s$ |
| $\{\ \}$ | = | column matrix (vector) |
| $[\ ]^T$ | = | transpose of a matrix |
| $[\ ]^{-1}$ | = | inverse of a square matrix |
| $[A]$ | = | modal matrix |
| $\{A\}$ , $\{B\}$ | = | coefficient vectors |
| $[C]$ | = | damping matrix |
| $\{F\}$ | = | amplitude vector of the forcing functions |
| $[H]$ | = | characteristic matrix |

Nomenclature and list of symbols (continued)

| | | |
|---|---|---|
| $[I]$ | = | diagonal unit matrix |
| $[J]$ | = | diagonal inertia matrix of the beam |
| $[K]$ | = | stiffness matrix |
| $[M]$ | = | diagonal mass matrix |
| $\{M_i\}$ | = | lumped mass as column vector |
| $\{P_i\}$ | = | principal coordinate vector |
| $[S]$ | = | stiffness matrix |
| $\{Y\}$ | = | coordinate displacement vector |
| $\{Y_r\}$ | = | relative coordinate displacement vector |
| $\{\Theta\}$ | = | rotation vector |
| $[\Phi]$ | = | normalized modal matrix |
| $(^{I})$ | = | derivative with respect to x |
| $(\dot{})$ | = | derivative with respect to t |

# I. INTRODUCTION

Vibration of mechanical systems are very common in nature. Common examples of such vibrations are the motion of a mass suspended from a spring, slender structures, and equipment mounted on a nonrigid foundation. Many kinds of vibrations are undesirable due to their damaging effects. For example, wind induced oscillations of tall antenna structures, vibration of bridges and airplane wings, and vibrations resulting from an unbalance in rotating machinery can become disasterous.

Isolation of such undesirable vibrations is of great importance in shipboard and aerospace applications. Isolating materials such as rubber pads, cork, felt, or metallic springs placed between the vibrating system and its support reduce the system response. A relatively recent means of reducing vibration response of some systems is to use an impact damper.

An impact or acceleration damper consists of a mass particle constrained to move between the two ends of a container. The container when attached to a vibrating mechanical system causes the particle to collide with the container ends. The collision of the particle reduces the vibration amplitude of the primary system through momentum transfer.

The feasibility of using such a system was first

suggested by Leiber and Jensen(1) in 1944. They investigated the response of an undamped, single degree of freedom system with a single active acceleration damper. These authors assumed that the response of the system to a sinusoidal forcing function was simple harmonic and that in every cycle two completely plastic impacts occured. They reported that the travel path of the particle is $\pi$ times the amplitude response for maximum energy dissipation.

Grubin(2) investigated the motion of a viscously damped single degree of freedom system subjected to the action of a single damper. He determined an analytical solution for the motion of the system from collision to collision by assuming two or more impacts per cycle. A similar system without viscous damping has also been investigated by Arnold (3). He expressed the force acting on the mass during impact in a Fourier Series and showed how different parameters affect the system behavior.

Masri(4,5,6) has performed extensive studies of impact dampers and he has defined two impacts per cycle as a "stable" type of motion. He determined the exact solution for a damped, single degree of freedom system with sinusoidal excitation and analyzed its stability. His results define the stable regions of solution. In later reports he presented a solution for the motion of the same system using a multiple-unit impact damper. He also investigated multidegree of freedom systems with an impact damper and presented the exact solution for the steady state motion

of the system in response to sinusoidal excitation. In all his research the assumption of two impacts per cycle was retained.

Other authors have studied the application of the impact damper attached to more complicated systems. Masri(5), McGoldrick(7), Leiber and Tripp(8), and Duckwald(9), have experimentally investigated single and multidegree of freedom systems, cantilever beam, and turbine buckets respectively.

The objective of the present study is to investigate the motion of a continuous system under the action of an impact damper located at any point along the structure. Two types of uniform continuous beams with sinusoidal base excitation were considered for investigation and the assumption of stability, i.e., two impacts per cycle common to all previous analysis, was not made. In this work the times of arbitrary impacts were determined numerically with a digital computer. Solutions valid between the impacts were obtained analytically by two separate approaches. These will be discussed in detail in later sections.

In Chapter II a viscously damped, Bernoulli-Euler beam with an impact damper attached to it is treated. It is assumed in this analysis that the mass of the damper container is very small and does not influence the normal modes of the system. The solution satisfying the initial conditions is determined in terms of the sum of an infinite

series. The solution defines the motion of the system from collision to collision and is complete when the time of impact is furnished.

In Chapter III the solution by the finite element method is discussed. The uniform continuous beam is replaced by a multidegree of freedom discrete structure and the set of governing differential equations are solved exactly. The solution satisfies the initial conditions and defines the motion of the system from collision to collision. The effect of the damper container mass is easily incorporated in the system response; this advantage was not available in the former solution.

The numerical technique which was used to compute the time of impact is described in Chapter IV. This is followed by Chapter V in which the description of the experimental effort is given and interpretation of the results are discussed. In Chapter VI the conclusions deduced are presented and the scope of future work is indicated.

# II. CONTINUOUS SYSTEM SOLUTION

## A. THE EULER EQUATION FOR THE BEAM

The differential equation of motion for the lateral vibration of a Bernoulli-Euler beam is

$$EI\ \partial^4 W(x,t)/\partial x^4 + \rho a\ \partial^2 W(x,t)/\partial t^2 = p(x,t) \qquad (2.1)$$

where $EI$ and $\rho a$ are respectively the stiffness and mass per unit length of the beam. The system under consideration consists of a uniform continuous beam with an impact damper of negligible container weight. The system is shown in Fig. 2.1. The response of any point on the beam between two consecutive impacts is given by the solution of Eq. (2.1).

In the absence of any distributed force on the beam and with sinusoidal base excitation

$$W(0,t) = W(L,t) = h\ \mathrm{Sin}\Omega t \qquad (2.2)$$

the equation of motion for the beam with internal and external relative damping becomes (see appendix A)

$$EI\ \partial^4 W_r/\partial x^4 + IC_{int}\partial^5 W_r/\partial x^4 \partial t + C_{ext}\ \partial W_r/\partial t$$

$$+ \rho a\ \partial^2 W_r/\partial t^2 = h\rho a\Omega^2\ \mathrm{Sin}\Omega t \qquad (2.3)$$

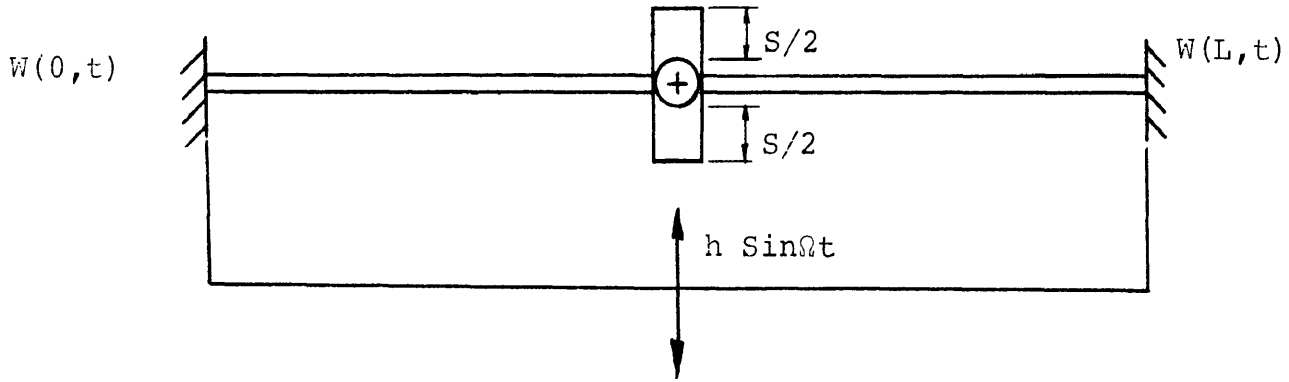


(a) Fixed beam

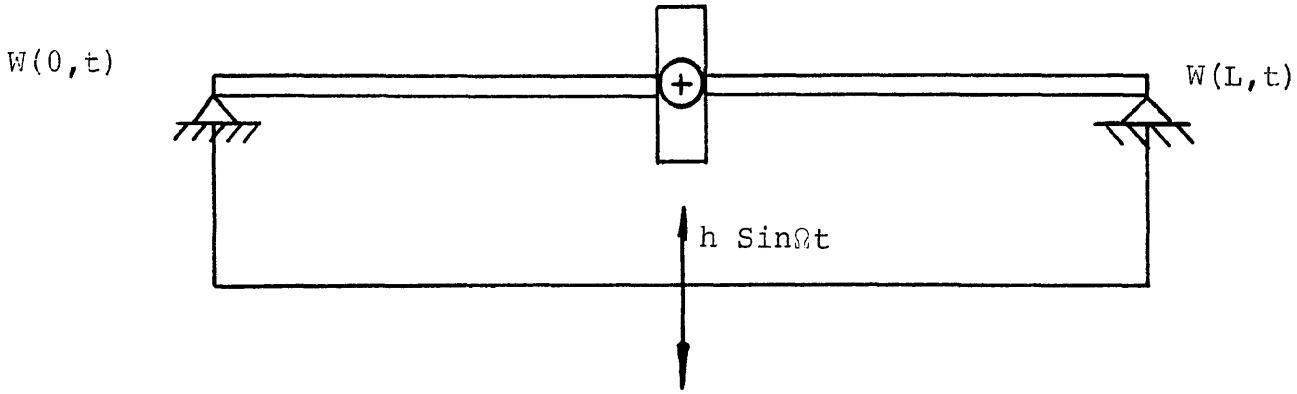


(b) Simply supported beam

Figure 2.1 Models of systems discussed in this report

where

$$W(x,t) = W_r(x,t) + h\,\mathrm{Sin}\Omega t \ . \tag{2.4}$$

The general solution of the equation of motion Eq. (2.3) when substituted in Eq. (2.4) becomes

$$W(x,t) = \sum_{n=1}^{\infty} \{ e^{-\beta_n t} (A_n \mathrm{Cos}(\omega_{dn} t) + B_n \mathrm{Sin}(\omega_{dn} t)) + F_n \mathrm{Sin}(\Omega t - \Psi_n) \} U_n(x) + h\,\mathrm{Sin}\Omega t \tag{2.5}$$

where

$$\beta_n = \xi_n \omega_n$$

$$\omega_n = K_n^2 \sqrt{EI/(\rho a)}$$

$$\omega_{dn} = \omega_n \sqrt{1 - \xi_n^2}$$

$$2\omega_n \xi_n = C_{ext}/(\rho a) + C_{int}\omega_n^2/E$$

$$F_n = \frac{H_n h \Omega^2}{L' \sqrt{(\omega_n^2 - \Omega^2)^2 + (2\beta_n \Omega)^2}}$$

$$\Psi_n = \tan^{-1} (2\beta_n \Omega/(\omega_n^2 - \Omega^2))$$

$$H_n = \int_0^L U_n(x)\, dx \ .$$

| For Fixed End Conditions | For Simply Supported End Conditions |
|---|---|
| $K_n$ are the roots of | |
| $\text{Cos}(KL)\ \text{Cosh}(KL) = 1$ | $\text{Sin}(KL)\ \text{Sinh}(KL) = 0$ |
| $U_n(x) = \text{Cosh}(K_n x) - \text{Cos}(K_n x)$ $- \alpha_n(\text{Sinh}(K_n x) - \text{Sin}(K_n x))$ | $U_n(x) = \text{Sin}(K_n x)$ |
| $\alpha_n = \dfrac{\text{Cos}(K_n L) - \text{Cosh}(K_n L)}{\text{Sin}(K_n L) - \text{Sinh}(K_n L)}$ | $\alpha_n = 0$ |
| $L' = \int_0^L U_n^2(x)\ dx = L$ | $L' = \int_0^L U_n^2(x)\ dx = L/2$ |

The orthogonality relations for these end conditions are

$$\int_0^L U_n(x)\ U_m(x)\ dx = \begin{cases} 0 & \text{for} \quad m \neq n \\ L' & \text{for} \quad m = n \end{cases}$$

which when coupled with zero initial displacement and relative velocity, gives

$$A_n = F_n\ \text{Sin}\Psi_n$$

and

$$B_n = (\beta A_n - F_n\ \Omega \text{Cos}\Psi_n)/\omega_{dn}$$

## B. SOLUTION FOR ARBITRARY IMPACT

Starting from rest, i.e., at t=0, if the time of the first collision is $t=t_1$, then the solution Eq. (2.5) for the beam displacement is valid for $0 \leq t \leq t_1$. The collision is assumed ideal in the sense that the position of the particle and the beam at all locations remain fixed. The velocities of all the beam particles and the damper particle are discontinuously changed. The time $t_1$ at which the first collision occurs and also the times for other collisions are found by a numerical technique which is discussed in Chapter IV.

The differential equation of motion Eq. (2.3) describes the movement of the beam between the time just after the first collision and until just before the second. Solutions for subsequent individual periods between collisions may be represented by

$$W(x,t) = \sum_{n=1}^{\infty} \{ e^{-\beta n t} \{A_{n+}\cos(\omega_{dn} t) + B_{n+}\sin(\omega_{dn} t)\} + F_n \sin(\Omega(t+t_1)-\Psi_n)\} U_n(x) + h \sin\Omega(t+t_1) \qquad (2.6)$$

where t is reckoned from the time of collision and $A_{n+}$, $B_{n+}$ are constants which are determined from the initial conditions just after the impact. Eq. (2.6) is Eq. (2.5) modified to show the change in coefficients $A_n$ and $B_n$ as a result of the collision.

For a single unit impact damper attached at any point along the beam, say at $x = x_d$, a particle of mass, $m$, is used. This particle is enclosed in a container assumed to be of negligible mass and it is also assumed that the particle makes point contact with the beam during a collision.

Just before the impact the beam displacement and velocity at the damper location are obtained from the solution Eq. (2.5). Using subscripts (-) and (+) to imply quantities before and after the collision, Eq. (2.5) at $t = t_1$ gives

$$W_-(x,t_1) = \sum_{n=1}^{\infty} \{e^{-\beta_n t_1}\{ A_n \cos(\omega_{dn} t_1) + B_n \sin(\omega_{dn} t_1)\} + F_n \sin(\Omega t_1 - \Psi_n)\} U_n(x) + h \sin\Omega t_1 \qquad (2.7)$$

and

$$\dot{W}_-(x,t_1) = \sum_{n=1}^{\infty} \{e^{-\beta n t_1}\omega_{dn}\{- A_n \sin(\omega_{dn} t_1) + B_n \cos(\omega_{dn} t_1)\} - \beta_n e^{-\beta_n t_1}\{ A_n \cos(\omega_{dn} t_1) + B_n \sin(\omega_{dn} t_1)\} + F_n\Omega \cos(\Omega t_1 - \Psi_n)\} U_n(x) + h\Omega \cos\Omega t_1 \qquad (2.8)$$

where $(\dot{})$ is used to denote differentiation with respect to $t$.

For Eq. (2.6) to be the solution for a period between

collisions it must give displacement and velocity of the beam just after the impact at t = 0, i.e.,

$$W_+(x,0) = \sum_{n=1}^{\infty} \{ A_{n+} + F_n \, \mathrm{Sin}(\Omega t_1 - \Psi_n) \} \, U_n(x) + h \, \mathrm{Sin}\Omega t_1 \tag{2.9}$$

and

$$\dot{W}_+(x,0) = \sum_{n=1}^{\infty} \{ B_{n+}\omega_{dn} - \beta_n A_{n+} + \Omega F_n \, \mathrm{Cos}(\Omega t_1 - \Psi_n) \} \, U_n(x) + h\Omega \, \mathrm{Cos}\Omega t_1 \, . \tag{2.10}$$

The velocity of the particle at this time (t = 0) is discontinuously changed from $v_-$ to $v_+$ .

Since the position of the particle and the beam remain unchanged during the collision, Eq. (2.7) and Eq. (2.9) can be equated to give

$$A_{n+} = e^{-\beta_n t_1} \{ A_n \, \mathrm{Cos}(\omega_{dn} t_1) + B_n \, \mathrm{Sin}(\omega_{dn} t_1) \} \, . \tag{2.11}$$

The beam is considered to sustain the collision with damper particles of mass m uniformly over the entire length. If the particle velocities are $v_-$ and $v_+$ before and after the collision respectively, then conservation of momentum applied to a beam element of length dx requires that

$$\rho a \, \dot{W}_+(x,0) \, dx + v_+ m \, dx = \rho a \, \dot{W}_-(x,t_1) \, dx + v_- m \, dx$$

where $v_{(+,-)}{}^m$ is considered to be the momentum acquired in the collision per unit length of the beam.

In the case of a collision at a point on the beam the momentum transferred through that point is assumed to be conserved over the whole length of the beam. Thus, for the entire system the momentum equation becomes

$$\int_0^L \rho a\{\dot{W}_+(x,0) - \dot{W}_-(x,t_1)\}\, dx = \int_0^L (v_- - v_+)m\, \delta(x - x_d)\, dx \tag{2.12}$$

where $x_d$ = location of damper along the beam and $\delta(x - x_d)$ is a Delta function having the properties

$$\delta(x - x_d) = 0 \qquad \text{for all} \quad x \neq x_d$$

$$\int_0^\infty U(x)\, \delta(x - x_d)\, dx = U(x_d) \qquad 0 < x_d < \infty$$

$$\int_0^L U(x)\, \delta(x - x_d)\, dx = U(x_d) \qquad 0 < x_d < L \quad .$$

Substituting $\dot{W}_-(x,t_1)$ and $\dot{W}_+(x,0)$ from Eq. (2.8) and Eq. (2.10), respectively into Eq. (2.12) yields

$$B_{n+} - D_n/\omega_{dn} = (v_- - v_+)\, G_n \tag{2.13}$$

where

$$G_n = mU_n(x_d)/(\rho L a \omega_{dn})$$

$$D_n = D_{1n} + D_{2n} + D_{3n}$$

$$D_{1n} = \beta_n A_{n+}$$

$$D_{2n} = e^{-\beta_n t_1} B_n\{ \omega_{dn} \cos(\omega_{dn} t_1) - \sin(\omega_{dn} t_1)\}$$

$$D_{3n} = e^{-\beta_n t_1} A_n\{ \omega_{dn} \sin(\omega_{dn} t_1) + \sin(\omega_{dn} t_1)\}.$$

According to the definition of the coefficient of restitution, e, between the particle and the beam

$$\dot{W}_+(x_d,0) - v_+ = - e(\dot{W}_-(x_d,t_1) - v_-). \qquad (2.14)$$

Substituting Eq. (2.8) and Eq. (2.10) in Eq. (2.14) gives

$$v_+ = \sum_{n=1}^{\infty} U_n(x_d)\omega_{dn} B_{n+} + E_2 \qquad (2.15)$$

where

$$E_2 = \sum_{n=1}^{\infty} U_n(x_d) E_n + E_1$$

and

$$E_n = e D_{2n} - e D_{3n} - D_{1n} + \Omega(1 + e) F_n \cos(\Omega t_1 - \Psi_n)$$

$$E_1 = \Omega(1 + e) h \cos\Omega t_1 - e v_- .$$

The solution of Eq. (2.15) and Eq. (2.13) for $B_{n+}$ results in

$$B_{n+} + G_n \sum_{i=1}^{\infty} Z_i B_{i+} = R_n \qquad (2.16)$$

where

$$Z_i = U_i(x_d)\ \omega_{di}$$

and

$$R_n = G_n v_- + D_n/\omega_{dn} - E_2 G_n .$$

Solutions Eq. (2.5) and Eq. (2.6) for the beam displacement before and after collision are expressed in the form of an infinite series of terms. For practical purposes however, only the first few terms are necessary to yield sufficiently accurate results.

Eq. (2.16) represents a system of k nonhomogeneous equations in k unknowns ($B_n$, n=1,2,....,k), where only first k terms are utilized. The system of equations Eq. (2.16) in matrix form are

$$\begin{bmatrix} (1+G_1Z_1) & G_1Z_2 & \cdot & \cdot & \cdot & G_1Z_k \\ G_2Z_1 & (1+G_2Z_2) & \cdot & \cdot & & G_2Z_k \\ \cdot & \cdot & \cdot & \cdot & \cdot & \cdot \\ \cdot & \cdot & \cdot & \cdot & \cdot & \cdot \\ G_kZ_1 & \cdot & \cdot & \cdot & \cdot & (1+G_kZ_k) \end{bmatrix} \begin{Bmatrix} B_{1+} \\ B_{2+} \\ \cdot \\ \cdot \\ B_{k+} \end{Bmatrix} = \begin{Bmatrix} R_1 \\ R_2 \\ \cdot \\ \cdot \\ R_k \end{Bmatrix} . \qquad (2.17)$$

The complete solution for the beam displacement between collisions is then given by Eq. (2.6), where $A_{n+}$ and $B_{n+}$

are determined by using Eq. (2.11) and Eq. (2.17), respectively.

The normal stress at a point on the surface of a beam is obtained by determining the bending moment at that section which is given by the relation

$$M(x,t) = EI\ \partial^2 W(x,t)/\partial x^2 \quad , \tag{2.18}$$

Accordingly, the flexural stress at a point located a perpendicular distance $d/2$ from the neutral surface becomes

$$\sigma = E\{\partial^2 W(x,t)/\partial x^2\}\{d/2\} \tag{2.19}$$

where $d$ is the thickness of the beam.

Computer programs were developed to numerically determine the time of impact and to evaluate the system response at any particular time. The numerical technique and the programs used are discussed in Chapter IV. To determine the accuracy of the results, the stress amplitude was computed using Eq. (2.19) and was compared with the experimentally observed values. Results of these computations for a simply supported beam are shown in Fig. 2.1 and Fig. 2.2. Damping ratios used in the computations were $\xi_1 = .0038$, $\xi_2 = .0025$ and $\xi_3 = \xi_4 = \ldots = \xi_n = .0016$. Among these, $\xi_1$ and $\xi_3$ were determined experimentally at

the first and third modes respectively from the width of the resonance curve at the half power points (see Fig. 2.4). These results do not include the effect of the weight of the container (of the impact damper) and this is exhibited by the relatively lower response amplitude in the graphs (Figs. 2.2 & 2.3). Similar calculations for a fixed beam also agreed with the corresponding experimental results.

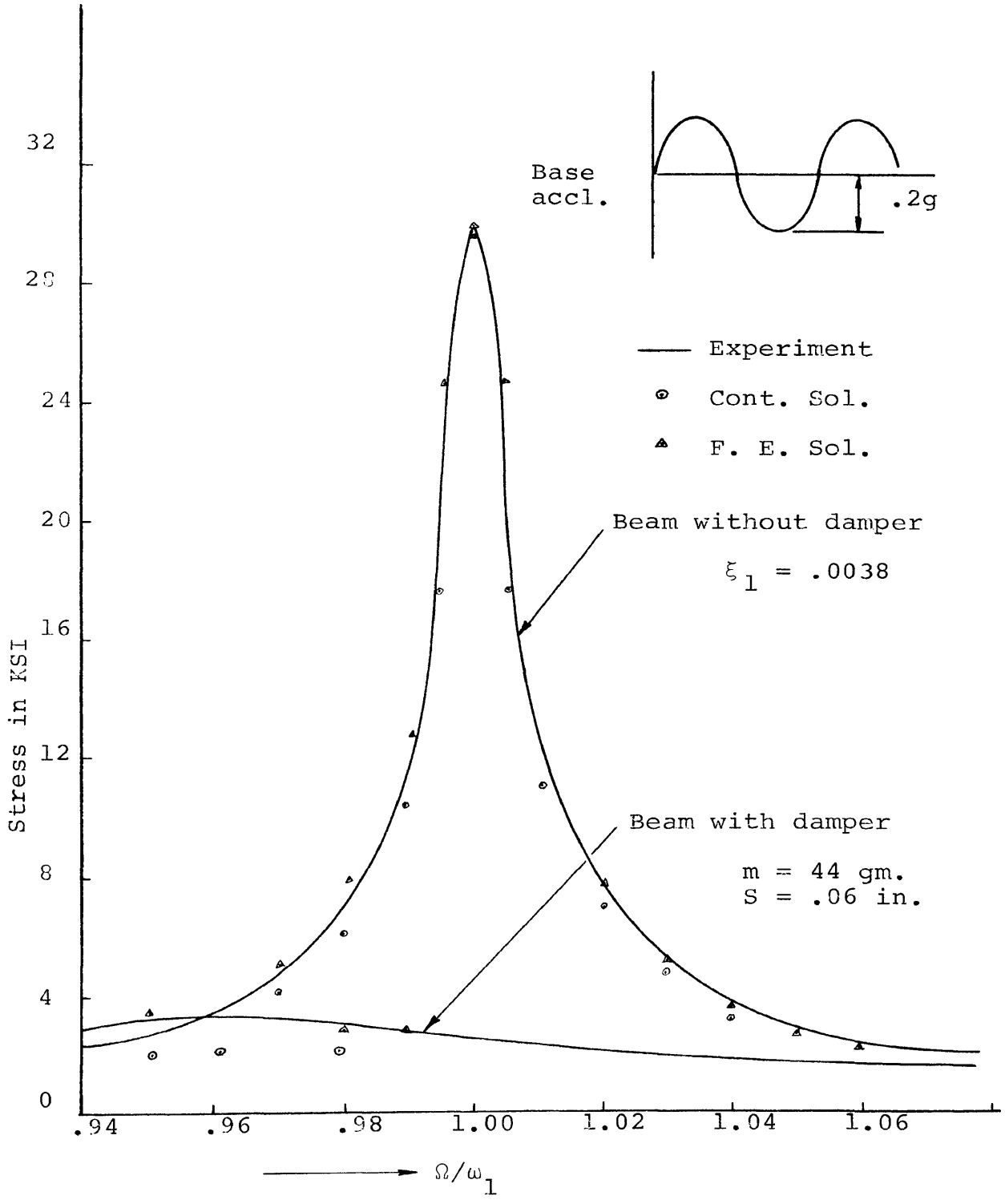


Figure 2.2 First mode frequency response of the simply supported beam

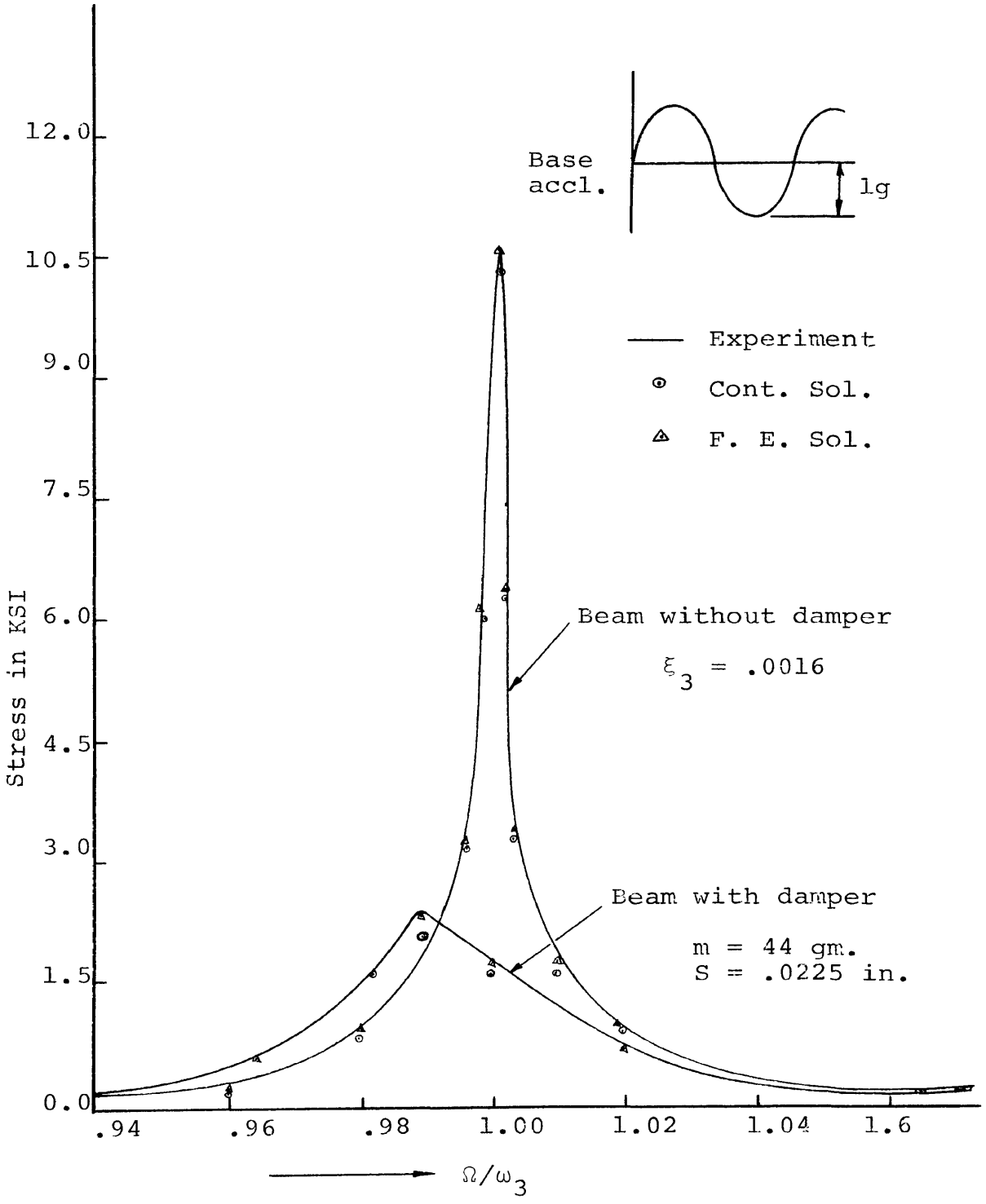


Figure 2.3 Third mode frequency response of the simply supported beam

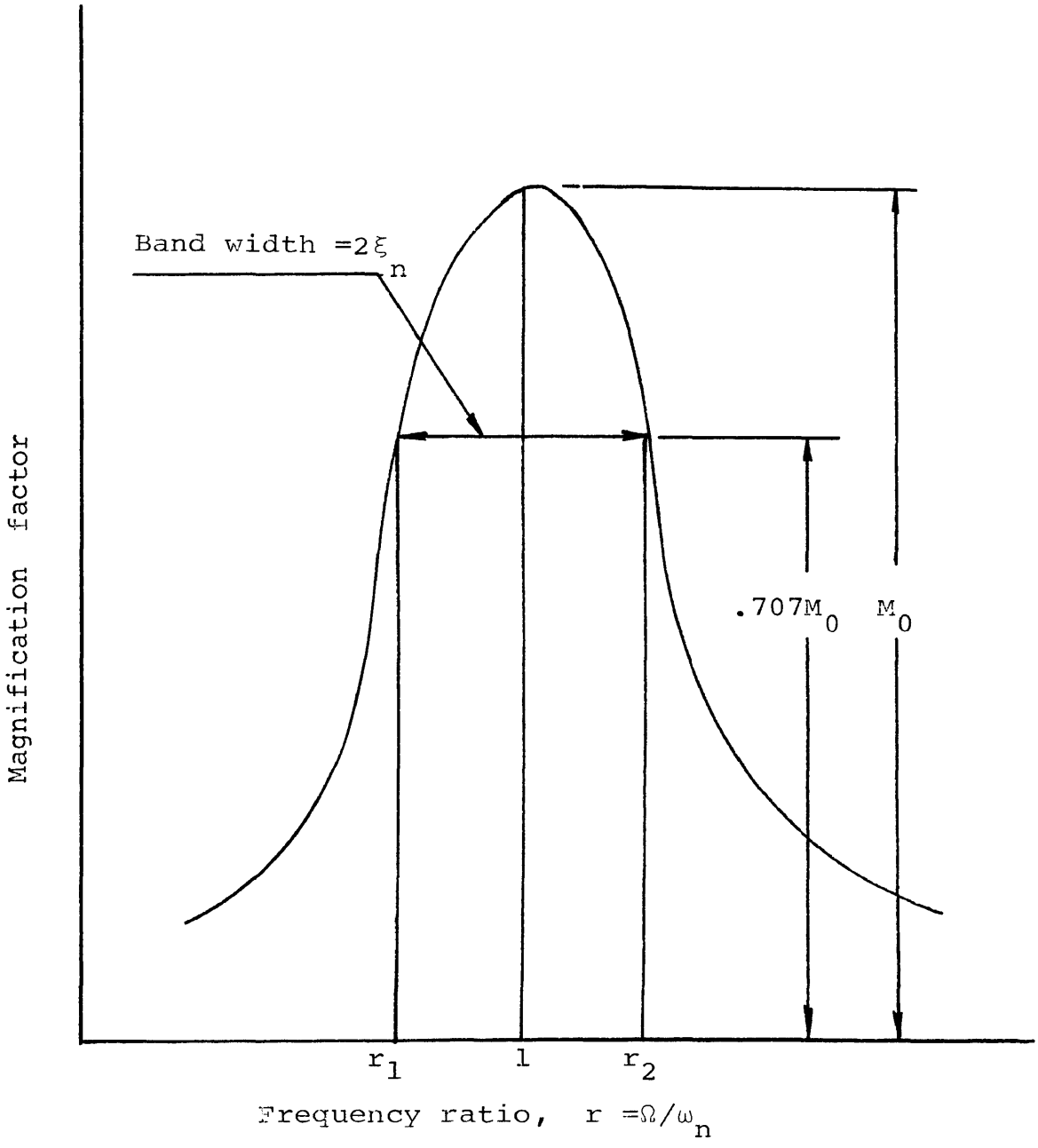


Figure 2.4 Width of the resonance curve at half-power points

# III. FINITE ELEMENT SOLUTION

## A. GOVERNING EQUATIONS

The governing differential equation of motion for a lumped mass model of a Bernoulli- Euler beam (see Fig. 3.1) can be represented in the form

$$\begin{bmatrix} M & 0 \\ 0 & J \end{bmatrix} \begin{Bmatrix} \ddot{Y} \\ \ddot{\Theta} \end{Bmatrix} + \begin{bmatrix} K_{11} & K_{12} \\ K_{21} & K_{22} \end{bmatrix} \begin{Bmatrix} Y \\ \Theta \end{Bmatrix} = \begin{Bmatrix} 0 \\ 0 \end{Bmatrix} \tag{3.1}$$

where $\{Y\}$ and $\{\Theta\}$ are the absolute displacements and rotations of the lumped masses.

Neglecting $J_i\ddot{\Theta}$ ($<<M_i\ddot{Y}_i$) for the lower modes, Eq. (3.1) can be reduced to

$$[M]\{\ddot{Y}\} + [S]\{Y\} = \{0\} \tag{3.2}$$

where

$$[S] = [K_{11}] - [K_{12}][K_{22}]^{-1}[K_{21}]$$

and

$$\{\Theta\} = -[K_{22}]^{-1}[K_{21}]\{Y\} \ . \tag{3.3}$$

## B. BASE EXCITATION SOLUTION

For systems with harmonic base excitation, h Sin$\Omega$t, and for the special case of proportional damping, the equations of motion become

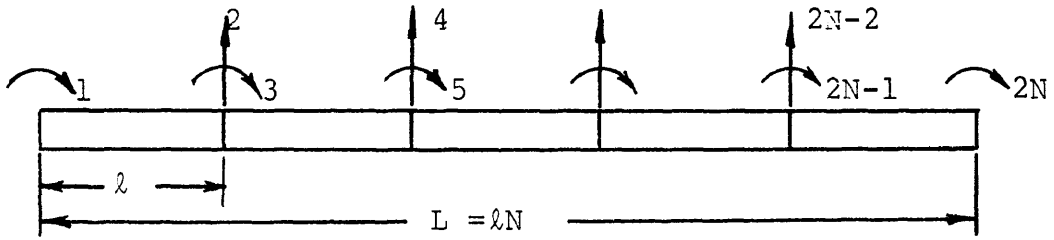


(a) Rotation and translation coordinates

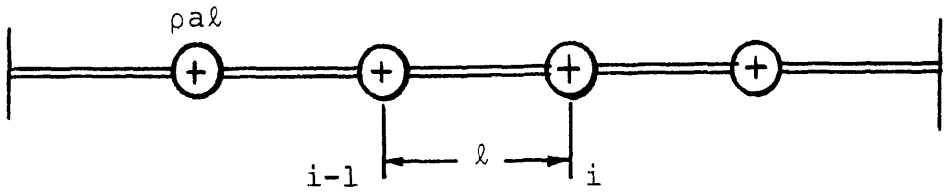


(b) Lumped mass model

Figure 3.1 Finite element model for fixed and simply supported beams

$$\left[M\right]\left\{\ddot{Y}_r\right\} + \left[C\right]\left\{\dot{Y}_r\right\} + \left[S\right]\left\{Y_r\right\} = \left\{M_i\right\} h\Omega^2 \, \mathrm{Sin}\Omega t \qquad (3.4)$$

where $\left\{Y_r\right\}$ are the coordinates relative to the support, i.e.,

$$\left\{Y\right\} = \left\{Y_r\right\} + \left\{1\right\} h \, \mathrm{Sin}\Omega t \; . \qquad (3.5)$$

The damping $\left[C\right]$ is a diagonal matrix obtained by a linear combination of $\left[M\right]$ and $\left[K\right]$ in the form

$$\left[C\right] = C_1\left[M\right] + C_2\left[K\right] ;$$

$C_1$ and $C_2$ are constants.

The eigenvalues and eigenvectors for the system are obtained by solving the undamped homogeneous equations

$$\left[M\right]\left\{\ddot{Y}_r\right\} + \left[S\right]\left\{Y_r\right\} = \left\{0\right\} . \qquad (3.6)$$

A coordinate transformation $\left\{Y_r\right\} = \left[M\right]^{-1/2}\left\{Z\right\}$ in Eq. (3.6) together with premultiplication by $\left[M\right]^{-1/2}$ uncouples the system of equations so that

$$\left\{\ddot{Z}\right\} + \left[H\right]\left\{Z\right\} = \left\{0\right\} \quad ; \qquad (3.7)$$

$$\left[H\right] = \left[M\right]^{-1/2}\left[S\right]\left[M\right]^{-1/2} \quad .$$

Since the eigenvalues, $\omega_i$, are independent of the

coordinate system, these are the same for both $[S]$ and $[H]$. The modal matrix for Eq. (3.6), however, becomes

$$[A'] = [M]^{-1/2}[A]$$

where $[A]$ is the modal matrix of Eq. (3.7) .

Further, as discussed in appendix B, $[A']$ is normalized with respect to the mass matrix to give $[\Phi]$ , the normalized modal matrix, such that

$$[\Phi]^T[M][\Phi] = [\bar{m}]$$

where $\bar{m}$ = a scalar quantity.

Substituting $\{Y_r\} = [\Phi]\{p\}$ into Eq. (3.4) and premultiplying by $[\Phi]^T$ yields

$$\{\ddot{p}_i\} + [2\xi_i\omega_i]\{\dot{p}_i\} + [\omega_i^2]\{p_i\} = [\Phi]^T\{M_i\}h_\Omega{}^2 \sin\Omega t/\bar{m} \tag{3.8}$$

where

$$2\xi_i\omega_i = C_1 + C_2\omega_1^2 \quad .$$

Following the standard approach used in the theory of differential equations, the complete solution of Eq. (3.8) can be cast in the form

$$\left\{p(t)\right\} = \left[E\right]\left\{\left[SIND\right]\left\{A\right\} + \left[COSD\right]\left\{B\right\}\right\} + \frac{1}{m}\left[\widetilde{(P_i^2 + Q_i^2)}\right]^{-1}\left[\widetilde{P_i \ Sin\Omega t - Q_i \ Cos\Omega t}\right]\left\{F\right\} \tag{3.9}$$

where

$$\left[E\right] = \left[\widetilde{e^{-\xi_i \omega_i t}}\right]$$

$$\left[SIND\right] = \left[\widetilde{Sin\omega_{di} t}\right]$$

$$\left[COSD\right] = \left[\widetilde{Cos\omega_{di} t}\right]$$

$$\omega_{di} = \omega_i\sqrt{1 - \xi_i^2}$$

$$\left\{F\right\} = \left[\Phi\right]^T \left\{M_i\right\} h\Omega^2$$

$$P_i = \omega_i^2 - \Omega^2$$

$$Q_i = 2\xi_i \omega_i \Omega \ ;$$

$\{A\}$ and $\{B\}$ are constants to be solved by initial conditions.

Therefore, the complete solution to Eq. (3.5) may be expressed in the original coordinates as

$$\left\{Y\right\} = \left[\Phi\right]\left[E\right]\left\{\left[SIND\right]\left\{A\right\} + \left[COSD\right]\left\{B\right\}\right\} + \frac{[\Phi]}{m}\left[\widetilde{(P_i Sin\Omega t - Q_i Cos\Omega t)/(P_i^2 + Q_i^2)}\right]\left\{F\right\} + \left\{1\right\} h Sin\Omega t \ . \tag{3.10}$$

If the initial conditions on the system are

$$\left\{Y_r(0)\right\} = \left\{Y_{r0}\right\} \qquad \text{and} \qquad \left\{\dot{Y}_r(0)\right\} = \left\{\dot{Y}_{r0}\right\}$$

the constants $\left\{A\right\}$ and $\left\{B\right\}$ are obtained by

$$\left\{B_i\right\} = \frac{1}{\bar{m}}\left[\Phi\right]^T\left[M\right]\left\{Y_{r0}\right\} + \frac{1}{\bar{m}}\left[\begin{array}{c} \\ \dfrac{Q_i}{P_i^2 + Q_i^2} \\ \\ \end{array}\right]\left\{F\right\} \tag{3.11a}$$

and

$$\left\{A_i\right\} = \frac{1}{\bar{m}}\left[\Phi\right]^T\left[M\right]\left\{\dot{Y}_{r0}\right\} + \left\{\xi_i \frac{\omega_i}{\omega_{di}} B_i\right\} - \frac{1}{\bar{m}}\left[\begin{array}{c} \\ \dfrac{1}{\omega_{di}} \\ \\ \end{array}\right]\left[\begin{array}{c} \\ \dfrac{P_i}{P_i^2 + Q_i^2} \\ \\ \end{array}\right]\left\{F\right\} \quad . \tag{3.11b}$$

## C. SOLUTION WITH ARBITRARY IMPACT

In the finite element method it is required that the damper be located at any one lumped mass points, i.e., a node point. While formulating the mass matrix for the system, the mass of the damper container is included in the computation along with the lumped mass at the node point. For collisions of very short duration ($<<$ period of oscillation), the displacement of this node point remains unchanged while its velocity is discontinuously changed. The displacements and velocities of all other nodal points remain unaffected during the collision.

Solution Eq. (3.10) represents the system response to

a sinusoidal base excitation and is valid until $t=t_1$, the time of first impact, which is found numerically as discussed in Chapter IV. The collision of the damper particle with this dynamical system produces a sudden impulse which gives rise to a response that is transient in nature. The solution after the impact can be established as

$$\begin{aligned}\left\{Y\right\} &= \left[\Phi\right]\left[E\right]\left\{\text{SIND}\left\{A_{i+}\right\} + \text{COSD}\left\{B_{i+}\right\}\right\} \\ &+ \frac{1}{m}\left[\Phi\right]\left[\sqrt{(P_i^2+Q_i^2)}\right]^{-1}\left[\sqrt{\phantom{x}}P_i\text{Sin}\Omega(t_1+t) - Q_i\text{Cos}\Omega(t_1+t)\right]\left\{F\right\} \\ &+ \left\{1\right\}h\ \text{Sin}\Omega(t_1+t) \qquad (3.12)\end{aligned}$$

where t is time elapsed after the impact and $A_{i+}$ and $B_{i+}$ are constants which are evaluated by using the initial conditions just after the impact. The displacements just before impact may be computed by evaluating Eq. (3.10) at $t=t_1$, thus

$$\begin{aligned}\left\{Y(t_1)\right\} &= \left[\Phi\right]\left\{e^{-\omega_i\xi_i t_1}(A_i\ \text{Sin}\omega_{di}t_1 + B_i\ \text{Cos}\omega_{di}t_1)\right\} \\ &+ \frac{1}{m}\left[\Phi\right]\left[\sqrt{\frac{P_i\text{Sin}\Omega t_1 - Q_i\text{Cos}\Omega t_1}{P_i^2 + Q_i^2}}\right]\left\{F\right\} + \left\{1\right\}h\text{Sin}\Omega t_1\ . \qquad (3.13)\end{aligned}$$

The displacements just after the impact are determined from Eq. (3.12) at t=0, as

$$\left\{Y(0)\right\} = \left[\Phi\right] B_{i+} + \frac{1}{\bar{m}} \left[\Phi\right] \left[ \frac{P_i \mathrm{Sin}\Omega t_1 - Q_i \mathrm{Cos}\Omega t_1}{P_i^2 + Q_i^2} \right] \left\{F\right\} + \left\{1\right\} h \, \mathrm{Sin}\Omega t \quad . \tag{3.14}$$

Since displacements during the impact remain unchanged, solving Eq. (3.14) and Eq. (3.13) yields

$$\left\{B_{i+}\right\} = \left\{ e^{-\omega_i \xi_i t_1} (A_i \mathrm{Sin}\omega_{di} t_1 + B_i \mathrm{Cos}\omega_{di} t_1) \right\} \quad . \tag{3.15}$$

The motion of the damper particle of mass m, and the total mass at the damper location, must satisfy the momentum equation during the impact. Therefore,

$$m_d \dot{Y}_{d-} - m v_- = m_d \dot{Y}_{d+} + m v_+ \tag{3.16}$$

where $\dot{Y}_{d-}$ , $v_-$ and $\dot{Y}_{d+}$ , $v_+$ are the system velocities before and after the impact, respectively.

If e is the coefficient of restitution between the impacting materials, then by definition

$$\dot{Y}_{d+} - v_+ = - e(\dot{Y}_{d-} - v_-) \quad . \tag{3.17}$$

Eq. (3.17) and Eq. (3.16) can be solved to give

$$v_+ = \frac{( C_m + e \, dv )}{( 1 + m/m_d )} \tag{3.18}$$

and

$$\dot{Y}_{d+} = \frac{( C_m + e\, dv )}{( 1 + m/m_d )} - e\, dv \qquad (3.19)$$

where

$$C_m = \dot{Y}_{d-} + v_- m/m_d$$

and

$$dv = \dot{Y}_{d-} - v_- \quad .$$

Differentiation of Eq. (3.10) yields the velocities of the lumped masses just before impact (at $t=t_1$), i.e.,

$$\begin{aligned}\dot{Y}_{i-} = &\left[\Phi\right]\left\{e^{-\omega_i\xi_i t_1}( A_i \cos\omega_{di} t_1 - B_i \sin\omega_{di} t_1 )\omega_{di}\right\} \\ &+ \left[\Phi\right]\left\{- \omega_i\xi_i e^{-\omega_i\xi_i t_1}(A_i\sin\omega_{di}t_1 + B_i\cos\omega_{di}t_1)\right\} \\ &+ \frac{1}{m}\left[\Phi\right]\left[\frac{(P_i\cos\Omega t_1 + Q_i\sin\Omega t_1)\Omega}{P_i^2 + Q_i^2}\right]\left\{F\right\} + \left\{1\right\} h\Omega \cos\Omega t_1 \quad .\end{aligned} \qquad (3.20)$$

Velocities of the lumped masses just after the impact thus become

$$\left\{\dot{Y}_+\right\} = \begin{Bmatrix} \dot{Y}_{1-} \\ \dot{Y}_{2-} \\ \cdot \\ \cdot \\ \dot{Y}_{d+} \\ \cdot \\ \cdot \\ \dot{Y}_{i-} \end{Bmatrix} \qquad (3.21)$$

where $\dot{Y}_{1-}$, $\dot{Y}_{2-}$ etc. are given by Eq. (3.20) and $\dot{Y}_{d+}$ by Eq. (3.19)

Since the solution Eq. (3.12) must satisfy these initial conditions Eq. (3.21), for velocities, the constants, $A_{i+}$, are obtained as follows

$$\left\{A_{i+}\right\} = \left[\omega_{di}\right]^{-1}\left\{\left\{\omega_i \xi_i B_{i+}\right\} - \frac{1}{m}\left[\Phi\right]^T\left[M\right]\left\{h\Omega\ \mathrm{Cos}\Omega t_1 - Y_{i+}\right\}\right\}$$

$$- \frac{1}{m}\left[\omega_{di}\right]^{-1}\left[\frac{(P_i\ \mathrm{Cos}\Omega t_1 - Q_i\ \mathrm{Sin}\Omega t_1)}{P_i^2 + Q_i^2}\right]\left\{F\right\} . \quad (3.22)$$

The complete solution for the displacement of the beam after the collision is obtained by evaluating Eq. (3.12) with the new values of $A_{i+}$ and $B_{i+}$ determined from Eq. (3.22) and Eq. (3.15), respectively. The corresponding rotation at each mode at the same time is computed by using Eq. (3.3).

Knowing the displacement and rotation of the lumped mass points, forces and moments acting on an element can be determined from the relation

$$\begin{Bmatrix} f_i \\ f_{i+1} \\ M_i \\ M_{i+1} \end{Bmatrix} = \frac{2EI}{\ell^3} \begin{bmatrix} 6 & -6 & -3\ell & -3\ell \\ -6 & 6 & 3\ell & 3\ell \\ -3\ell & 3\ell & 2\ell^2 & \ell^2 \\ -3\ell & 3\ell & 2\ell & 2\ell^2 \end{bmatrix} \begin{Bmatrix} Y_i \\ Y_{i+1} \\ \Theta_i \\ \Theta_{i+1} \end{Bmatrix} \qquad (3.23)$$

which is derived in Appendix B. Thus, the bending stress on the surface of the beam at the ith node is

$$\sigma = \frac{M_i}{I} \frac{d}{2} .$$

The computer program developed for this method is discussed in detail in Chapter IV C. The initial part of the computation involves the determination of the eigenvectors and eigenvalues of the system for a certain assumed number of segments comprising the beam. To determine the accuracy of the finite element method, the frequency roots obtained by this method for various numbers of beam segments are compared with the corresponding exact values. The comparison has been interpreted as a percentage of frequency root error, giving the extent by which the roots obtained by this method deviate from those given by the exact solutions. The percentage error has been expressed in the following manner

$$e_r = \frac{| \omega_0 - \omega_e |}{\omega_e} \times 100 \qquad (3.24)$$

where

$\omega_0$ = the frequency root obtained by the finite element method

$\omega_e$ = the exact frequency root

$e_r$ = the percentage frequency root error .

Percentage errors have been calculated for the first, second, third, fourth and fifth modes for a simply supported beam and a plot of these values as a function of the number of segments in the beam is shown in Fig. 3.2. It can be observed from this plot that the percentage error for 8 segments is well below 1% in the first three modes. Similar calculations for fixed beams also revealed less than 1% error in the first and third modes for 8 segments in the beam.

Following the determination of the error associated with various numbers of segments, 8 segments in the beam were chosen for the remainder of the calculations. Equations derived in this chapter were programmed and solutions were evaluated for all the desired parameters. Damping ratios used in the computations were calculated from experimental results using the width of the resonance curve at half power points, for both systems in the first and third modes. Values of the damping ratios at other modes are insignificant when the response at the first and third modes are considered and therefore were assigned arbitrarily small values. The results of these computations are

compared with the corresponding experimental values and are presented in Figs. 3.3 & 3.4. In the finite element approach the mass of the damper container is included with the lumped mass at the nodal point and the results showed excellent agreement with the corresponding experimental values.

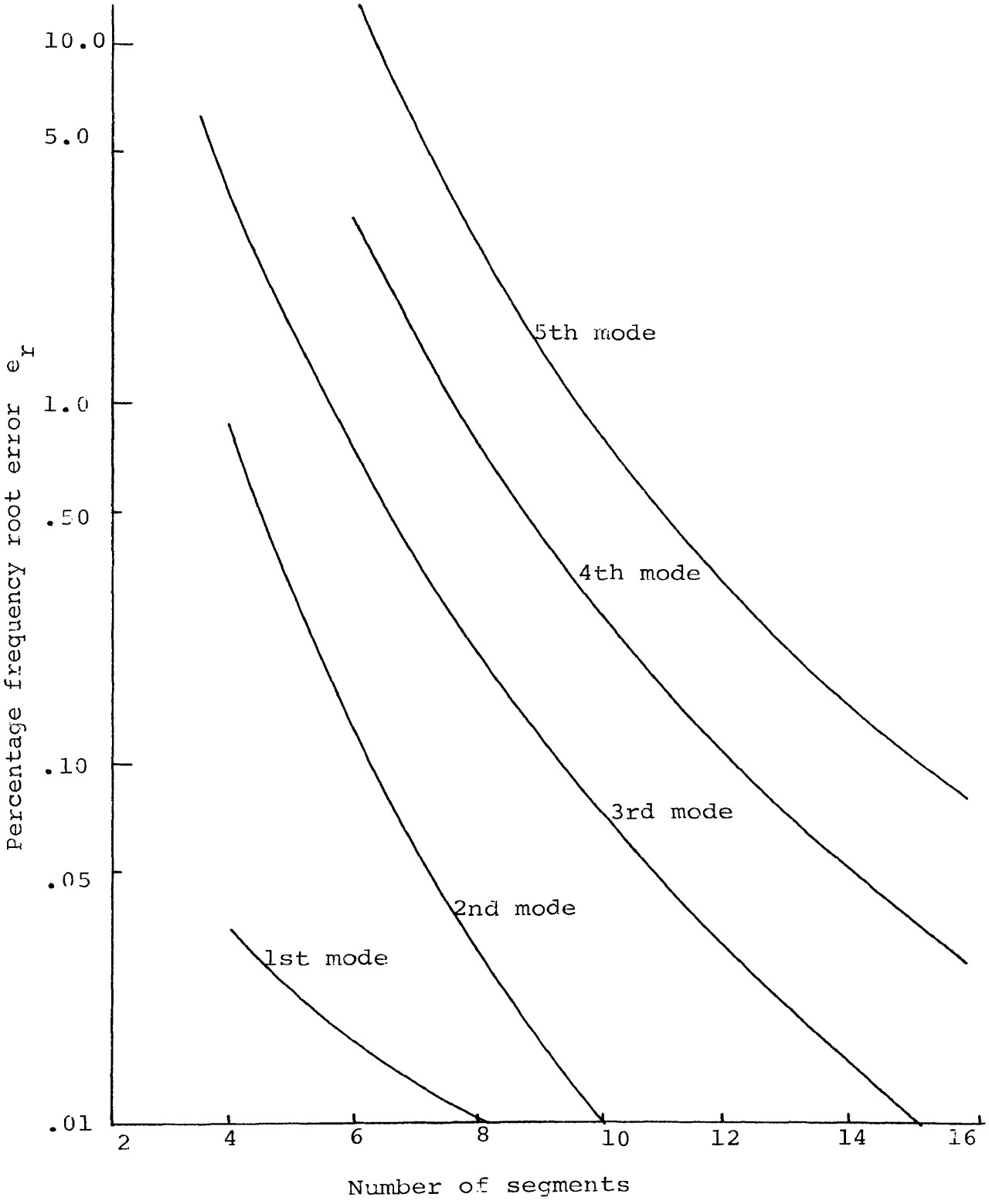


Figure 3.2 Non-dimensional frequency root errors for the simply supported beam

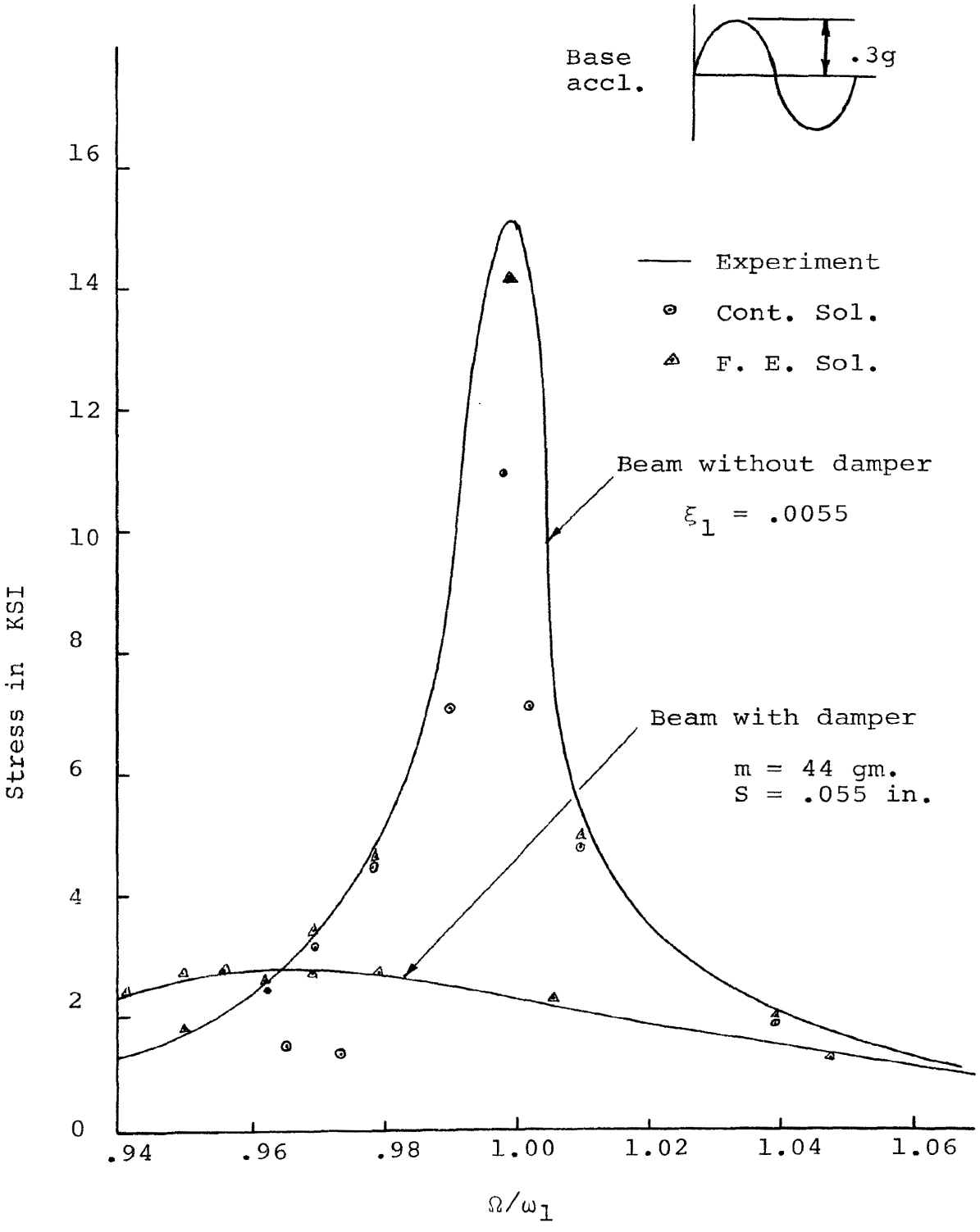


Figure 3.3 First mode frequency response of the fixed beam

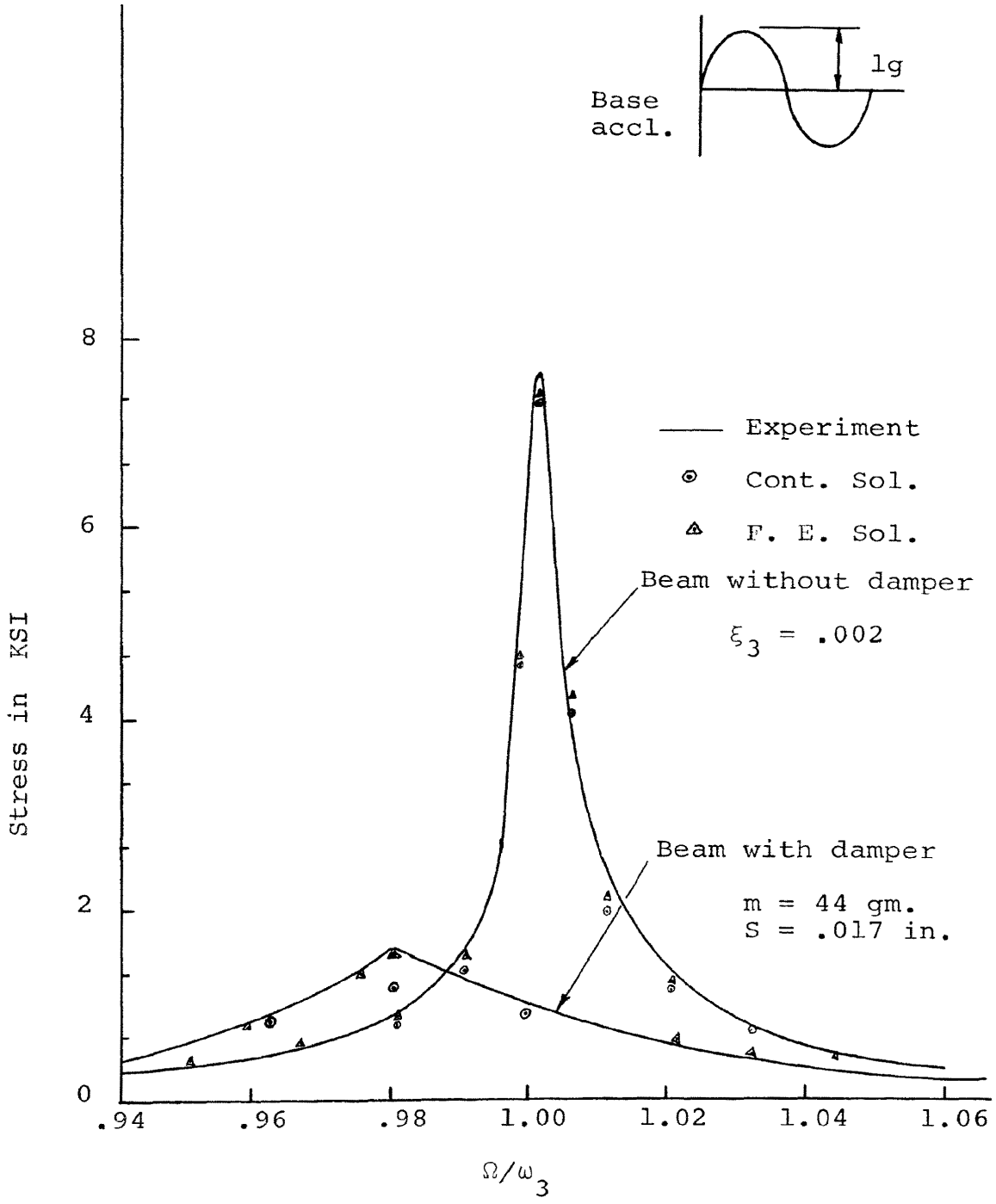


Figure 3.4 Third mode frequency response of the fixed beam

# IV. DIGITAL COMPUTER SOLUTION

## A. THE COLLISION CRITERION

In the previous two chapters solutions have been derived which are valid during the time immediately after the first impact until the next. In so doing, the time $t_1$ at which the first impact occurs is assumed to be known. The times of first impact and subsequent impacts are actually determined by numerical computation with the help of a digital computer. The following sections explain the technique involved.

If the beam displacement at the damper location is denoted by $U_d(t)$ then

$$U_d(t) = \begin{cases} \text{either the solution Eq. (2.6) evaluated at } x=x_d \\ \text{or one of the solutions Eq. (3.12) for the lumped mass plus the damper mass.} \end{cases}$$

The particle displacement, $U_p(t)$, is measured from the initial reference position of the damper location on the beam. Then, in order that the particle might come in contact with either of the container surfaces, $U_d(t)$ and $U_p(t)$ must satisfy

$$\left| U_d(t) - U_p(t) \right| = S/2 \tag{4.1}$$

where $S$ is the clearance as shown in Fig. 2.1.

A measure of how close the system is to an impact is indicated by the difference of the quantities appearing on the left and the right hand sides of the condition expressed in Eq. (4.1). This difference is expressed as follows

$$C_c(t) = S/2 - \left|U_d(t) - U_p(t)\right| \qquad (4.2)$$

where $C_c(t)$ is dependent on time and is termed the collision function. The roots of

$$C_c(t) = 0 \quad , \qquad (4.3)$$

are the times of the collisions. Since the particle is constrained to move within the clearance S, $C_c(t)$ is never negative.

## B. FINITE INTERVAL METHOD OF DETERMINING TIME OF IMPACT

The function, $C_c(t)$, may be expressed either explicitly as a polynomial in time t, or as a transcendental function. Geometrically a root of the equation is a time, $t=t_r$ , for which the curve $Y=C_c(t)$ intersects the line Y=0 (Fig. 4.1). It may, of course, happen that these curves do not intersect, in which case the condition given by Eq. (4.3) is not satisfied and as such no impact will occur.

Computer programs to evaluate $C_c(t)$ were written in FORTRAN IV language using the solution expressed by

Eq. (2.6) and Eq. (3.12). Values of $C_c(t)$ were computed at $t = 0, \Delta t, 2\Delta t, 3\Delta t$, and so on until $C_c(t)$ changed sign. This means that an impact has occured. A linear iteration technique namely, the method of false position, was used at this point to obtain a root of the equation. For this method, it is assumed that there exist a simple root, $t_i$, within the interval between $t_{i-1}$ and $t_{i+1}$ such that $C_c(t_{i-1})$ and $C_c(t_{i+1})$ are opposite in sign. An approximation $t_i'$ of $t_i$ is (see Fig. 4.1) the geometrical intersection of the line connecting $\{t_{i-1}, C_c(t_{i-1})\}$ and $\{t_{i+1}, C_c(t_{i+1})\}$ with the $t$ axis, and can be mathematically expressed as

$$t_i' = \frac{t_{i-1}\, C_c(t_{i+1}) - t_{i+1}\, C_c(t_{i-1})}{C_c(t_{i+1}) - C_c(t_{i-1})} \quad . \qquad (4.4)$$

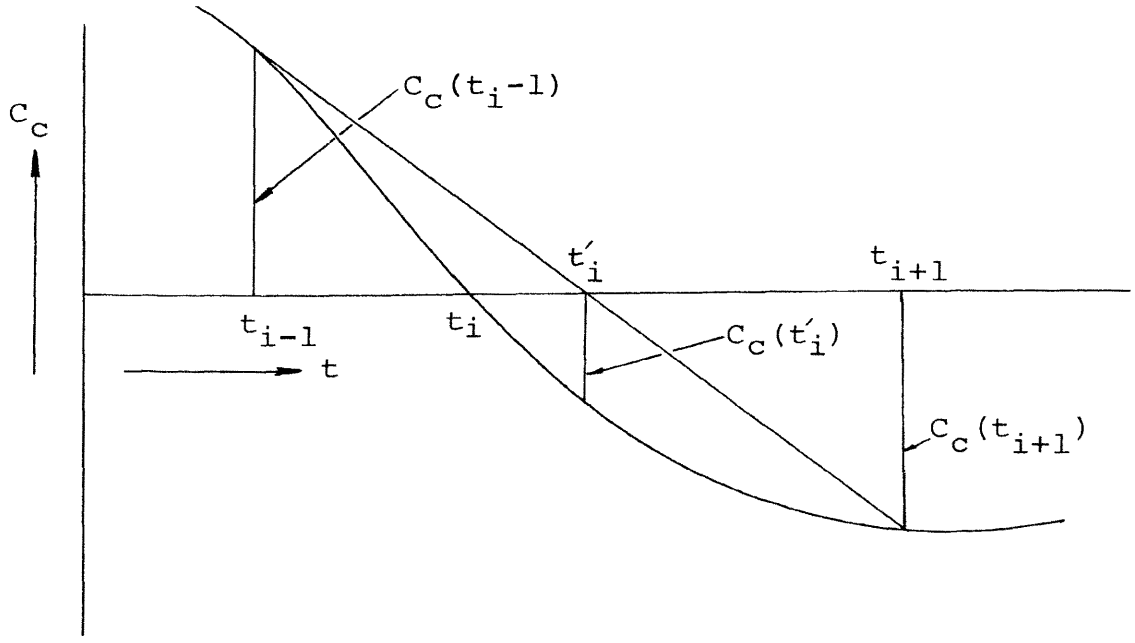


Figure 4.1 Plot of the collision function

If $C_c(t_i)$ and $C_c(t_{i-1})$ are opposite in sign, as can be seen in Fig. 4.1, $t_{i+1}$ is replaced by $t_i$, $t_{i-1}$ is unchanged, and a new approximation is obtained from Eq. (4.4). Otherwise $t_{i-1}$ is replaced by $t_i$, $t_{i+1}$ is left unchanged, and again another approximation is obtained.

## C. COMPUTER PROGRAMS

Digital computer programs were written to find the step by step solutions of the basic equations of motion as related to the system under investigation. Two separate programs were developed to evaluate results for the same system using the series and the finite element analysis. Major programs were written in FORTRAN IV language, and executed on the University of Missouri-Rolla, computer system, which is an IBM 360, Model 50, with IBM 2314 disk storage. Each program required a maximum core storage of 150 k bytes. Small check programs were executed through CPS, IBM 2741 terminal and an IBM teletype using the PL 1 language. The Calcomp Plotter was used to plot computer outputs.

The finite element solution was completed in two separate programs. Quantities such as eigenvalues, eigenvectors, stiffness matrices etc., which are characteristics of the system, are calculated in one program. The output from this code (punched cards) is used as input to the second program which computes system response at any time. Brief outlines of these are shown in Figs. 4.2, 4.3, & 4.4.

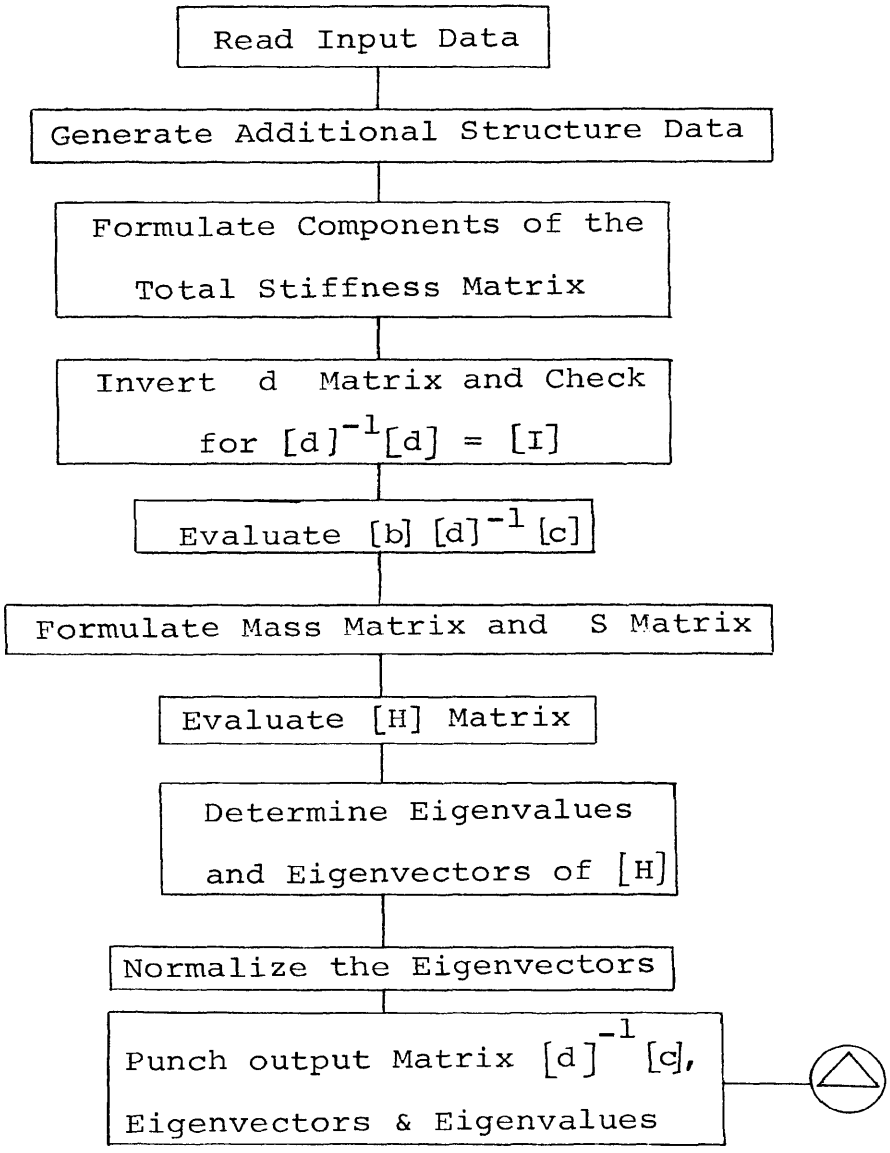


Figure 4.2 Program outline for the finite element method - step one

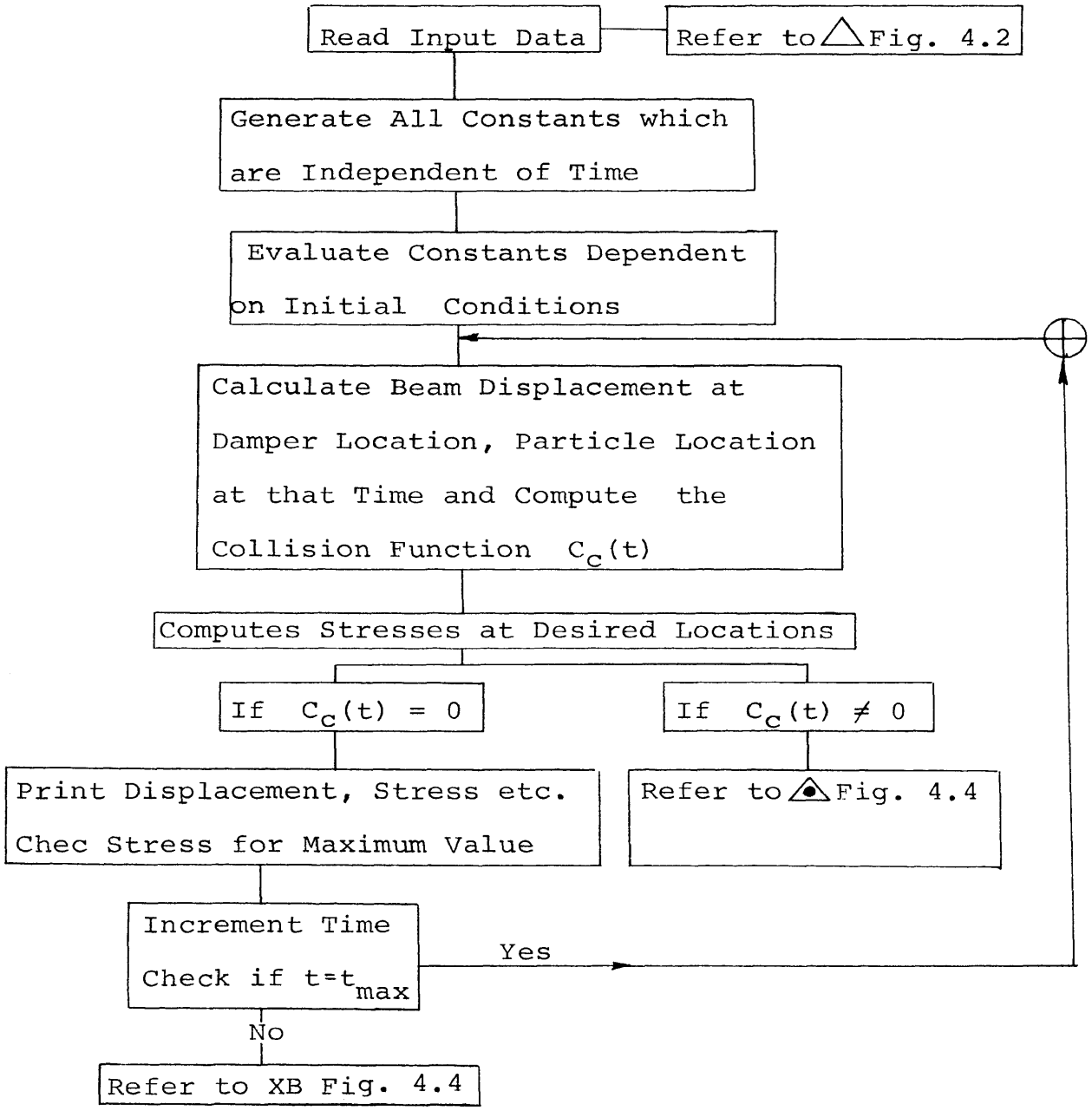


Figure 4.3 Program outline for the finite element method - step two

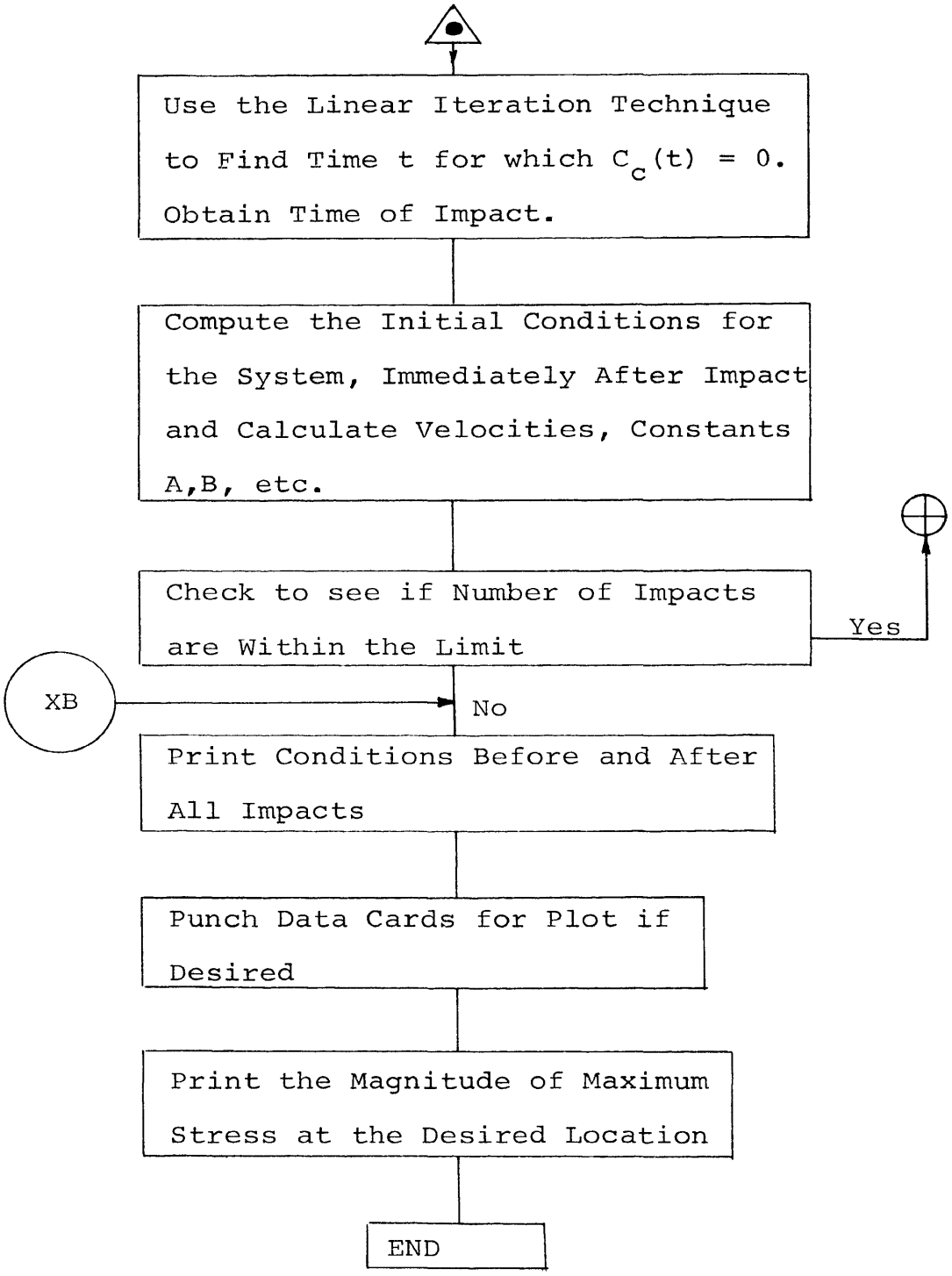


Figure 4.4 Continuation of the program outline for the finite element method-step two

The program for the series solution uses the characteristic frequencies given by Volterra(10) and follows similar lines of computation as the second step of the finite element code mentioned above.

## D. EQUIVALENT SINGLE DEGREE OF FREEDOM SYSTEM

Two beam systems, clamped and simply supported, were experimentally studied and the results obtained were compared with analytical solutions. Each of these actual systems can be described as an equivalent discrete spring-mass model with viscous damping and an impact damper, as shown in Fig. 4.5 and Fig. 4.6. The mass of the equivalent system is such that the period of vibration of the massless beam loaded at the center by this equivalent mass is the same as the fundamental period of vibration of the actual system. The equivalent mass, $M_e$, of the system is found by substituting the experimentally determined, fundamental natural frequency in

$$f_1 = (1/2\pi) \sqrt{(K_e/M_e)} \quad ,$$

which gives

$$M_e = M_d + .367\ (\rho aL)$$

for the clamped beam and

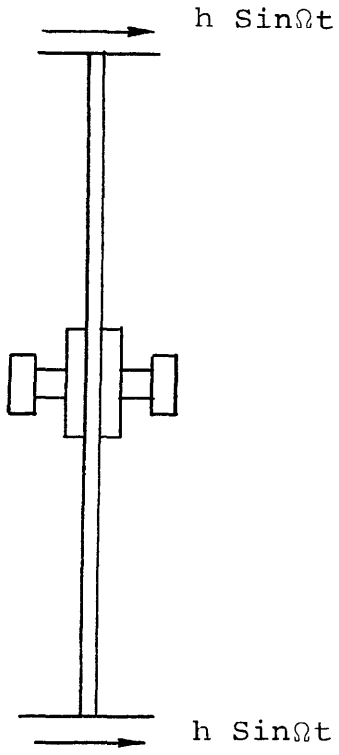


Figure 4.5 Uniform beam with an impact damper attached at the middle

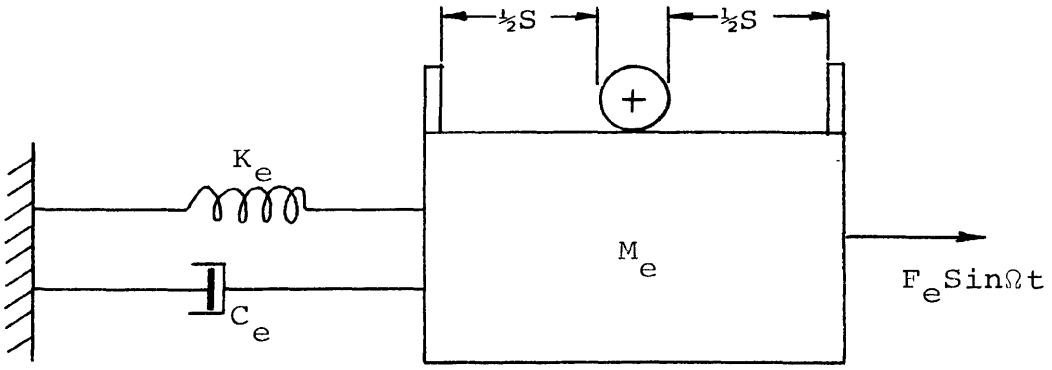


Figure 4.6 Equivalent single spring-mass model

$$M_e = M_d + .485\ (\rho aL)$$

for the simply supported beam, where $M_d$ is the mass of the damper container assumed to be concentrated at the center of the beam.

The equivalent spring constant, $K_e$, can be obtained by considering the static deflection of a massless beam loaded in the center and is $(192EI)/L^3$ and $(48EI)/L^3$ for clamped and simply supported beams, respectively.

The base excitation, h Sin$\Omega$t, of the actual system is equivalent to an acceleration force amplitude

$$F_e = M_e h\Omega^2$$

on the equivalent mass and acts as shown in Fig. 4.6.

Such simplification of the actual continuous system to a single degree of freedom system, will allow a comparison of these results with those of previous investigators. The following two cases are considered in this study.

Two steel beams each of length 25½", width 1½", and thickness 1/8" for which $E=30\times10^6$ psi., $\rho g=.283$ lbs./in$^3$. and $x_d=L/2$ ;

Case 1: Clamped beam

| | |
|---|---|
| $M_d$ = 99gm. | $\xi_1$ = .0055 |
| $M_p$ = 44 gm. | $\Omega/\omega_1$ = 1.0 |
| e = .8 | $h\Omega^2$ = .3g (base acceleration) |

$S = .06$ in.

i.e.,

$$M_e = M_d + .367\ (\rho aL) = 324 \text{ gm.}$$

$$K_e = 192EI/L^3 = 84.809 \text{ lbs./in.}$$

$$F_e = M_e h\Omega^2 = .2142 \text{ lbs.}$$

$$\mu = M_p/M_e = .136$$

$$\frac{S}{F_e/K_e} = 13.85 \quad ;$$

Case 2: Simply supported beam

$M_d = 90.5$ gm. $\qquad \xi_1 = .0038$

$M_p = 44$ gm. $\qquad \Omega/\omega_1 = 1.0$

$e = .8$ $\qquad h\Omega^2 = .2g$ (base acceleration)

$S = .06$ in.

i.e.,

$$M_e = 389 \text{ gm.}$$

$$K_e = 21.2 \text{ lbs./in.}$$

$$F_e = .1716$$

$$\mu = .113$$

$$\frac{S}{F_e/K_e} = 7.4 \quad .$$

For both the above cases, stresses were computed using analytical solutions (Eqs. 2.19 & 3.24) and found to agree favorably with the experimental results (see Figs.

4.7 & 4.8). The stress amplitude ratio for case (1) and case (2) were found as $A_d/A_0$ = .185 and .190 respectively. Masri(4), using $\Omega/\omega = 1$, $\mu = .1$, $e = .8$ and $S = .1$ in his investigation, obtained $(X/A)_{max} = .2$ for $\frac{d}{F/K} = 17.0$.

Numerical solutions for a wide range of parameters obtained by computer have been compared with the experimental results and are shown in Figs. 4.7 through 4.10.

## E. DISCUSSION OF ANALYTICAL SOLUTIONS

The analytical solution for a continuous system as determined in Chapter II is expressed as the sum of an infinite series of terms. Comparison of computer results for various numbers of terms in the series showed that sufficiently accurate (<.1% error) results are obtained by considering only the first few terms. Based on these findings, computations were carried out using the first 10 terms in the series.

The solutions by the finite element method can be evaluated by assuming any number of segments in the beam. A study of the computer results showed that the greater the number of segments in the beam the better the results obtained, but required correspondingly longer computation time. The extent of the frequency root errors for various segments in the beam is shown in Fig. 3.2. As a result of this study, all computations for finite element solutions were carried out using 8 segments in the beam.

Damping ratio used in all computations were predetermined experimentally. The impact damper was applied at the center of the beam for this phase of the investigation , and the following features were noted:

a. The computer programs evaluated stress at x = 11.165" (strain gage location on the test models) on the beam as well as displacement and velocity at the mid-point. The effect of gravitation on the free action of the damper particle was neglected.

b. Initially, the damper particle was assumed to be at rest at the zero displacement position. If the clearance, S, were made sufficiently large such that S/2 was greater than the beam displacement at all times, the system response was the same as that without the damper.

c. The right hand side of Eq. (4.2) was evaluated with a finite interval, $\Delta t$, starting with t equal to zero. The linear iteration process for determining the time was continued until

$$|C_c(t_i) - C_c(t_{i+1})| \leq \varepsilon$$

where $\varepsilon$ was chosen to be $1\times10^{-8}$ and usually required less than 8 iterations.

d. Impact between the damper particle and the beam excited the system in many normal modes. For example, when the excitation was at the first natural frequency, the impact produced transients which were predominantly

that of the third mode. This gave rise to multiple impacts within a single cycle of the base excitation.

e. The system response for a given set of parameters was computed over a range of impacts usually (30 or 40), until the response amplitude ceased to increase.

f. Double precision and single precision arithmetic were used for the computations with the continuous and the finite element solutions, respectively. The programs required approximately 80 seconds for compilation and 25 seconds for execution to carry out computations through 40 impacts.

g. Analytical solutions yielded results which compared more favorably with experimental results when larger values of S were used.

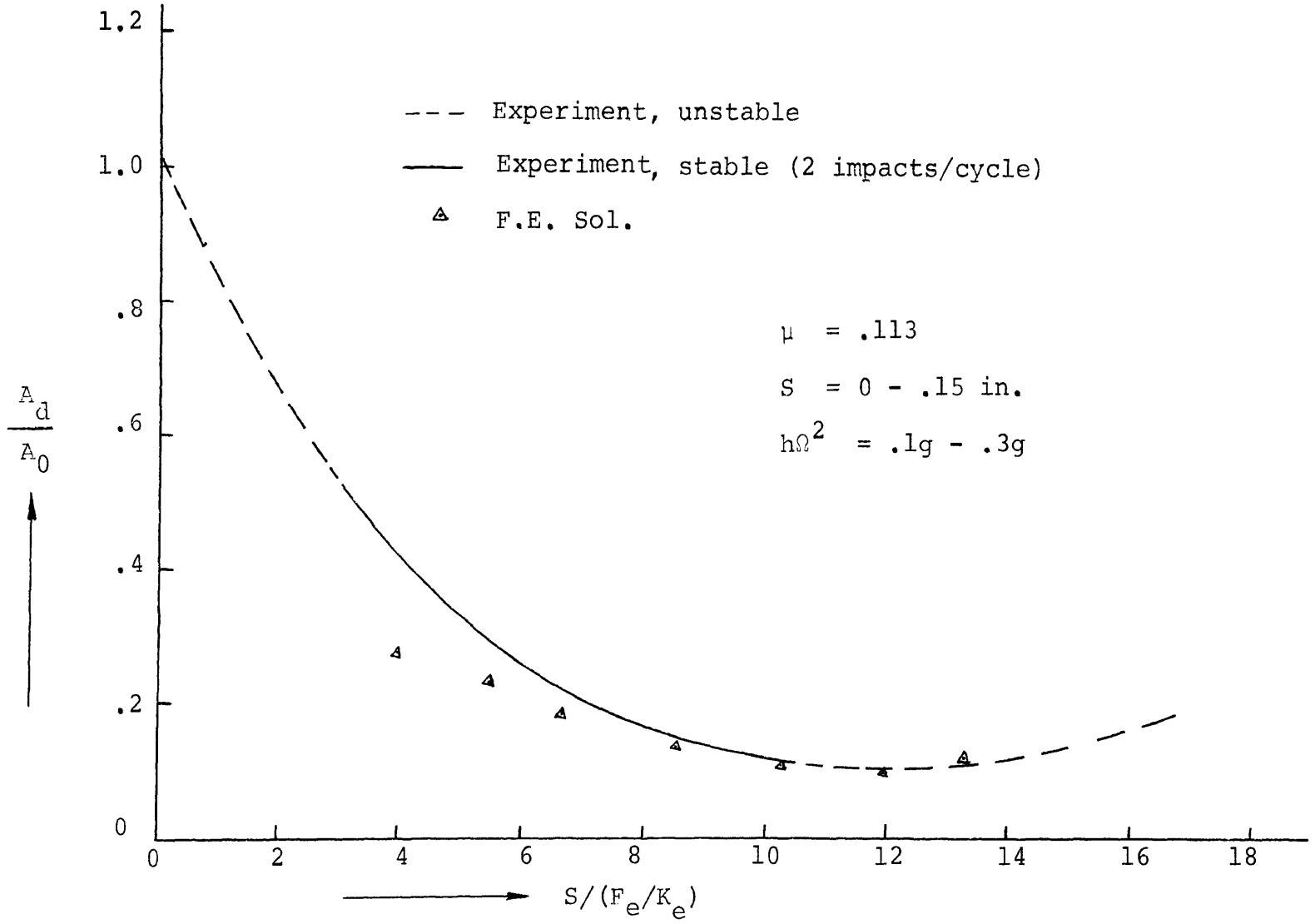


Figure 4.7 Solution curve for the simply supported beam ( 44 gm. damper )

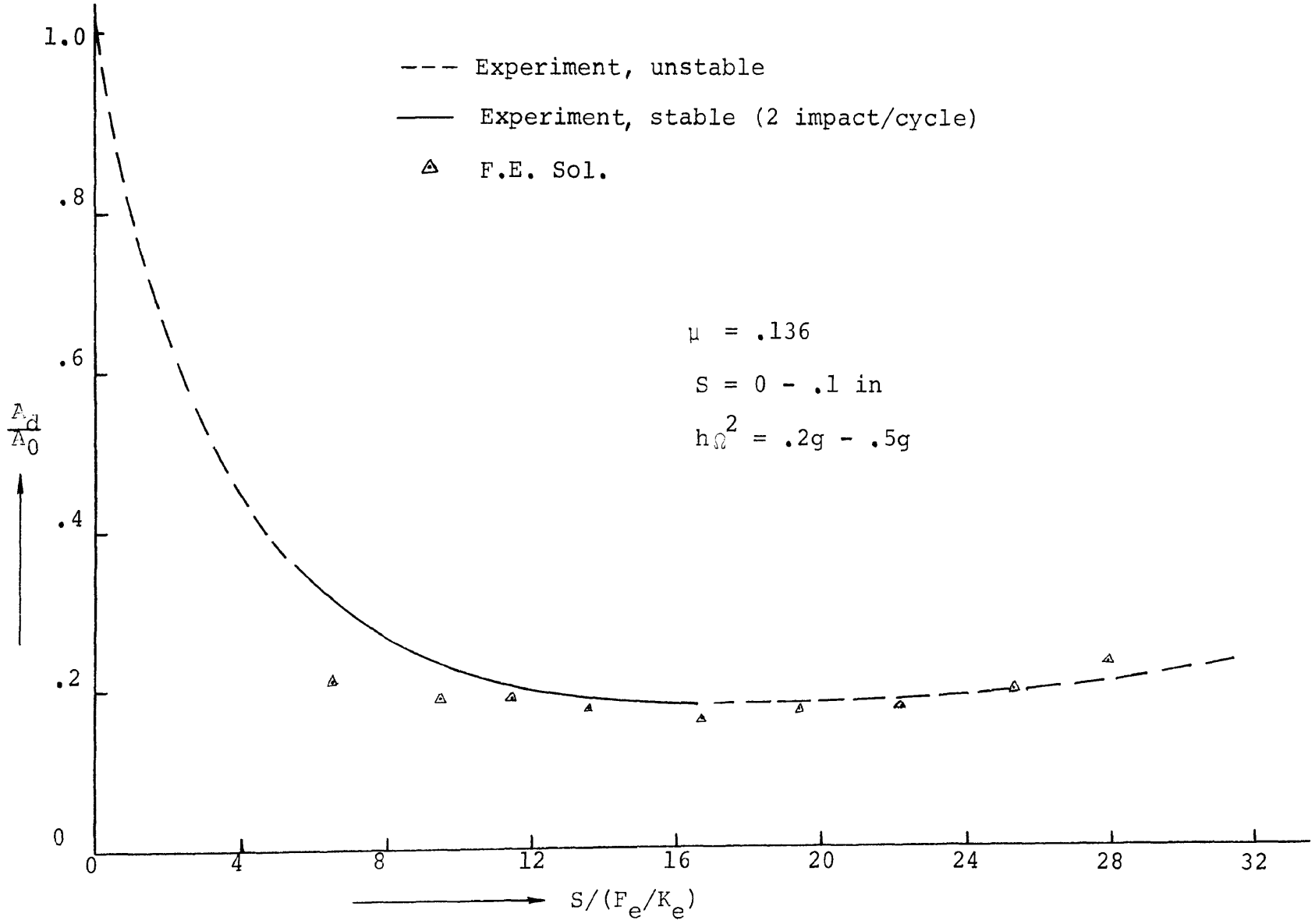


Figure 4.8 Solution curve for the fixed beam ( 44 gm. damper )

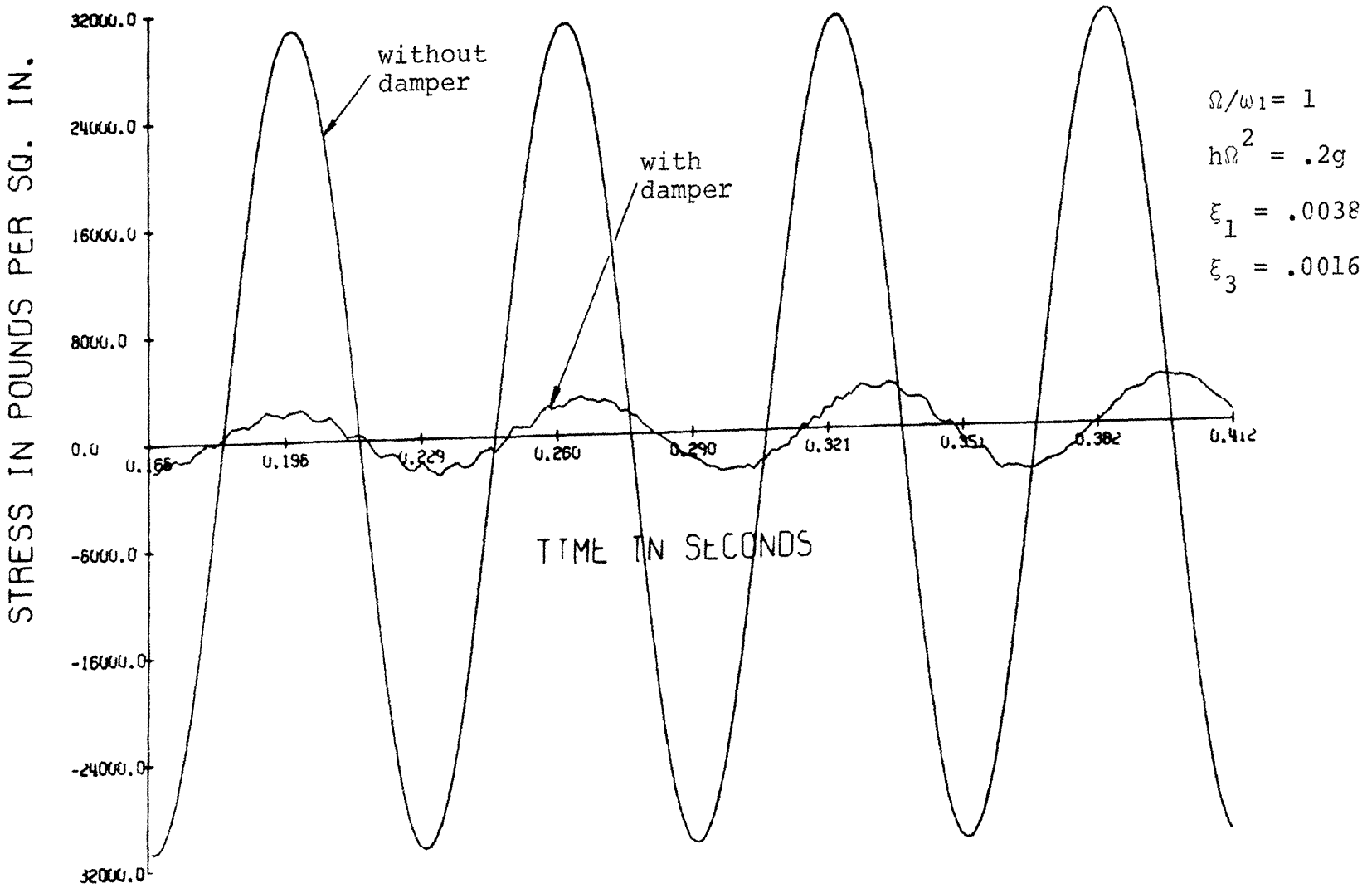


Figure 4.9 Typical response of the simply supported beam using the finite element program

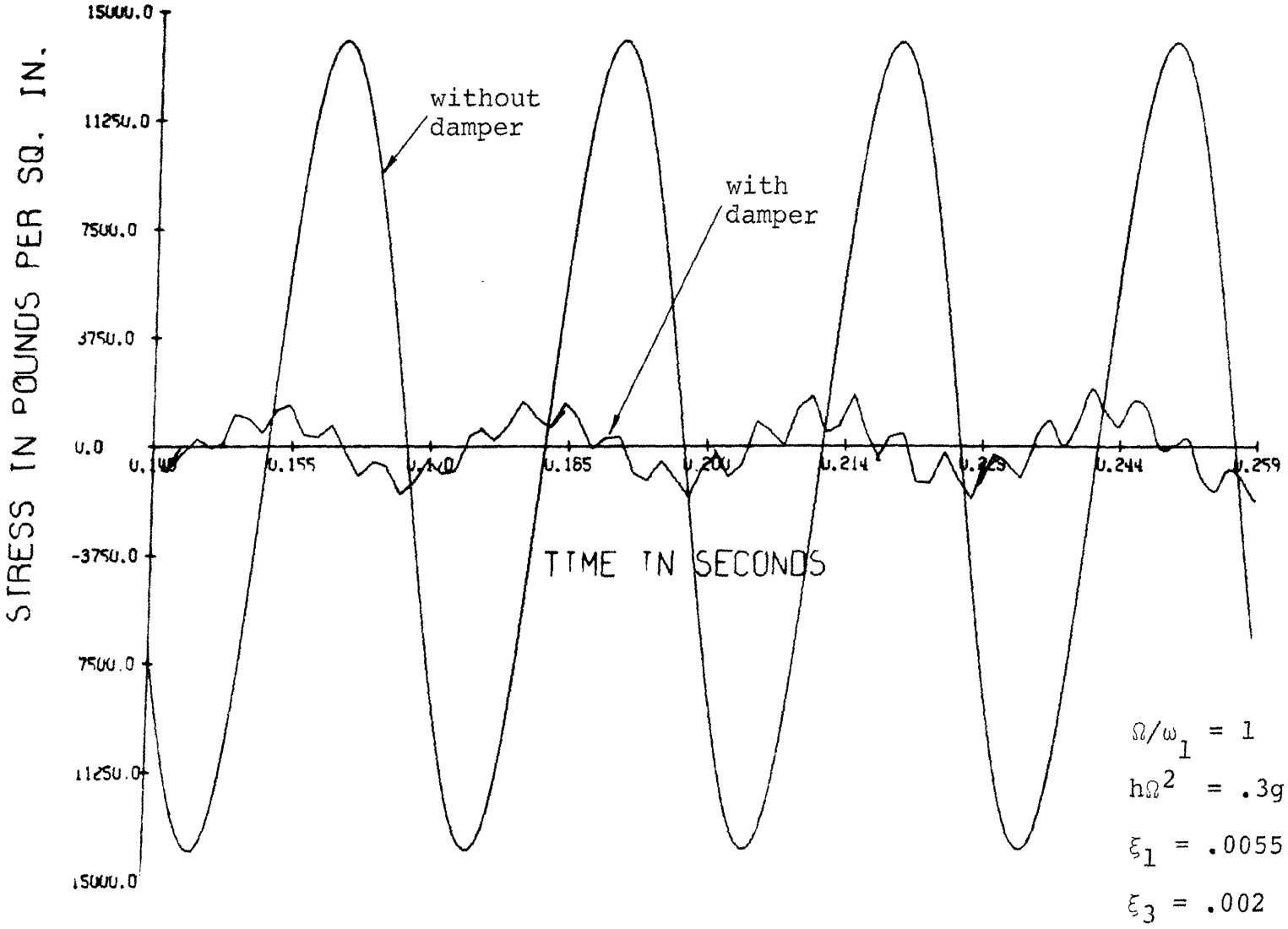


Figure 4.10 Typical response of the fixed beam using the finite element program

# V. EXPERIMENTAL INVESTIGATION

## A. INTRODUCTION AND OBJECTIVES

In the theoretical determination of the solution for the motion of the system, certain parameters were assumed to be arbitrary. In practice, however, some of these were unique to the system. For example, the damping of the system at different modes were dependent on the end conditions, forcing function, driving frequency, and other factors. Certain parameters such as the mass of the particle, m, the clearance, S, and the coefficient of restitution had to be properly selected to obtained realistic results.

With a view toward estimating the accuracy of the finite element method discussed in Chapter III, the computer solution was compared with that of the continuous system discussed in Chapter II, for a few theoretical cases. This comparison was favorably concluded and, although it established the validity of the analytical solutions, it did not however, assure selection of damper parameters for the following reasons:

a. Lack of information concerning the design and use of impact dampers on continuous systems.

b. Design problems involved in the construction of the damper unit as well as the system concerned.

To obtain some of the information mentioned above, tests were conducted with two types of steel beams. The

objectives of the tests were:

1. To determine damping present in the system for the first few modes.
2. To compare results of previously obtained analytical solutions with observed values.
3. To encounter and solve design problems of these types of systems and study the range of size of the damper unit to render maximum effectiveness.
4. To determine the effects of variations of mass and clearance on the action of the damper.

## B. TEST DESCRIPTION AND RESULTS

The experimental part of the investigation was conducted in the Engineering Mechanics Laboratory of the University of Missouri-Rolla. Two steel beams each of 25½" by 1½" were machined from 1/8" thick steel plate. Support fixtures were designed to permit positioning of these beams as either clamped or simply supported for two different tests. The entire experimental work was conducted on a 3500 pound-force MB C25H vibration exciter. An additional fixture was designed and attached to the exciter to permit mounting the beam systems on the vibration shaker. Schematic diagrams of the mechanical models that were used are shown in Figs. 5.1 & 5.2 and photographs of the actual beams are shown in Figs. 5.3 & 5.4.

Endevco, piezoelectric accelerometers and electric resistance strain gages were used to measure the accelera-

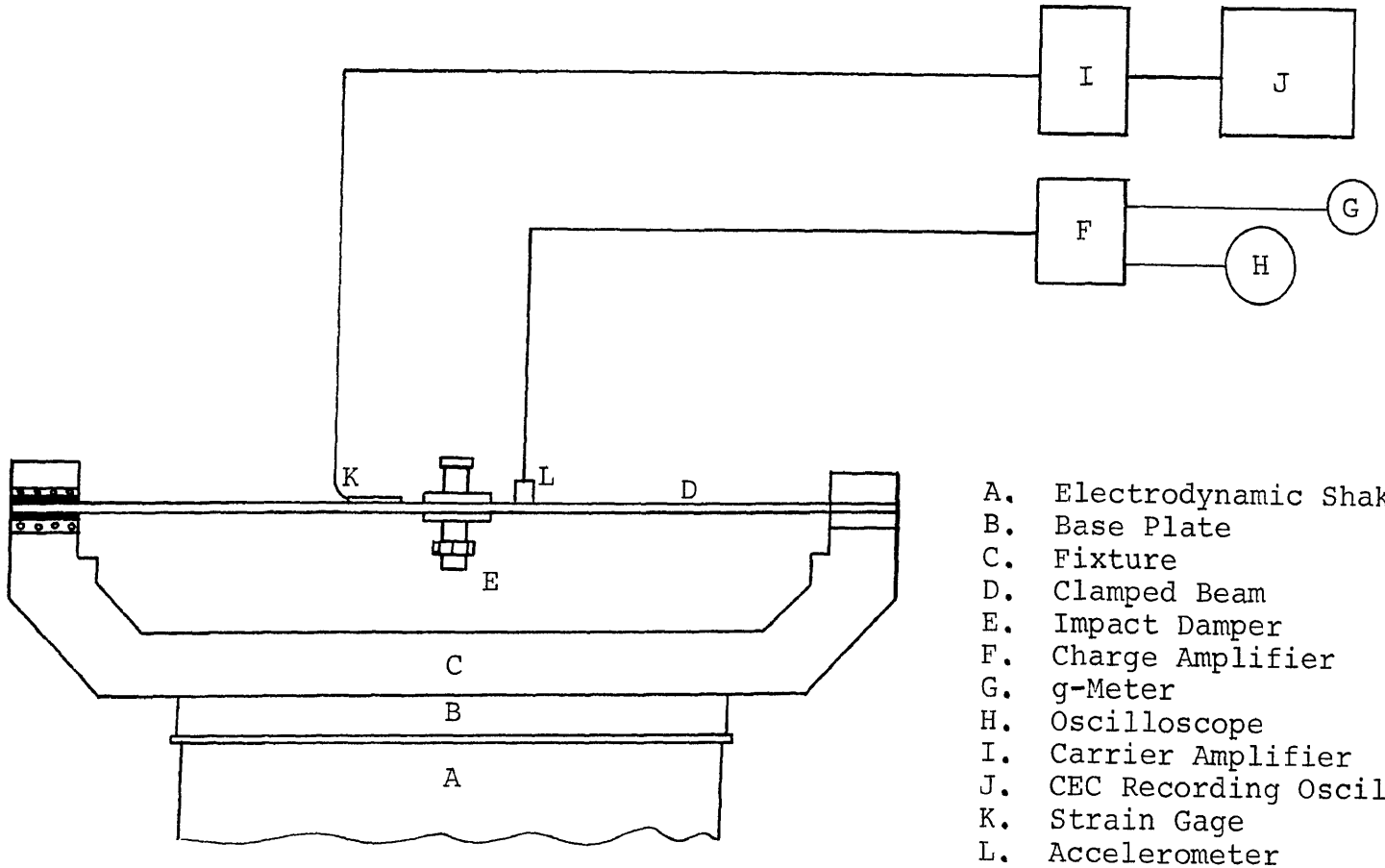


A. Electrodynamic Shaker
B. Base Plate
C. Fixture
D. Clamped Beam
E. Impact Damper
F. Charge Amplifier
G. g-Meter
H. Oscilloscope
I. Carrier Amplifier
J. CEC Recording Oscillograph
K. Strain Gage
L. Accelerometer

Figure 5.1 Mechanical model of the fixed beam

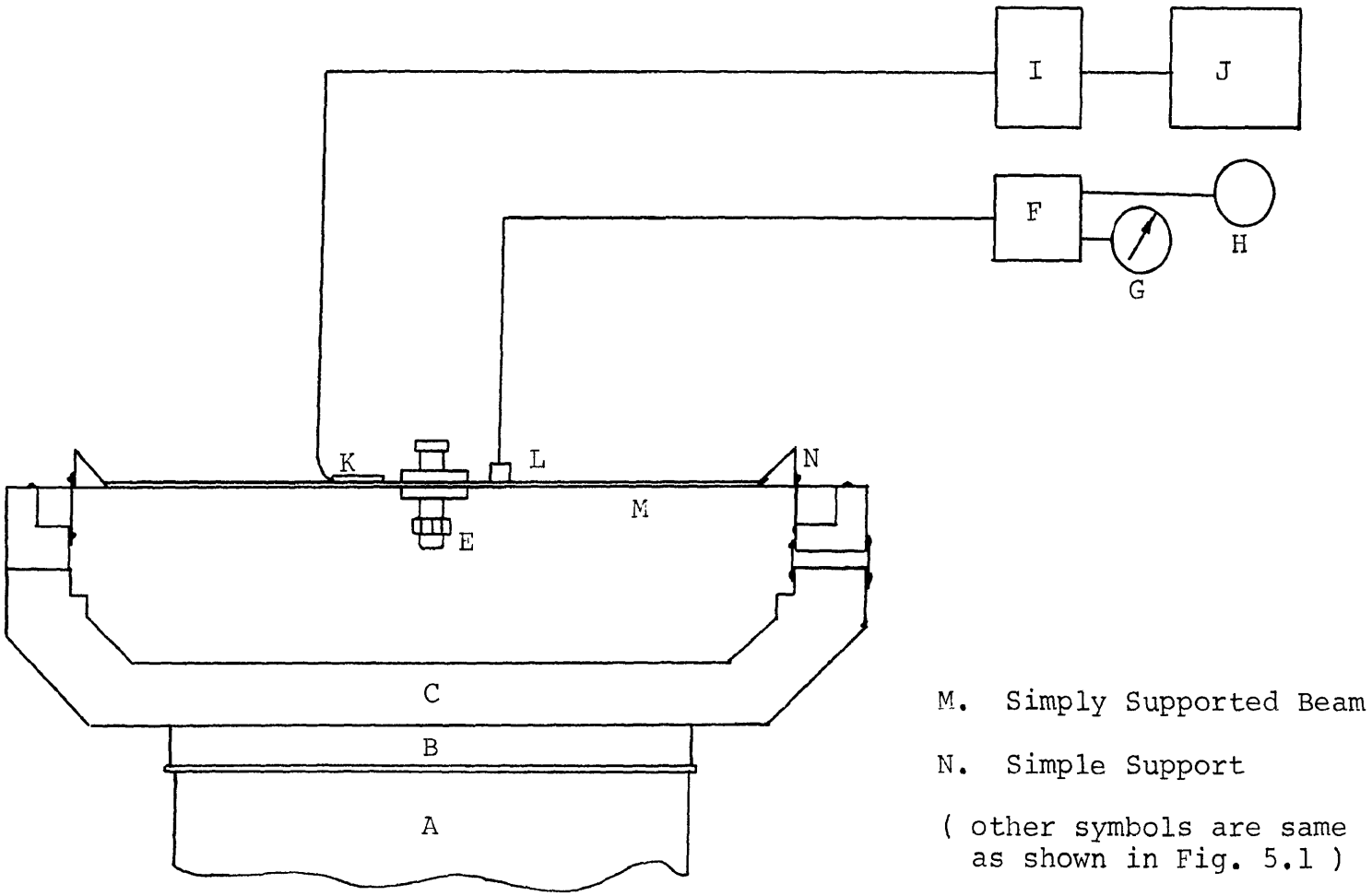


Figure 5.2 Mechanical model of the simply supported beam

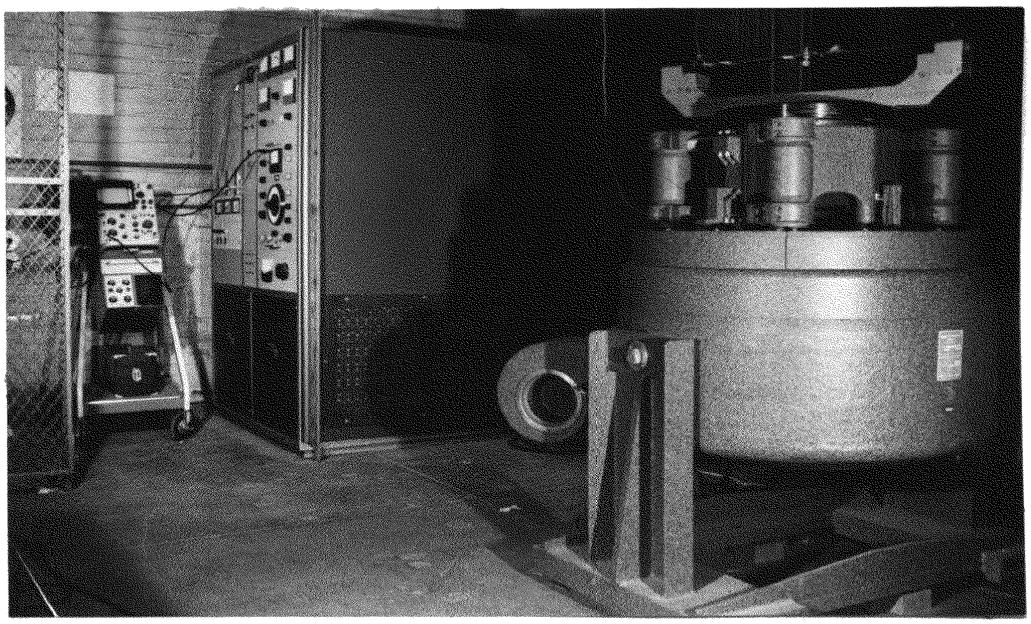

General View of the Vibration Excitation System

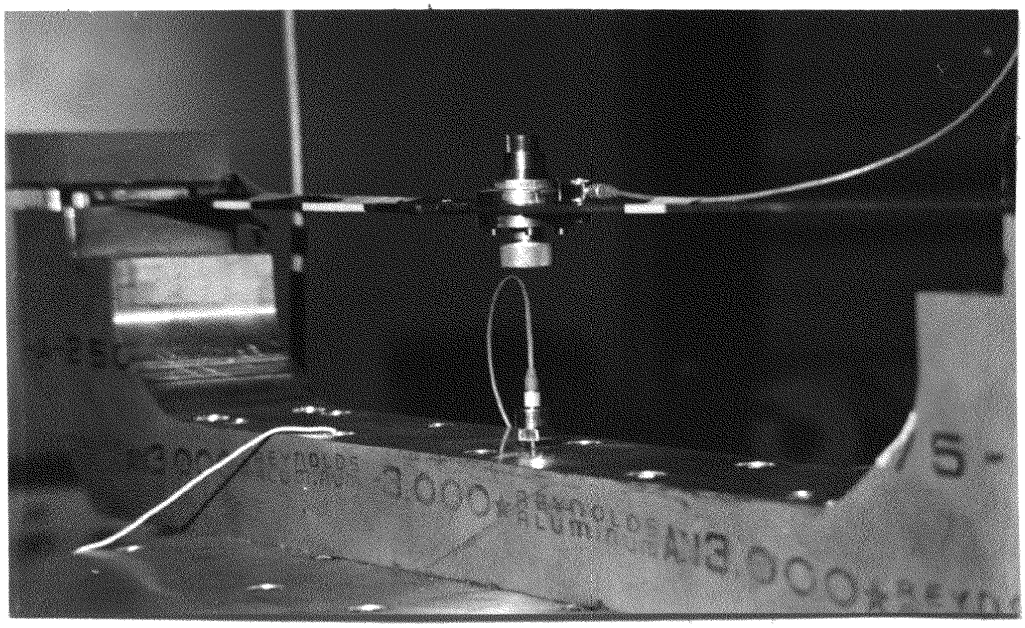

Impact Damper Mounted on a Clamped Beam

Figure 5.3 Photograph of the mechanical model and vibration exciter

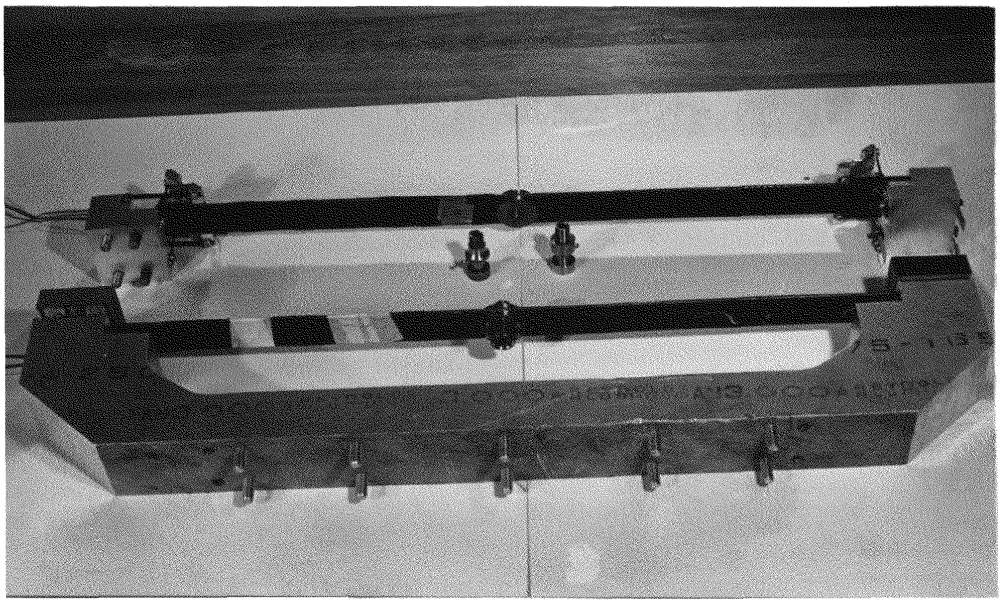

Test Fixture

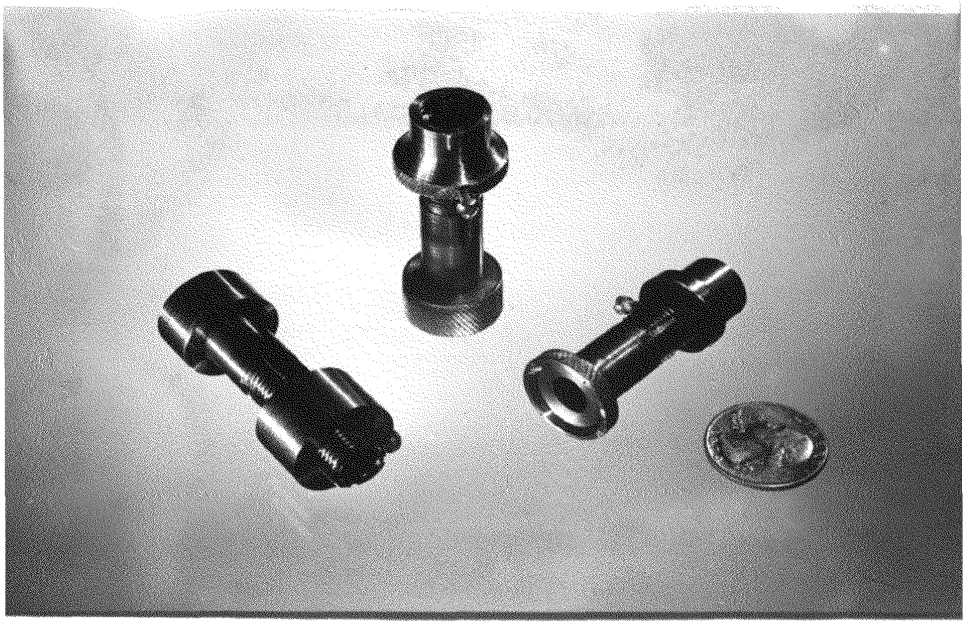

Damper Particles

Figure 5.4 Photograph of the test fixture and the damper particles used

tion and strains respectively at desired locations. Signals from these transducers were monitored on a Tektronix dual trace oscilloscope and recorded by means of a CEC recording oscillograph. A Beckman counter was used to time the periods of oscillations.

The impact damper in both models was located at the center of each beam. For the two cases of symmetrical end excitation the beams could be excited only in symmetrical modes (odd numbered modes).

The damper unit consisted of a pair of hard steel collars attached to the beam and an alloy steel,nut and bolt assembly. The bolt was fitted into a hole drilled through the beam and was constrained to oscillate within a certain magnitude of clearance. To vary the clearance distance, adjustments were made by turning a threaded lock nut.

Strain and acceleration of both types of beams were recorded at x=11.165" and x=14.36" respectively, along the length. Impacts between the particle and the beam produced a very complex oscilloscope trace of the accelerations making it impossible to use for comparative purposes. The sharpness of the strain trace,on the other hand, remained unaffected by the impacts and,since it was possible to measure accurately the strain amplitude, it was utilized for purposes of comparison.

During the course of this investigation the following

observations were made:

a. The damper was most effective when its operating axis was horizontal. In this position, 2 impacts/cycle motion was observed over a wider frequency range than in the vertical direction. At the higher acceleration levels (>8g), the effect of gravity was negligible and the damper showed the same effectiveness in both the vertical and horizontal directions of action. For the vertical operation the lightest possible particle gave the most stable motion over the widest range.

b. The effect of the damper weight on the system was studied by making the clearance, S=0. This, in most cases, resulted in slightly larger amplitude of vibration than that without the damper particle attached. Following this, the damper was activated by gradually increasing the clearance. The amplitude response was observed to reduce to a minimum for a particular clearance and increase from the low as the clearance was gradually increased.

For a given damper particle, the frequency range of the 2 impacts/cycle type of motion, discussed in reference (4), varied as the clearance varied. Other type of motions were irregular with arbitrary numbers of impacts per cycle. The 2 impacts/cycle motion was superior to the other types of motions, in the sense that it produced a steady response. The other types of motion, however, were also effective in reducing the amplitude of response in most cases.

c. A heavier damper particle was more effective in reducing response in the primary mode but produced transients of larger magnitude. The weight of the particle lowered the frequency of resonance of the system.

d. For a given base acceleration, the displacement amplitude at the third mode resonance is much smaller than that at the first. Therefore, the application of the damper in this mode required a more sophisticated design for clearance adjustment. The investigation at the third mode was carried out with only one value of the clearance.

e. The primary nature of the response was sinusoidal.

f. The damper unit used in the experimental investigation was relatively smaller than those used by other workers in the field, and as such, the level of the noise generated was a minimum. Illustrative of this, it may be stated that the noise of the damper impact was literally inaudible due to the noise of the operating accessories of the exciter.

The frequency response of the system is illustrated in Figs. 5.5 & 5.6 as plots of stress versus the frequency ratio through the third mode. The reduction in stress amplitude when dampers were applied was interpreted as the ratio of the stress amplitudes with the damper to that without it (for the same base excitation). The amount of isolation obtained near the first and third mode resonance with various damper particles is shown in Figs. 5.7 through 5.14. Assuming the actual system to behave as an equivalent single degree of freedom system, the first mode test

results were plotted in non-dimensional form and are shown in Figs. 5.15 & 5.16. These curves, along with those shown in Figs. 4.7 & 4.8, provide information which will allow application of impact dampers to similar systems.

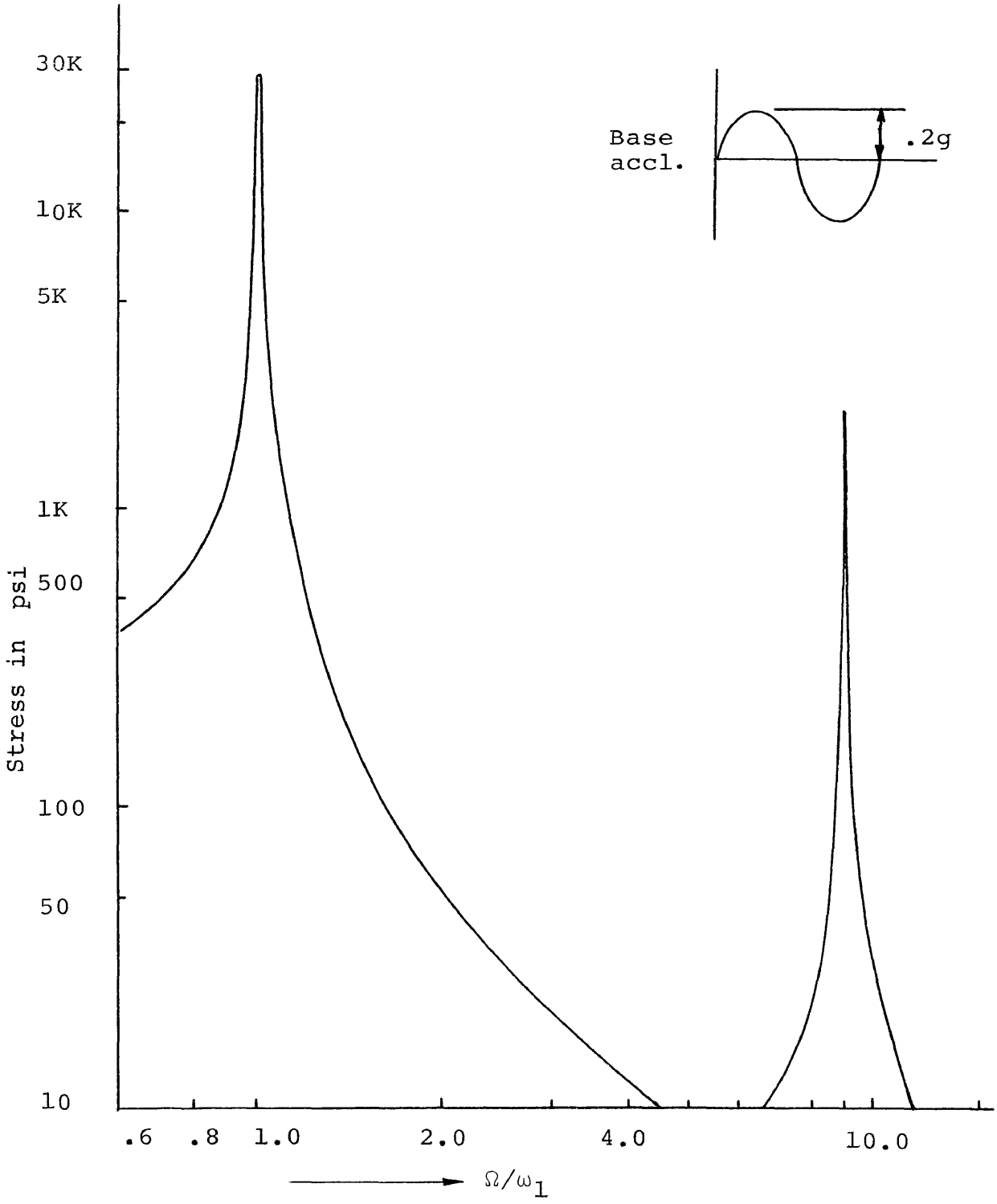


Figure 5.5 Experimentally determined frequency response of the simply supported beam

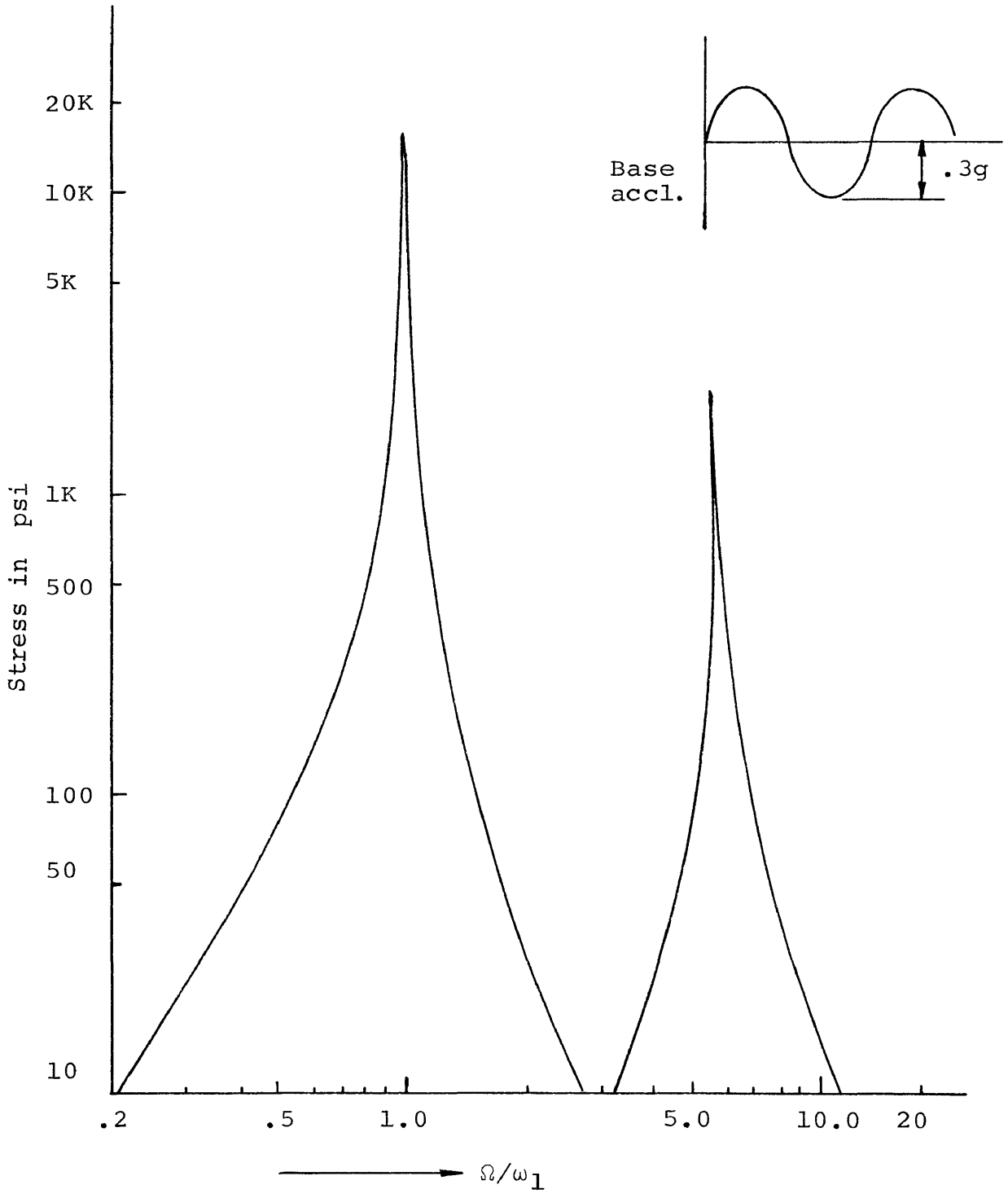


Figure 5.6 Experimentally determined frequency response of the fixed beam

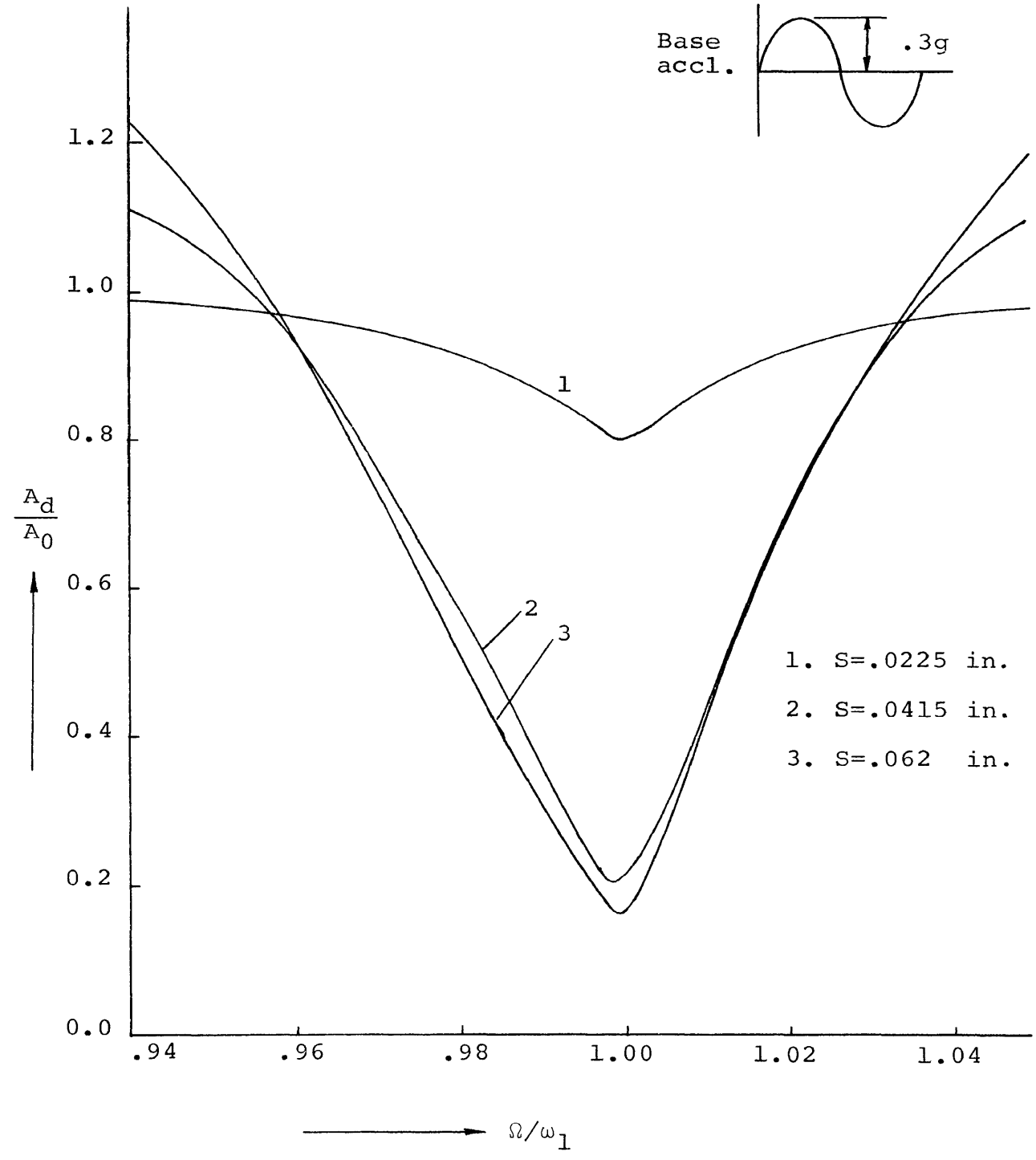


Figure 5.7 First mode isolation curves for the fixed beam (17 gm. damper)

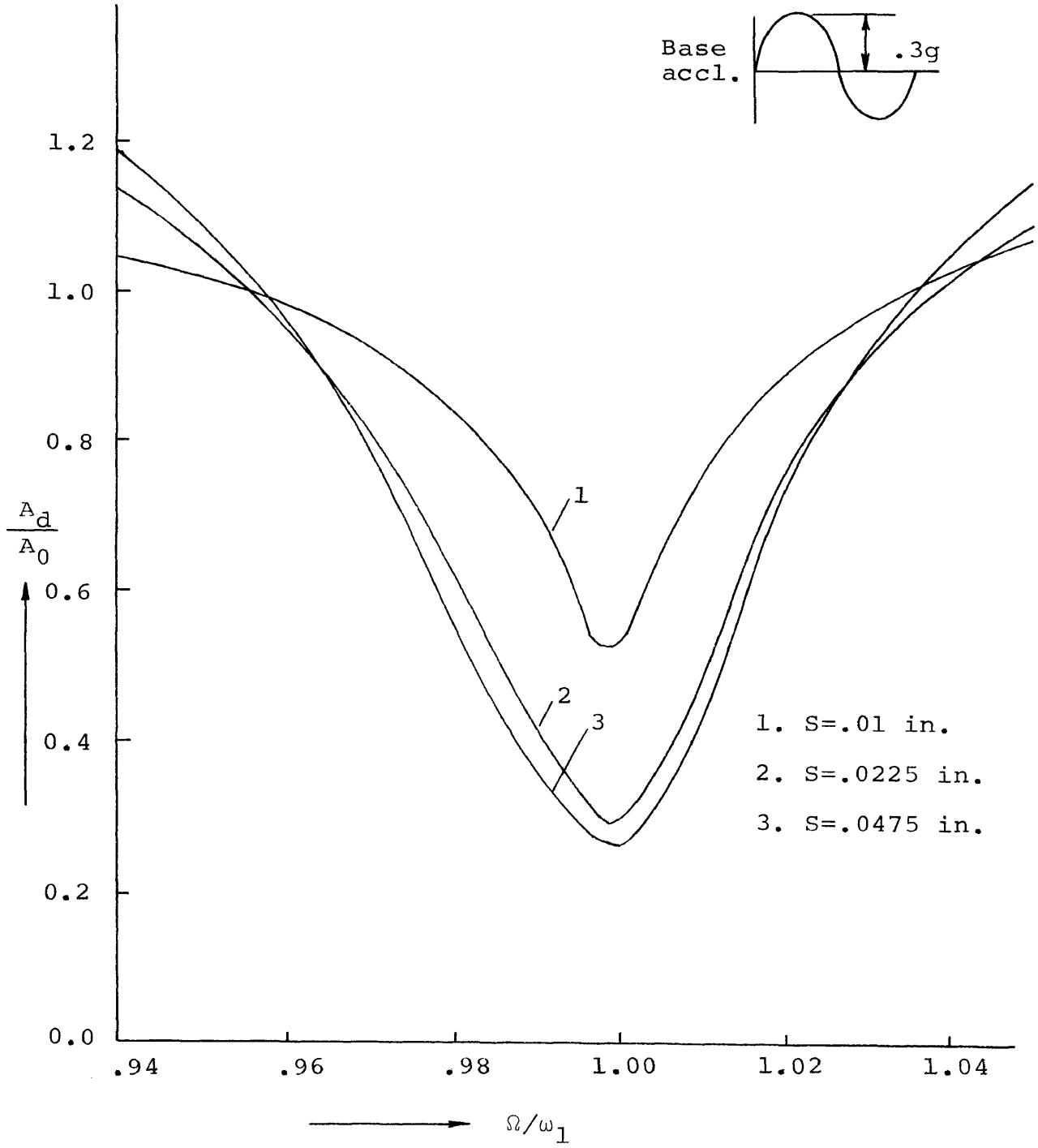


Figure 5.8 First mode isolation curves for the fixed beam (44 gm. damper)

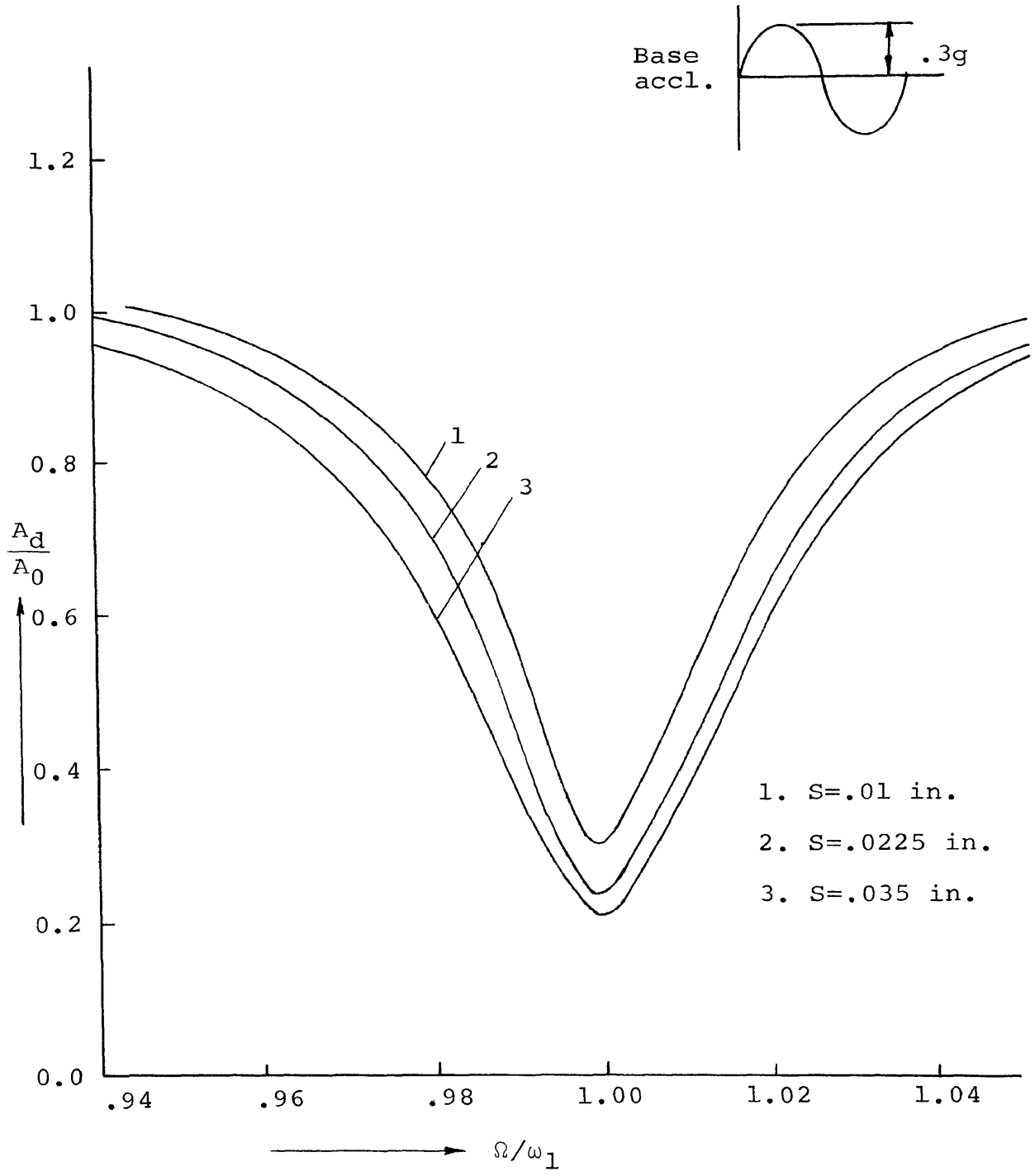


Figure 5.9 First mode isolation curves for the fixed beam (73 gm. damper)

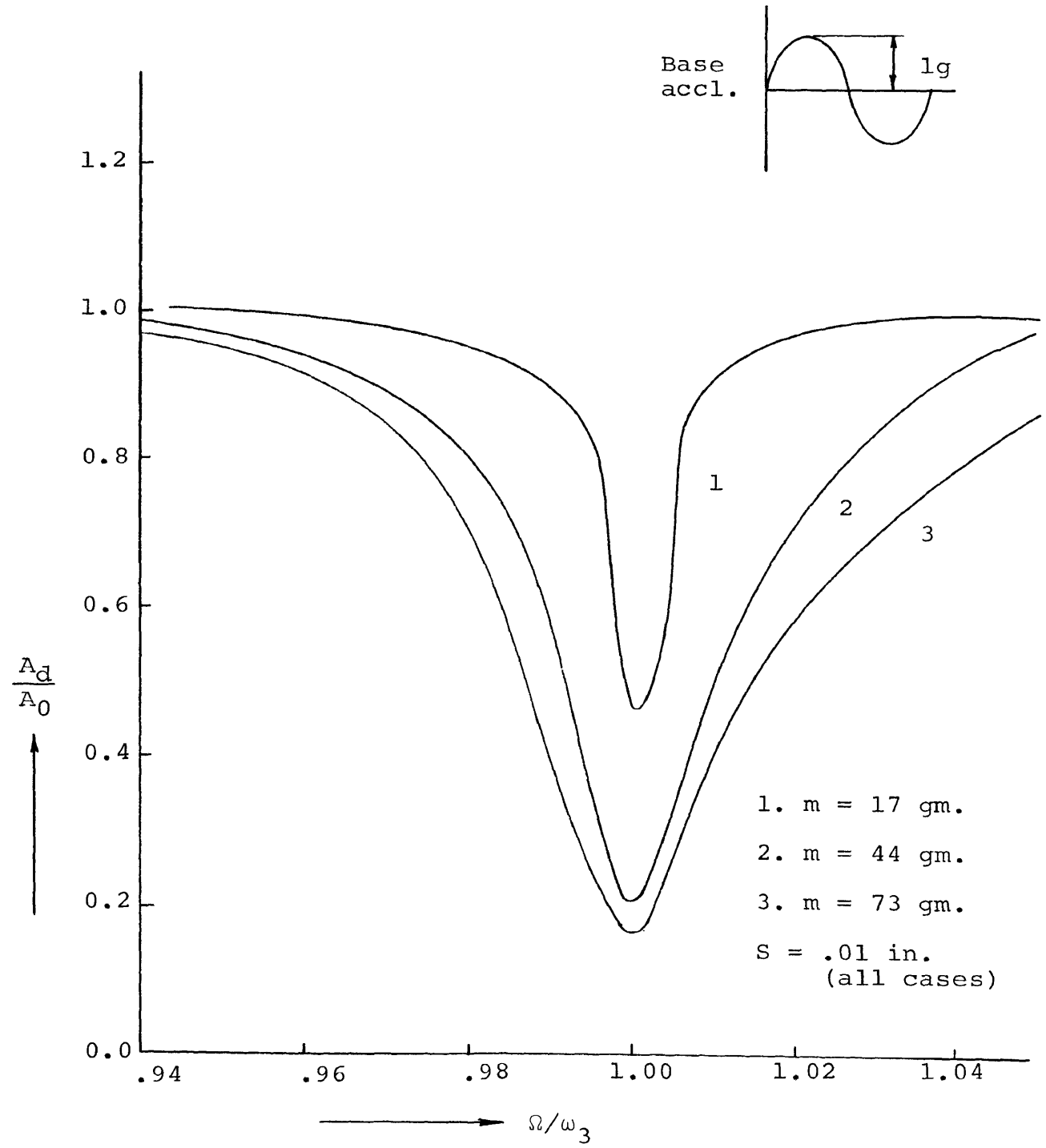


Figure 5.10 Third mode isolation curves for the fixed beam

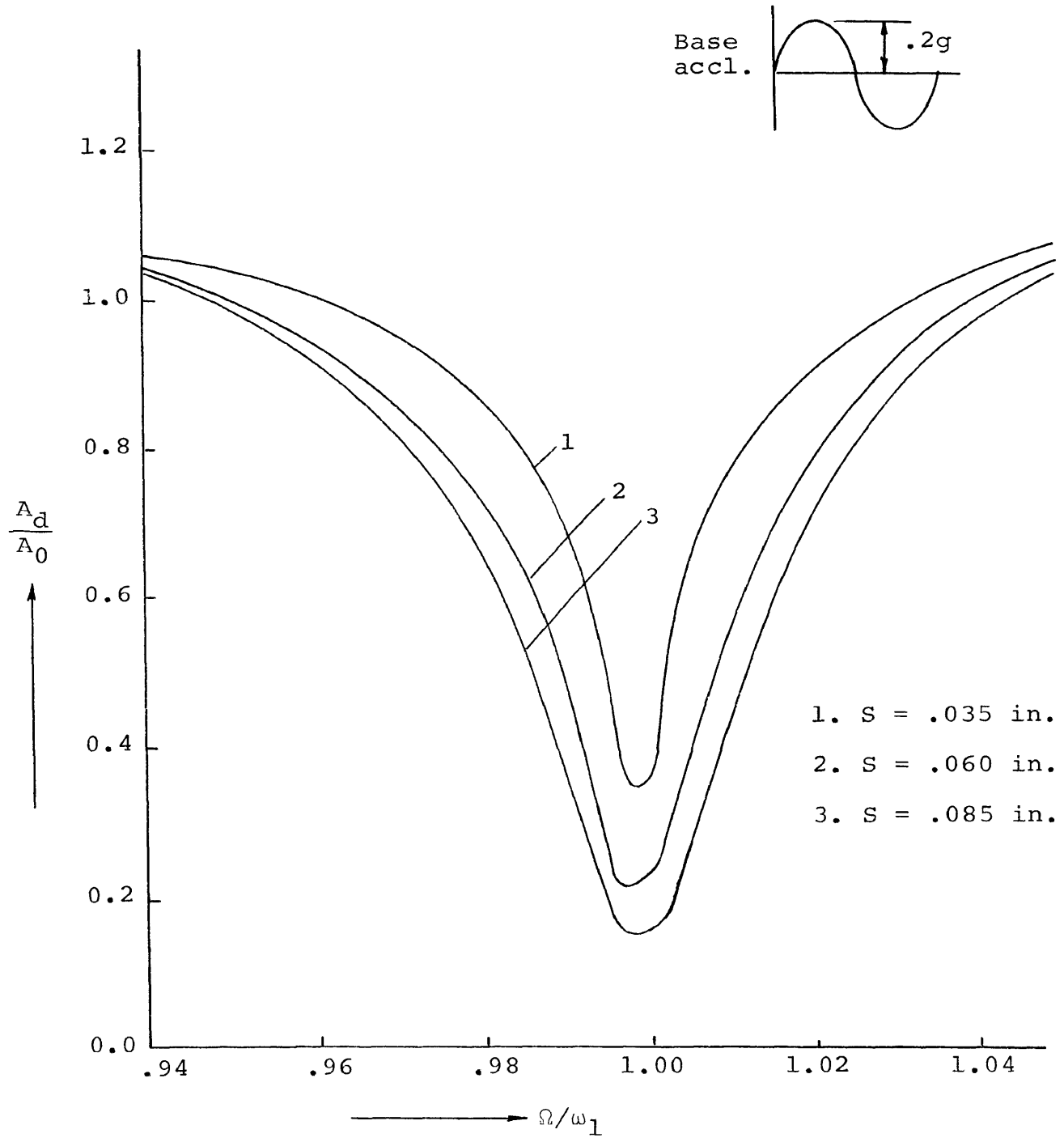


Figure 5.11 First mode isolation curves for the simply supported beam (17 gm. damper)

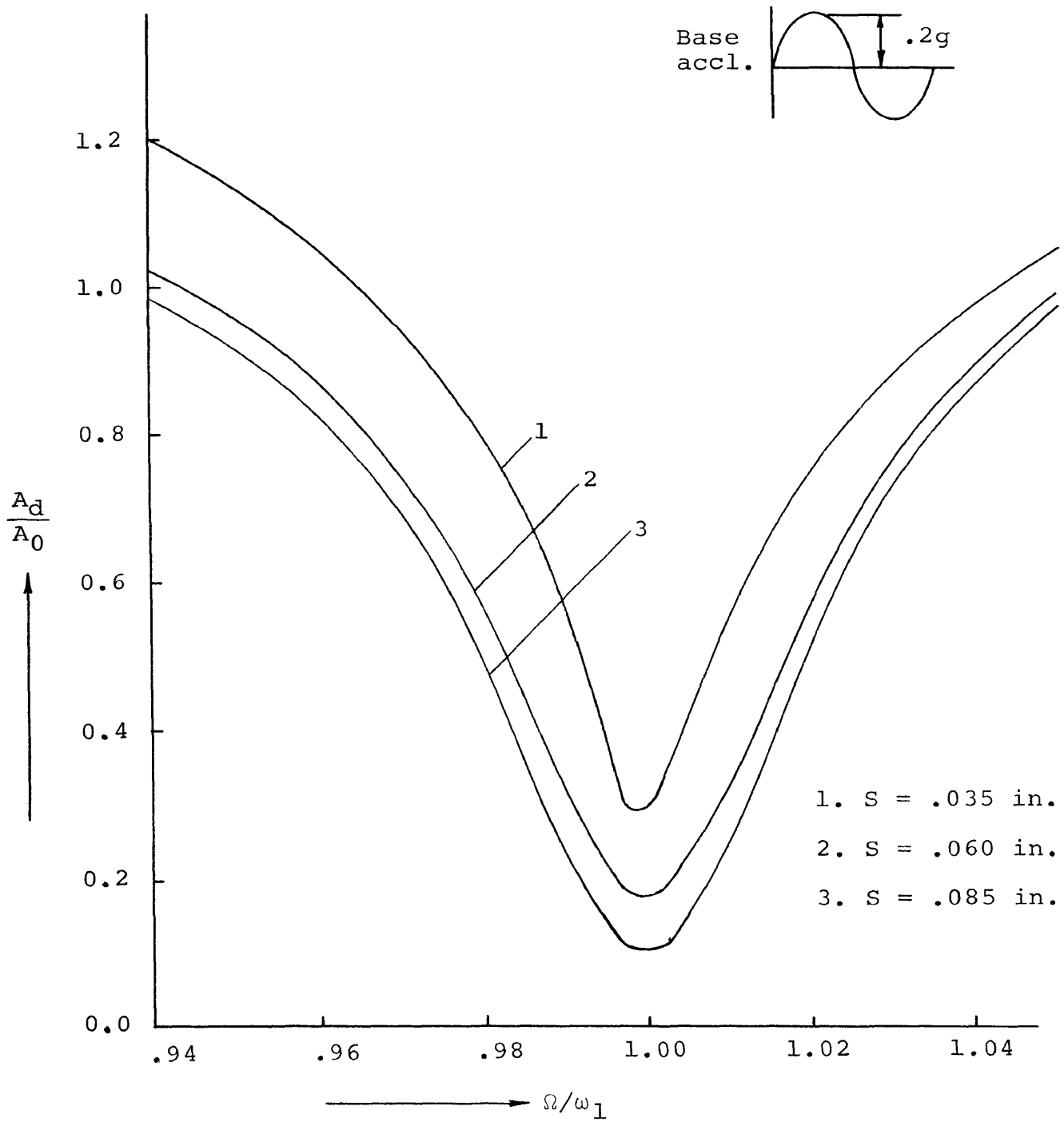


Figure 5.12 First mode isolation curves for the simply supported beam (44 gm. damper)

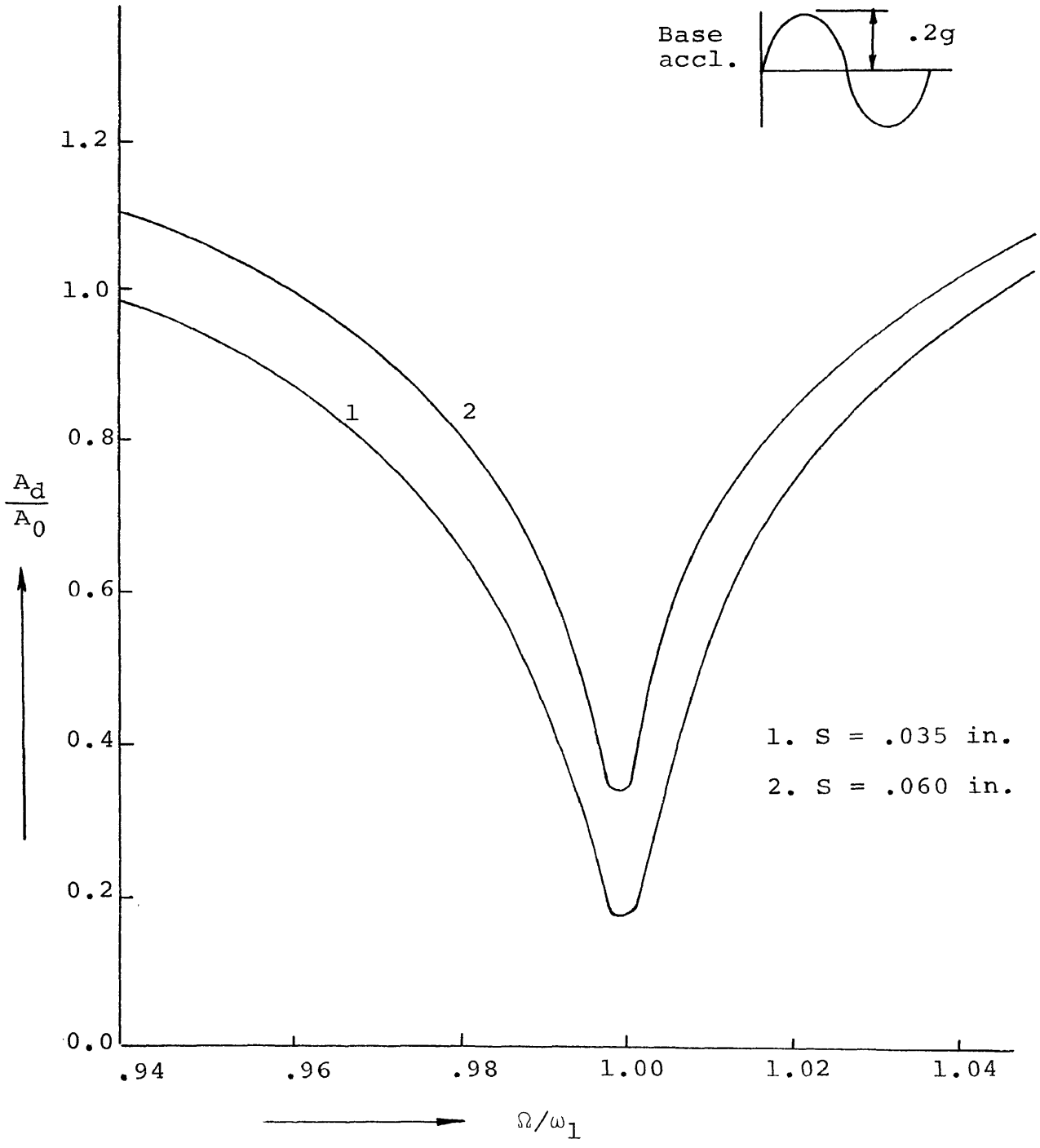


Figure 5.13 First mode isolation curves for the simply supported beam (73 gm. damper)

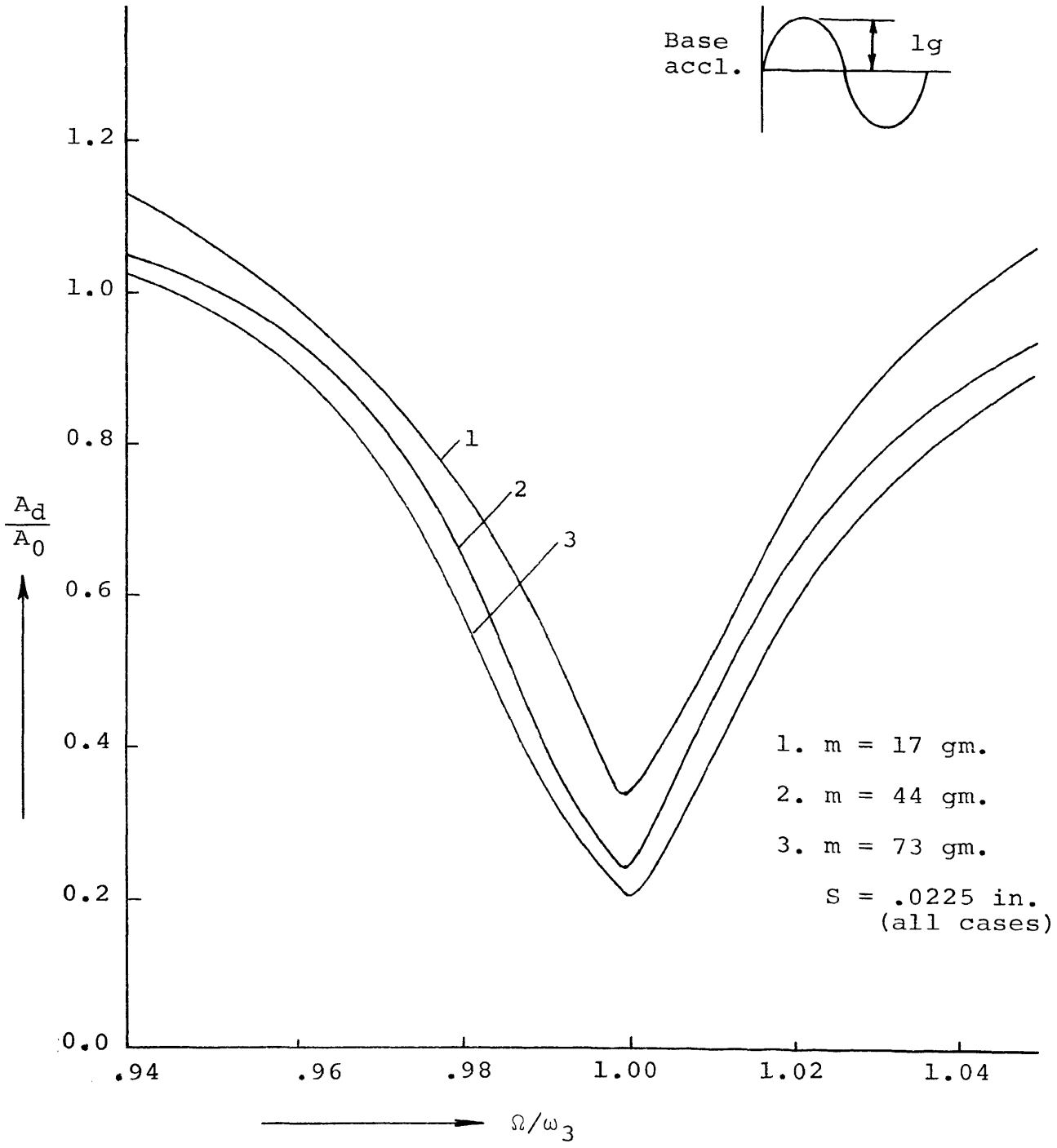


Figure 5.14 Third mode isolation curves for the simply supported beam

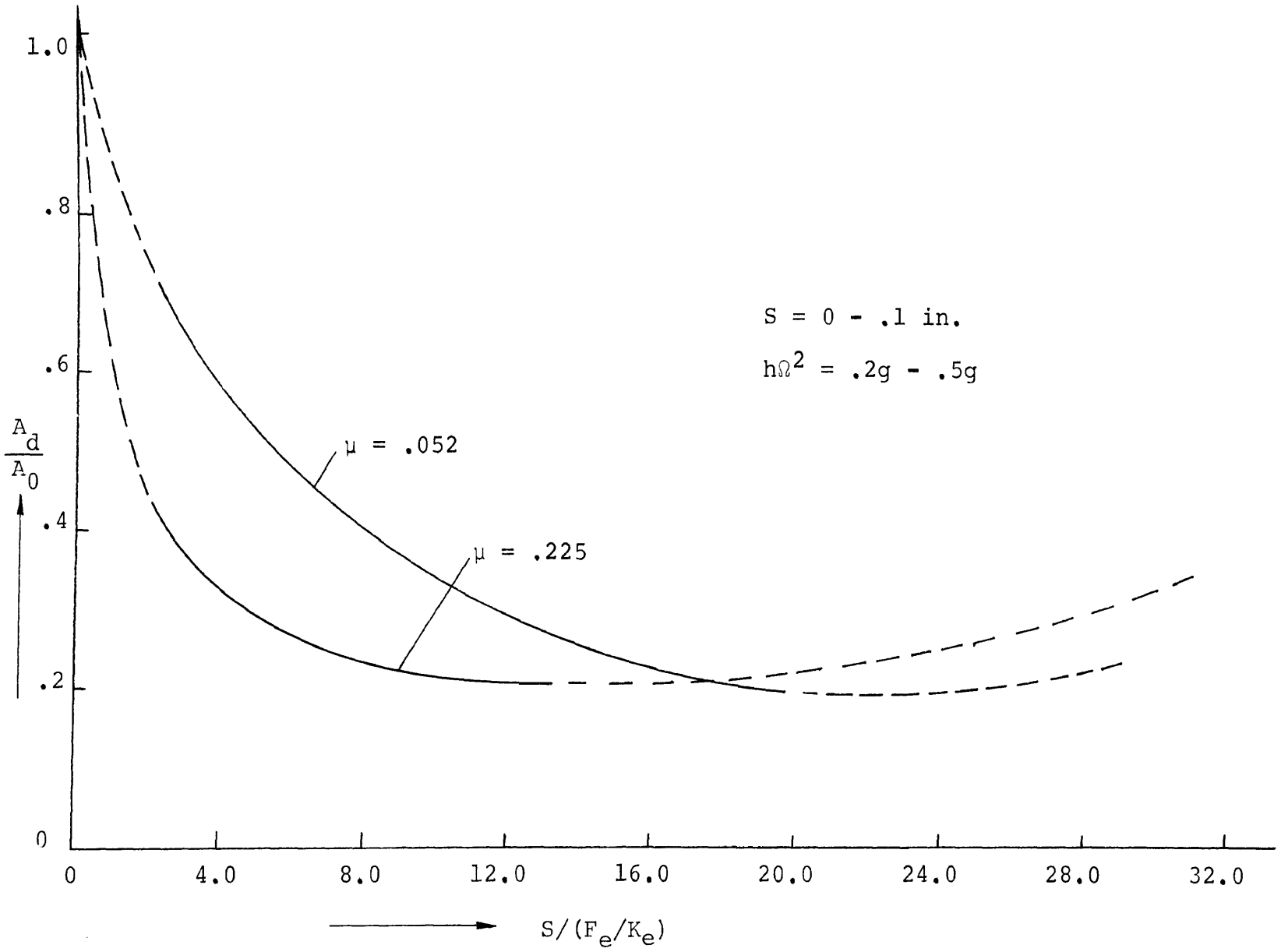


Figure 5.15 Solution curves for the fixed beam (17 gm. and 73 gm. damper)

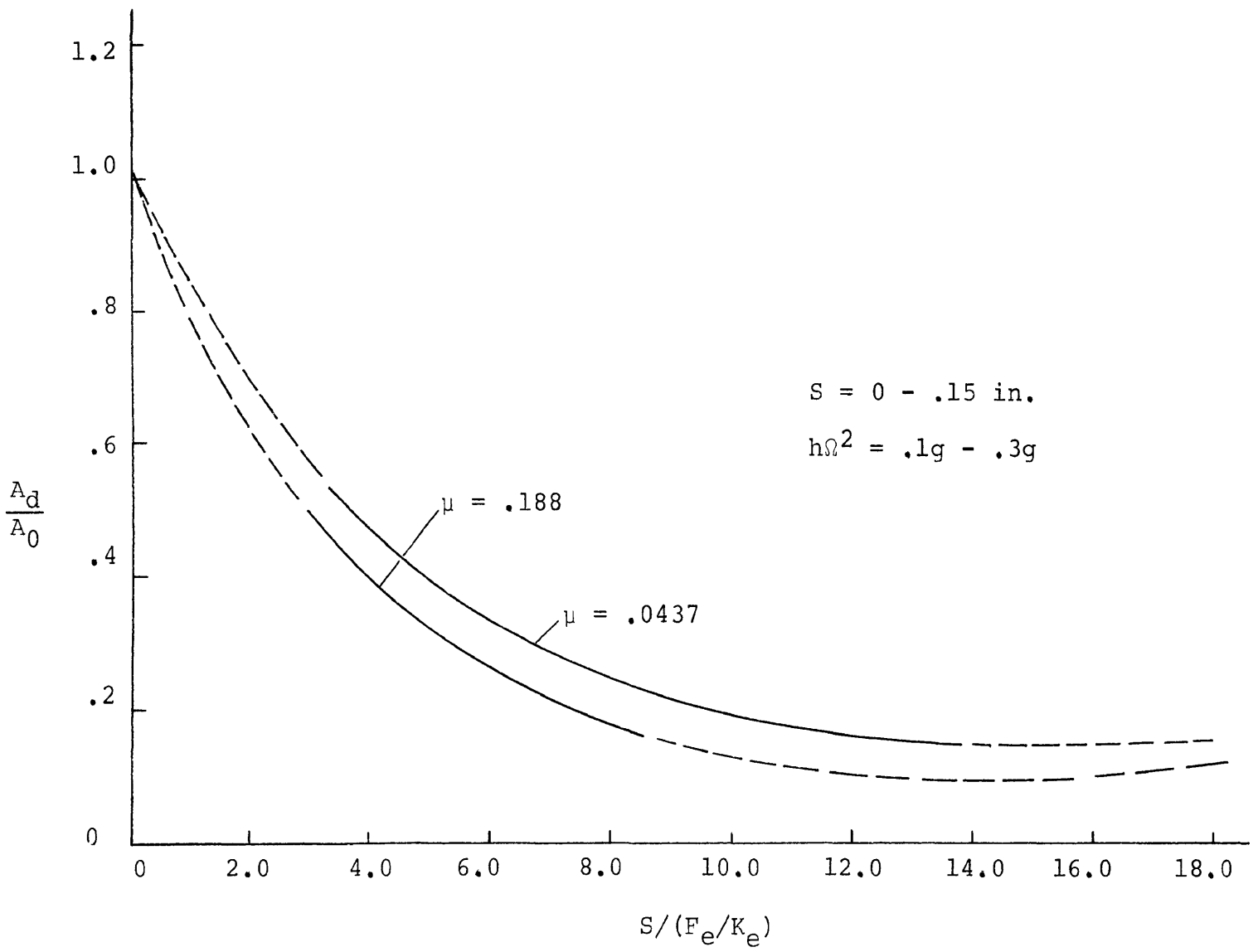


Figure 5.16 Solution curves for the simply supported beam ( 17 gm. and 73 gm. damper )

# VI. CONCLUSIONS AND FUTURE WORK

A seminumerical technique has been developed to describe the motion of sinusoidally excited, continuous systems with impact dampers attached. The solutions for an arbitrary number of impacts per cycle have been determined by two different approaches. In the first method, starting with the Bernoulli-Euler beam equation, the motion of the system is determined in terms of the sum of an infinite series. In the second approach, the system is described by a lumped parameter model and solutions have been obtained using the finite element method. For both procedures, the motion from collision to collision was determined analytically and the times of collisions were obtained with a computer.

The predictions of the theory were substantiated by an extensive experimental study with two types of uniform beams, and three different damper particles. The system response to the base excitation was observed near the first and the third resonant frequencies.

On the basis of the numerical calculations with the computer and the experimental investigation using the electrodynamic exciter, the following conclusions were drawn:

1. The impact damper was observed to be very effective near and at the resonant frequency of the system where

damage might be expected to occur. Steady response was obtained for 2 impacts/cycle motion only for certain system parameters. Other kinds of motions were often effective in reducing system response near resonance but would be difficult to analyze theoretically.

2. The collision of the damper particle with the beam often produced response in many resonant modes. For example, at the first natural frequency the collision often caused response oscillations in the third mode. This effect, of other mode participation, increased with heavier damper particles and was responsible for an increase of vibration amplitude at some frequencies, removed from resonance.

3. The performance of the impact damper was observed to be dependent on the magnitude of the base excitation, showing thereby the nonlinear character of the damper unit.

4. For motions of higher acceleration, i.e., at resonance, the impact damper was equally effective with either a vertical or a horizontal operating axis.

5. Heavier damper particles usually produced more isolation near resonance. For a damper of a given mass, a particular clearance produced the most effective reduction of vibration amplitude.

6. Results obtained by analytical solution showed better agreement with experimental results when greater values of clearance were used.

The investigations presented in this report do not

exhaust the scope of further research in this field. One general area of interest would be the determination of the effectiveness of impact dampers applied to more complicated systems, such as plates and shells by an extension of the finite element technique. Further, damper location on the structures to give optimum isolation could be investigated. A problem with equal bearing on the present study is the effect of multiple impact dampers on continuous systems.

These studies could also be expanded to include the contact resonance problem, such as the vibration of shafts within bearings with a given clearance. This latter problem area could include the vibration of beams with curved boundaries and with motion limiting stops at particular locations along the length direction.

# REFERENCES


1. Lieber, P. and Jensen, D.P., "An Acceleration Damper: Development, Design and some Applications", Trans. A.S.M.E. vol. 67(1945), pp. 523 - 530.

2. Grubin, C., "On the theory of the Acceleration Damper", Journal of Applied Mechanics, Trans. A.S.M.E., Sept. 1956, pp. 373 - 378.

3. Arnold, R.N., "Response of an Impact Vibration Absorber to Forced Vibration", Ninth International Congress of Applied Mechanics (1956).

4. Masri, S.F., and Caughey, T.K., "On the Stability of the Impact Damper", Journal of Applied Mechanics, Trans. A.S.M.E., Sept. 1966, pp. 586 - 592.

5. Masri, S.F., "Analytical and Experimental studies of Multi-unit Impact Dampers", The Journal of the Acoustical Socity of America, vol. 45, No. 5 (1969), pp. 1111 - 1117.

6. Masri, S.F., "Steady Response of a Multidegree system with an impact damper", Journal of Applied Mechanics, Paper No. 72 - APM - 39.

7. McGoldrick, R.T., "Experiments with an Impact Vibration Damper", David Taylor Model Basin Report No. 816.

8. Lieber, P. and Tripp, F., "Experimental Results on the Acceleration Damper", Rensselaer Polytechnic Institute Aeronautical Laboratory, Report No. TR AE 5401(1954).

9. Duckwald, C.S., "Impact Damping for Turbine Buckets", General Engineering Laboratory, General Electric, Report No. R 55GL108(1955).

10. Volterra, E. and Zachmanoglou, E.C., Dynamics of Vibrations, Charles E. Merrill Books, Inc. , Columbus, Ohio. (1965), pp. 310 - 377.

11. Thomson, W.T., Vibration Theory and Applications, Prentice-Hall, Inc., Englewood Cliffs, N.J., Sixth Edition (1965).

12. Timoshenko, S., Vibration Problems in Engineering, D.Van Nostrand Company, Inc., New York, Second Edition (1941), pp. 83 - 89.

13. Pestel, E.C., and Leckie, F.A., Matrix Methods in Elasto-Mechanics, McGraw-Hill Book Co., Inc., New York, N.Y.

14. Rocke, R.D., "Transmission Matrices and Lumped Parameter Models for Continuous Systems", Dynamics Laboratory Report, Calif. Institute of Technology (1966), pp. 82-98.

15. Rocke, R.D. and Roy, R., "Application of Approximate Transmission Matrices to Describe Transverse Beam Vibrations", The Shock and Vibration Bulletin, Bulletin 41, December 1970, pp. 133-145.

16. Archer, J.S., "Consistent Mass Matrix for Distributed Mass Systems", Journal of The Structural Division, A.S.C.E., vol. 89, No. ST4, Aug. 1963, pp. 161-178.

17. Meirovitch, Leonard, Analytical Methods in Vibrations, The Macmillan Company, New York, N.Y. (1967), pp. 287-291.

18. Snowdon, J.C., Vibration and Shock in Damped Mechanical Systems, John Wiley & Sons, Inc., New York, N.Y. (1968).

19. Chen, Y., Vibrations: Theoretical Methods, Addison-Wesley Publishing Company, Inc., Raeding, Mass. (1966).

20. Fox, L., An Introduction to Numerical Linear Algebra, Oxford University Press, New York, N.Y. (1965), pp. 175.

21. Warburton, G.B., Discussion of "On the theory of the Acceleration Damper, " Journal of Applied Mechanics, Trans. A.S.M.E., June. 1957. pp. 322 - 324.

22. Wen, R.D., "Dynamic Response of Beams with Lumped Parameters", Journal of Applied Mechanics, Trans. A.S. M.E., June 1965, pp. 453 - 454.

23. Conte, S.D., Elementary Numerical Analysis, McGraw-Hill Book Company, New York, N.Y. (1965), pp. 20 - 43.

# VITA

Ranjit Kumar Roy was born on January 1, 1947, in the District of Barisal, Bangladesh. He attended Model High School, Khulna, and matriculated in the year 1961. In 1962, he emigrated to India and completed the Pre-University Course in Science at the University of Calcutta in 1963. He received a Bachelor of Engineering Degree in Mechanical Engineering from Regional Engineering College, Durgapur, in 1968.

He has been enrolled in the Graduate School of the University of Missouri-Rolla since September 1968, and received a Master of Science Degree in Mechanical Engineering in January 1970. During the entire period of graduate study, he held a Teaching Assistantship in the Engineering Mechanics and Mechanical Engineering Departments and taught undergraduate mechanics courses.

He was married to Miss Krishna Majumder in April 1970, in Cleveland, Ohio. Mrs. Roy is a native of Calcutta, India.

# APPENDIX A

# CONTINUOUS SYSTEM SOLUTION

## A.1 THE DIFFERENTIAL EQUATION OF MOTION FOR THE BEAM

For the beam under consideration (see Fig. A.1) the following assumptions were made:

1. Shear deformation and rotatory inertia effects are negligible.
2. The beam is of homogeneous material and uniform in cross section (a, $\rho$, and E are constants).
3. The internal damping is proportional to strain rate and external damping proportional to velocity.

The stress in the material is a function of strain and strain rate as follows

$$\sigma = E\varepsilon + C_{int}\partial\varepsilon/\partial t \quad . \tag{A.1}$$

Strain in a fiber at a distance Y from the neutral surface is

$$\varepsilon = - Y/R \tag{A.2}$$

where R is the radius of curvature and is expressed as

$$1/R = \frac{\partial^2 W/\partial x^2}{\left[1 + (\partial W/\partial x)^2\right]^{3/2}} \cong \partial^2 W(x,t)/\partial x^2 \tag{A.3}$$

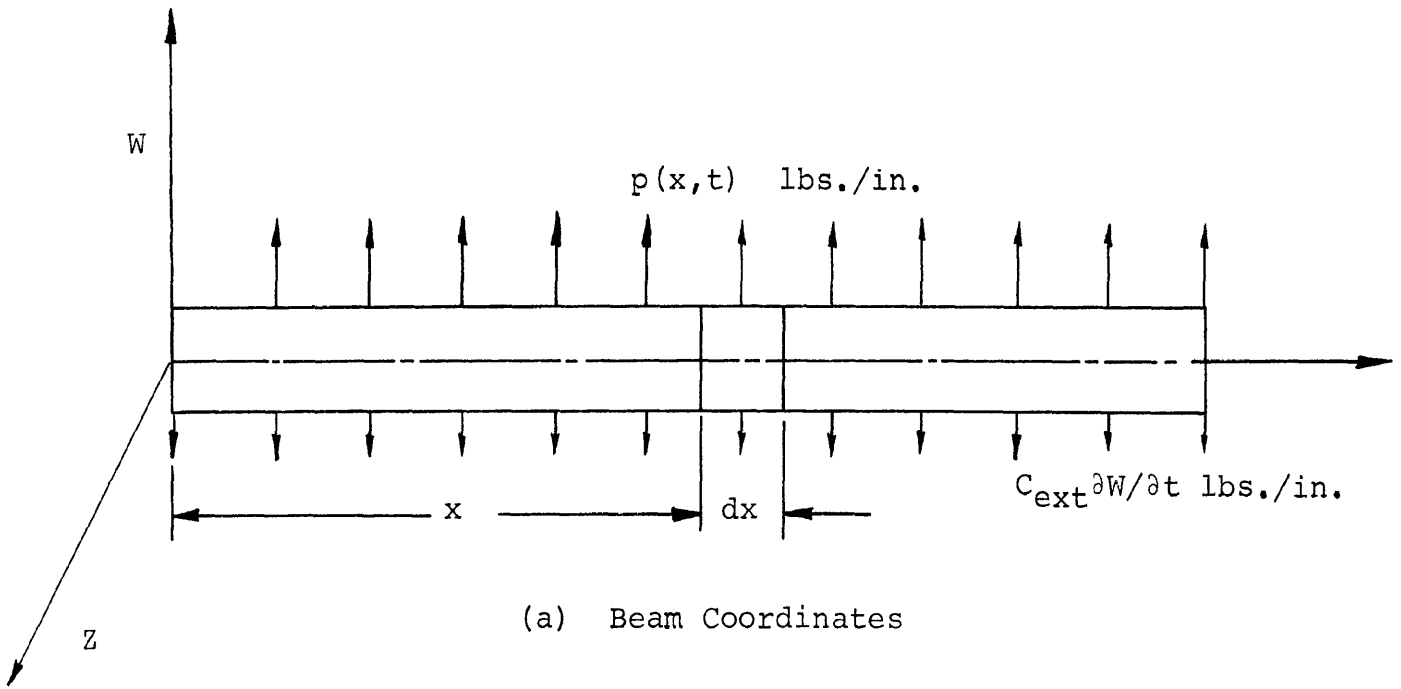


(a) Beam Coordinates

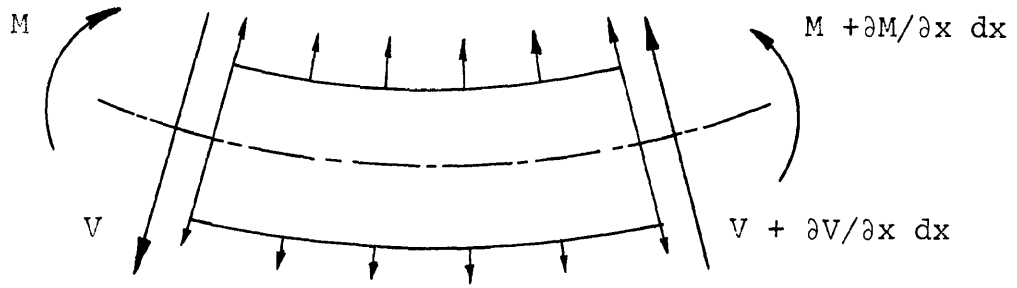


(b) Elastic Beam Increment

Figure A.1 Bernoulli-Euler beam discussed in the report

since $(\partial W/\partial x)^2 << 1$.

Upon substituting the latter relation into Eq. (A.2) there results

$$\varepsilon = - y(\partial^2 W/\partial x^2) \quad . \tag{A.4}$$

From basic mechanics of material the moment at a section is

$$M(x) = - \int_a y\sigma \, da \quad . \tag{A.5}$$

Substitution of Eq. (A.1) and Eq. (A.4) into Eq. (A.5) gives

$$M(x) = - EI \, \partial^2 W/\partial x^2 + IC_{int} \, \partial^3 W/(\partial x^2 \partial t) \tag{A.6}$$

where $I = \int_a y^2 da$ , the area moment of inertia.

Summing forces on the beam element of length dx, gives (see Fig. A.1)

$$- V + V + \partial V/\partial x \, dx - \rho a(\partial^2 W/\partial t^2)dx + p(x,t)\,dx$$

$$- C_{ext}(\partial W/\partial x)\, dx = 0$$

or

$$\partial V/\partial x = \rho a \, \partial^2 W/\partial t^2 - p(x,t) + C_{ext}\partial W/\partial t \quad . \tag{A.7}$$

Summing moments (about the Z-axis passing through the right end of the element) gives

$$- M - \partial M/\partial x\, dx + M - \rho a\, (\partial^2 W/\partial t^2)\, dx\, dx/2 - V\, dx$$

$$+ p(x,t)dx\, dx/2 - C_{ext}(\partial W/\partial t)\, dx\, dx/2 = 0 \qquad \text{(A.7a)}$$

and neglecting terms of order $O(dx)^2$ reduces the equation to

$$\partial M/\partial x = - V \quad .$$

On differentiating further this reduces to

$$\partial^2 M/\partial x^2 = - \partial V/\partial x \quad . \qquad \text{(A.8)}$$

Substituting Eq.(A.7) and Eq.(A.6) into Eq. (A.8) gives

$$\frac{\partial^2}{x^2}\left[ EI\ (\partial^2 W/\partial x^2) + IC_{int}(\partial^3 W/\partial x^2 \partial t)\right] + \rho a(\partial^2 W/\partial t^2)$$

$$+ C_{ext}\partial W/\partial t = p(x,t) \qquad \text{(A.9)}$$

which is the differential equation of motion for the beam.

## A.2 SOLUTION WITHOUT OR BETWEEN THE IMPACTS

Eq. (A.9) is the equation of motion for the beam which

under sinusoidal base excitation and in the absence of external forces reduces to

$$EI\ \partial^4 W_r/\partial x^4 + IC_{int}(\partial^5 W_r/\partial x^4 \partial t) + \rho a\ \partial^2 W_r/\partial t^2 + C_{ext}\partial W_r/\partial t = \rho a\ h\Omega^2\ Sin\Omega t \qquad (A.10)$$

where

$$W(x,t) = W_r(x,t) + h\ Sin\Omega t\ .$$

The displacement, $W_r(x,t)$, is measured relative to the base and the damping is assumed to be proportional to the relative velocity.

Using the technique of separating variables, a solution to Eq. (A.10) can be expressed in the form

$$W_r(x,t) = U(x)\ Q(t)\ .$$

Accordingly

$$\partial^4 W_r/\partial x^4 = U^{IV}\ Q$$

$$\partial^5 W_r/(\partial x^4 \partial t) = U^{IV}\ \dot{Q}$$

and

$$\partial^2 W_r/\partial t^2 = U\ \ddot{Q}$$

where $(^{I})$ denotes $\frac{d}{dx}$ and $(\dot{})$ denotes $\frac{d}{dt}$.

A homogeneous solution of Eq. (A.10) is obtained by equating the right hand side to zero so that

$$\frac{U^{IV}}{U}\left\{\frac{EI}{\rho a}\right\} = -\frac{\left[\ddot{Q} + C_{ext}\dot{Q}/(\rho a)\right]}{\left[Q + C_{int}\dot{Q}/E\right]} = \omega^2$$

or

$$U^{IV} - K^4 U = 0 \qquad \text{(A.11)}$$

and

$$\ddot{Q} + \left[C_{ext}/(\rho a) + \omega_n^2 C_{int}/E\right]\dot{Q} + \omega_n^2 Q = 0 \quad . \qquad \text{(A.12)}$$

In the above $\omega$ is a constant and

$$K^4 = \omega^2 \rho a/EI \quad . \qquad \text{(A.13)}$$

The general solution of Eq. (A.11) is

$$U(x) = C_1 \text{Cosh}(Kx) + C_2 \text{Cos}(Kx) + C_3 \text{Sinh}(Kx) + C_4 \text{Sin}(Kx) \qquad \text{(A.13a)}$$

where $C_1, C_2, .. C_4$ are arbitrary constants.

The use of the boundary conditions in the above equation allows evaluation of these constants $(C_1, C_2, ..C_4)$ as well as determination of the eigenvalues $(K_n)$.

The general solution of Eq. (A.12) is

$$Q(t) = e^{-\xi\omega t}\left(A\ \mathrm{Cos}(\omega_d t) + B\ \mathrm{Sin}(\omega_d t)\right) \qquad (A.14)$$

where

$$2\xi\omega = C_{ext}/\rho a + C_{int}\omega^2/E \qquad (A.15)$$

and

$$\omega_d = \omega\sqrt{1 - \xi^2} \quad . \qquad (A.16)$$

A.2.1 SIMPLY SUPPORTED BEAM

In this case displacements and bending moments are zero at both ends of the beam which lead to the following conditions

$$\left.\begin{array}{ll} W(0,t) = 0 & \partial^2 W_r(0,t)/\partial x^2 = 0 \\ W(L,t) = 0 & \partial^2 W_r(L,t)/\partial x^2 = 0 \end{array}\right\} \cdot (A.17)$$

These boundary conditions imply that

$$\left.\begin{array}{lll} \text{(a)} & U(0) = 0 & \text{(c)} \quad d^2U(0)/dx^2 = 0 \\ \text{(b)} & U(L) = 0 & \text{(d)} \quad d^2U(L)/dx^2 = 0 \end{array}\right\} (A.18) \ .$$

Imposing these relations on Eq. (A.13a) yields

$$C_1 = C_2 = 0$$

and

$$\left.\begin{aligned} C_3\ \mathrm{Sinh}(KL) + C_4\ \mathrm{Sin}(KL) &= 0 \\ C_3\ \mathrm{Sinh}(KL) - C_4\ \mathrm{Sin}(KL) &= 0 \end{aligned}\right\} \qquad (A.19)$$

.

The latter two equations are a system of homogeneous equations in two unknowns $C_3$ and $C_4$. In order that $C_3$ and $C_4$ may have nontrivial solutions, the determinant of the coefficients must be equal to zero, i.e.,

$$\mathrm{Sin}(KL)\ \mathrm{Sinh}(KL) = 0 \qquad (A.20)$$

which is the frequency equation.

Neglecting the solution, $K=0$, since $\mathrm{Sinh}(KL) \neq 0$ for $K\neq 0$ it follows that

$$\mathrm{Sin}(KL) = 0 \qquad (A.21)$$

or

$$KL = n\pi \qquad (n=1,2,3,.....\infty). \qquad (A.22)$$

In view of Eq. (A.13), the characteristic frequencies are

$$\omega_n = K_n^2 \sqrt{EI/\rho a} \quad . \tag{A.23}$$

Using Eq. (A.19), substitution can be made into Eq. (A.13a) to give

$$U(x) = C \, \mathrm{Sin}(n\pi x/L)$$

where C is another arbitrary constant.

Thus for each characteristic value $K_n$ there corresponds a characteristic function

$$U_n(x) = C_n \, \mathrm{Sin}(n\pi x/L) \tag{A.24}$$

or further, normalized displacements

$$W_n(x,t) = \mathrm{Sin}(n\pi x/L) \quad . \tag{A.25}$$

## A.2.2 FIXED BEAMS

For fixed ends, the slope and displacement must be zero, that is,

$$\left.\begin{array}{ll} W_r(0,t) = 0 & \partial W_r(0,t)/\partial x = 0 \\ W_r(L,t) = 0 & \partial W_r(L,t)/\partial x = 0 \end{array}\right\} \quad . \tag{A.26}$$

Following the procedure previously discussed, the characteristic frequencies are

$$\omega_n = K_n^2 \sqrt{EI/\rho a} \quad . \tag{A.27}$$

The characteristic functions are

$$U_n(x) = \text{Cosh}(K_n x) - \text{Cos}(K_n x) - \alpha_n \left[\text{Sinh}(K_n x) - \text{Sin}(K_n x)\right] \tag{A.28}$$

where

$$\alpha_n = \frac{\text{Cos}K_nL - \text{Cosh}K_nL}{\text{Sin}K_nL - \text{Sinh}K_nL} \quad , \tag{A.29}$$

$K_n (n=1,2,3,....)$ are the roots of

$$\text{Cos}(KL)\ \text{Cosh}(KL) = 1 \tag{A.30}$$

and the normalized displacements are

$$W_n(x,t) = U_n(x)\ Q_n(t) \quad .$$

## A.2.3 RESPONSE TO HARMONIC BASE EXCITATION

The general solution of the equation of motion, Eq. (A.10), with the forcing function is the sum of all the characteristic vibrations

$$W_r(x,t) = \sum_{n=1}^{\infty} U_n(x)\ Q_n(t) \qquad (A.31)$$

where $U_n(x)$ are the functions given by Eq. (A.24) or Eq. (A.28).

Substitution of Eq. (A.31) into Eq. (A.10) gives

$$\frac{\omega_n^2}{K_n^4} \sum_{n=1}^{\infty} U_n^{IV}(x)\ Q_n(t) + \frac{C_{ext}}{\rho a} \sum_{n=1}^{\infty} U_n(x)\ \dot{Q}_n(t)$$

$$+ \frac{IC_{int}}{\rho a} \sum_{n=1}^{\infty} U_n^{IV}(x)\dot{Q}_n(t) + \sum_{n=1}^{\infty} U_n(x)Q_n(t) = h\Omega^2 \mathrm{Sin}\Omega t \ . \qquad (A.32)$$

The orthogonality relations for these two types of boundary conditions are

$$\int_0^L U_n(x)U_m(x)\ dx = 0 \quad \text{for} \quad n \neq m \qquad (A.33)$$

$$L' = \int_0^L U_n^2(x)\ dx = L/2 \quad \text{for simply supported ends}$$

$$= L \quad \text{for fixed ends} \ .$$

Multiplying both sides of Eq. (A.32) by $U_m(x)\ dx$, integrating from zero to $L$ and using the orthogonality relations, the latter equation reduces to

$$\ddot{Q}_n(t) + 2\xi_n\omega_n\dot{Q}_n(t) + \omega_n^2\ Q_n(t) = \frac{1}{L} h\Omega^2 H_n \mathrm{Sin}\Omega t \qquad (A.34)$$

where

$$H_n = \int_0^L U_n(x)\ dx \ . \qquad (A.35)$$

By integration, the constants, $H_n$, for the simply supported case become

$$H_n = \begin{cases} 2/K_n & \text{for } n=1,3,5,.... \\ 0 & \text{for } n=2,4,6,.... \end{cases} \qquad (A.36)$$

and for the fixed beam is

$$H_n = \frac{2}{K_n}\left\{\alpha_n - \frac{\text{Sinh}(K_nL) \quad \text{Sin}(K_nL)}{\text{Sinh}(K_nL) - \text{Sin}(K_nL)}\right\} \qquad n=1,2,3,... \; n \; . \qquad (A.37)$$

Eq. (A.33) can be compared with the equation of motion of a single degree of freedom system and its particular solution can be expressed as

$$Q_n(t)_P = \frac{H_n}{L'} h\Omega^2 \frac{\text{Sin}(\Omega t - \Psi_n)}{\sqrt{(\omega_n^2 - \Omega^2)^2 + (2\xi_n\omega_n\Omega)^2}} \qquad (A.38)$$

where

$$\Psi_n = \tan^{-1} \frac{2\xi_n\omega_n\Omega}{\omega_n^2 - \Omega^2} \; . \qquad (A.39)$$

The homogeneous solution of Eq. (A.3) is of the same form as Eq. (A.14), i.e.,

$$Q_n(t)_H = e^{-\xi_n\omega_n t}\left(A_n\text{Cos}(\omega_{dn}t) + B_n\text{Sin}(\omega_{dn}t)\right) \; . \qquad (A.40)$$

The total solution of Eq. (A.34) is

$$Q_n(t) = Q_n(t)_H + Q_n(t)_P \tag{A.41}$$

which can be incorporated into Eq. (A.31). The relative displacement then becomes

$$W_r(x,t) = \sum_{n=1}^{\infty} \left[ e^{-\beta_n t} \left( A_n \cos(\omega_{dn} t) + B_n \sin(\omega_{dn} t) \right) + F_n \sin(\Omega t - \Psi_n) \right] U_n(x) \tag{A.42}$$

where

$$\left.\begin{aligned} \omega_{dn} &= \omega_n \sqrt{1 - \xi_n^2} \\ B_n &= \xi_n \omega_n \end{aligned}\right\} \tag{A.43}$$

and

$$F_n = \frac{H_n h \Omega^2}{L' \sqrt{(\omega_n^2 - \Omega^2)^2 + (2\xi_n \omega_n \Omega)^2}} \; .$$

The first two terms on the right hand side of Eq. (A.42) represent free vibrations of the system while the third represents forced response.

The coefficients $A_n$ and $B_n$ are constants and depend on the initial conditions

$$\left.\begin{aligned} W_r(x,0) &= W_0(x) \\ \dot{W}_r(x,0) &= V_0(x) \end{aligned}\right\} \quad \text{for} \quad 0 \leq X \leq L \tag{A.44}$$

For zero initial conditions these becomes

$$W_r(x,0) = \sum_{n=1}^{\infty} U_n(x) \left[ (A_n + 0)e^{0} + F_n \, \mathrm{Sin}(-\Psi_n) \right] = 0 \tag{A.45a}$$

and

$$\dot{W}_r(x,0) = \sum_{n=1}^{\infty} U_n(x) \left[ B_n\omega_{dn} - A_n\beta_n + \Omega F_n \, \mathrm{Cos}\Psi_n \right] = 0 \, . \tag{A.45b}$$

When these equations are multiplied by $U_m(x)\,dx$ and integrated from 0 to L there results

$$A_n = F_n \, \mathrm{Sin}\Psi_n \tag{A.46}$$

$$B_n = -\frac{1}{\omega_{dn}} \left(\beta_n A_n - F_n \Omega \, \mathrm{Cos}\Psi_n\right) \quad . \tag{A.47}$$

Finally the general solution for the motion of both beam systems can be expressed as

$$W(x,t) = \sum_{n=1}^{\infty} \Big[ e^{-\beta_n t} \left( A_n \mathrm{Cos}(\omega_{dn} t) + B_n \mathrm{Sin}(\omega_{dn} t) \right) + F_n \mathrm{Sin}(\Omega t - \Psi_n) \Big] U_n(x) + h\mathrm{Sin}\Omega t \quad . \tag{A.48}$$

## A.3 SOLUTION FOR AN ARBITRARY IMPACT

Assumptions:

1. Impact between the particle and the beam is elastic.
2. The duration of impact is negligible compared to the time of travel of the particle.
3. The beam as well as the particle do not change position during impacts.
4. Momentum is conserved between the particle and the beam.
5. The velocity of the particle between impacts remains constant.

Let

$t_1$ = the time when the first impact occurs.

$v_-$ = velocity of the particle before the impact.

$v_+$ = velocity of the particle after the impact .

The solution for the displacement of any point on the beam at a distance $x$ and time $t$ is given by Eq. (A.48) until impact occurs. The solution after the impact may be expressed as follows

$$W(x,t) = \sum_{n=1}^{\infty} \Big[ e^{-\beta_n t} \{ A_{n+} \operatorname{Cos}(\omega_{dn} t) + B_{n+} \operatorname{Sin}(\omega_{dn} t) \} + F_n \operatorname{Sin}(\Omega(t+t_1) - \Psi_n) \Big] U_n(x) + h \operatorname{Sin}(\Omega(t+t_1)) . \tag{A.49}$$

Just after the impact Eq. (A.49) with $t=0$ describes the beam displacement while $t=t_1$ in Eq. (A.48) describes the displacement just before impact. With the assumption

$$W_+(x,0) = W_-(x,t_1) \quad ,$$

from Eq. (A.49) and Eq. (A.48) there results

$$\sum_{n=1}^{\infty}\left[A_{n+} + F_n \, \mathrm{Sin}(\Omega t_1 - \Psi_n)\right] U_n(x) + h \, \mathrm{Sin}\Omega t_1 =$$

$$\sum_{n=1}^{\infty}\left[e^{-\beta_n t_1}\{A_n \mathrm{Cos}(\omega_{dn} t_1) + B_n \mathrm{Sin}(\omega_{dn} t_1)\} + F_n \mathrm{Sin}(\Omega t_1 - \Psi_n)\right] U_n(x)$$

$$+ h \, \mathrm{Sin}\Omega t_1 \quad .$$

Use of the orthogonality condition reduces the latter equation to

$$A_{n+} = e^{-\beta_n t_1}\{A_n \, \mathrm{Cos}(\omega_{dn} t_1) + B_n \, \mathrm{Sin}(\omega_{dn} t_1)\}. \qquad (A.51)$$

Assuming the beam has an impact over the entire length with an impacting particle of mass m and velocity v, an incremental beam length must satisfy

$$\rho a \, \dot{W}_+(x,0) \, dx + v_+ m \, dx = \rho a \, \dot{W}_-(x,t_1) \, dx + v_- m \, dx$$

during the impact.

Integrating over the entire length of the beam gives

$$\int_0^L \rho a \, \{\dot{W}_+(x,0) - \dot{W}_-(x,t_1)\} \, dx = \int_0^L (v_- - v_+) m \, dx \quad . \qquad (A.52)$$

If the impact is restricted to occur only at a particular point, $x_d$, Eq. (A.52) can be modified to include point impact as

$$\int_0^L \rho a\{\dot{W}_+(x,0) - \dot{W}_-(x,t_1)\}\, dx = \int_0^L (v_- - v_+)m\delta(x - x_d)\, dx \quad . \tag{A.53}$$

Substituting for $\dot{W}_+$ and $\dot{W}_-$ and multiplying both sides of Eq. (A.53) by $U_m(x)$ gives

$$\begin{aligned}
&\rho a \int_0^L U_m(x)\Big[\sum_{n=1}^{\infty} U_n(x)\{B_{n+}\omega_{dn} - \beta_n A_{n+} + \Omega F_n \cos(\Omega t_1 - \Psi_n)\} \\
&+ h\Omega\cos\Omega t_1 - \sum_{n=1}^{\infty} U_n(x)\{e^{-\beta_n t_1}\omega_{dn}(-A_n \sin\omega_{dn} t_1 \\
&+ B_n \cos\omega_{dn} t_1) + (-\beta_n)e^{-\beta_n t_1}(A_n \cos\omega_{dn} t_1 + B_n \sin\omega_{dn} t_1) \\
&+ \Omega F_n \cos(\Omega t_1 - \Psi_n)\} - h\Omega \cos\Omega t_1\Big]\, dx \\
&= \int_0^L U_m(x)(v_- - v_+)m\,\delta(x - x_d)\, dx \quad .
\end{aligned} \tag{A.54}$$

Using orthogonality conditions and the relation

$$\int_0^L U_m(x)\ \delta(x - x_d)\ dx = U_m(x_d) \tag{A.55}$$

Eq. (A.54) reduces to

$$\rho L'a \left[ B_{n+}\omega_{dn} - \beta_n A_{n+} - \{e^{-\beta_n t_1}\omega_{dn}(A_n \sin\omega_{dn}t_1 + B_n \cos\omega_{dn}t_1) - \beta_n e^{-\beta_n t_1}( A_n \cos\omega_{dn}t_1 + B_n \sin\omega_{dn}t_1)\}\right] = ( v_- - v_+ ) m U_n(x_d)$$

or

$$B_{n+}\omega_{dn} - \beta_n A_{n+} - e^{-\beta_n t_1} A_n(\omega_{dn} \sin\omega_{dn}t_1 + \beta_n \cos\omega_{dn}t_1) - e^{-\beta_n t_1} B_n(\omega_{dn} \cos\omega_{dn}t_1 - \beta_n \sin\omega_{dn}t_1) = ( v_- - v_+ ) mU_n(x_d)/(\rho aL') \quad .$$

Substituting

$$\left.\begin{aligned} D_n &= D_{1n} + D_{2n} + D_{3n} \\ D_{1n} &= \beta_n A_{n+} \\ D_{2n} &= e^{-\beta_n t_1} B_n(\omega_{dn} \cos\omega_{dn}t_1 - \beta_n \sin\omega_{dn}t_1) \\ D_{3n} &= e^{-\beta_n t_1} A_n(\omega_{dn} \sin\omega_{dn}t_1 + \beta_n \cos\omega_{dn}t_1) \end{aligned}\right\} \quad (A.57)$$

and

$$G_n = m U_n(x_d)/(\rho L'a_{dn})$$

into Eq. (A.56) gives

$$B_{n+} - D_n/\omega_{dn} = ( v_- - v_+ ) G_n \quad . \qquad (A.58)$$

Using the coefficient of restitution between the particle and the beam (at the damper location) gives

$$\dot{W}_+(x_d,0) - v_+ = - e( \dot{W}_-(x_d,t_1) - v_- ) \qquad (A.59)$$

or

$$v_+ = \dot{W}_+(x_d,0) + e ( \dot{W}_-(x_d,t_1) - v_-) \quad . \qquad (A.60)$$

In the above equation, e is the coefficient of restitution; $\dot{W}_+$ contains $A_{n+}$ which is known, and $B_{n+}$.

Substituting for $\dot{W}_+(x_d,0)$ and $\dot{W}_-(x_d,t_1)$ in Eq. (A.60) gives

$$\begin{aligned} v_+ = & \sum_{n=1}^{\infty} U_n(x)\{\omega_{dn}B_{n+} - \beta_n A_{n+} + F_n\Omega \cos(\Omega t_1 - \Psi_n)\} \\ & + h\Omega \cos\Omega t_1 + e \sum_{n=1}^{\infty} U_n(x_d)\{e^{-\beta_n t_1}(-A_n \sin\omega_{dn}t_1 + B_n \cos\omega_{dn}t_1) \\ & + (B_n \sin\omega_{dn}t_1 + A_n \cos\omega_{dn}t_1)(-\beta_n e^{-\beta_n t_1}) \\ & + F_n\Omega \cos(\Omega t_1 - \Psi_n)\} + eh\Omega \cos\Omega t_1 - e\, v_- \quad . \end{aligned}$$

Using Eq. (A.57) the latter equation can be put in

the form

$$v_+ = \sum_{n=1}^{\infty} U_n(x_d)(\omega_{dn} B_{n+} - D_{1n}) + e \sum_{n=1}^{\infty} U_n(x_d)(D_{2n} - D_{3n})$$

$$+ \Omega(1 + e) \sum_{n=1}^{\infty} U_n(x_d) F_n \cos(\Omega t_1 - \Psi_n)$$

$$+ \Omega(1 + e) h \cos\Omega t_1 - e v_- \quad . \qquad (A.61)$$

Defining the following

$$F_n = eD_{2n} - eD_{3n} - D_{1n} + \Omega(1 + e) F_n \cos(\Omega t_1 - \Psi_n)$$

$$E_1 = \Omega(1 + e) h \cos\Omega t_1 - e v_-$$

and

$$E_2 = \sum_{n=1}^{\infty} U_n(x_d) E_n + E_1 \quad ,$$

Eq. (A.61) reduces to

$$v_+ = \sum_{n=1}^{\infty} U_n(x_d)\omega_{dn} B_{n+} + E_2 \quad .$$

Substituting this result into Eq. (A.58) gives

$$B_{n+} \omega_{dn} - D_n = \{v_- - \sum_{n=1}^{\infty} U_n(x_d)\omega_{dn} B_n - E_2\} G_n$$

or

$$B_{n+} + G_n \sum_{i=1}^{\infty} U_i(x_d)\omega_{di}\, B_{i+} = (G_n\, v_- + D_n/\omega_{dn} - E_2\, G_n)\ . \tag{A.62}$$

Further defining

$$R_n = G_n\, v_- + D_n/\omega_{dn} - E_n\, G_n$$

and

$$Z_i = U_i(x_d)\omega_{di}$$

Eq. (A.62) becomes

$$B_{n+} + G_n \sum_{i=1}^{\infty} Z_i\, B_i = R_n \quad . \tag{A.63}$$

For $n=1,2,\ldots,5$, Eq. (a.63) can be expanded to give

$$\begin{array}{lllllll}
B_{1+}(1+G_1Z_1) & B_{2+}G_1Z_2 & B_{3+}G_1Z_3 & \cdot\ \cdot\ \cdot & B_{5+}G_1Z_5 & = & R_1 \\
B_{1+}G_2Z_1 & B_{2+}(1+G_2Z_2) & B_{3+}G_2Z_3 & \cdot\ \cdot\ \cdot\ \cdot & & = & R_2 \\
\cdot\ \cdot & \cdot\ \cdot & \cdot\ \cdot\ \cdot & \cdot\ \cdot\ \cdot\ \cdot\ \cdot & & = & \cdot \\
\cdot\ \cdot & \cdot\ \cdot & \cdot\ \cdot\ \cdot & \cdot\ \cdot\ \cdot\ \cdot\ \cdot & & = & \cdot \\
B_{1+}G_5Z_1 & \cdot\ \cdot & \cdot\ \cdot\ \cdot & \cdot\ \cdot\ \cdot & B_{5+}(1+G_5Z_5) & = & R_5
\end{array}$$

which is a system of n (n=5) nonhomogeneous linear equations in n unknowns. In the computer program the unknowns, $B_{n+}$, are solved by the Gauss Elimination Process.

# APPENDIX B

## FINITE ELEMENT SOLUTION

Assumptions:

1. Bernoulli-Euler beam ; $\rho$ , a, E are constants.
2. All external loads, if any, act only at the node points.

### B.1 THE STIFFNESS MATRIX

The beam is divided into N equal segments as shown in Fig. (B.1). The stiffness matrix connecting forces and displacement for the ith segment is

$$\begin{Bmatrix} f_i \\ M_i \\ f_{i+1} \\ M_{i+1} \end{Bmatrix} = \frac{2EI}{\ell^3} \begin{bmatrix} 6 & -3\ell & -6 & -3\ell \\ -3\ell & 2\ell^2 & 3\ell & \ell^2 \\ -6 & 3\ell & 6 & 3\ell \\ -3\ell & \ell^2 & 3\ell & 2\ell^2 \end{bmatrix} \begin{Bmatrix} Y_i \\ \Theta_i \\ Y_{i+1} \\ \Theta_{i+1} \end{Bmatrix} \qquad \text{(B.1)}$$

or

$$\begin{Bmatrix} f_i \\ f_{i+1} \\ M_i \\ M_{i+1} \end{Bmatrix} = \frac{2EI}{\ell^3} \begin{bmatrix} 6 & -6 & -3\ell & -3\ell \\ -6 & 6 & 3\ell & 3\ell \\ -3\ell & 3\ell & 2\ell^2 & \ell^2 \\ -3\ell & 3\ell & \ell^2 & 2\ell^2 \end{bmatrix} \begin{Bmatrix} Y_i \\ Y_{i+1} \\ \Theta_i \\ \Theta_{i+1} \end{Bmatrix} . \qquad \text{(B.2)}$$

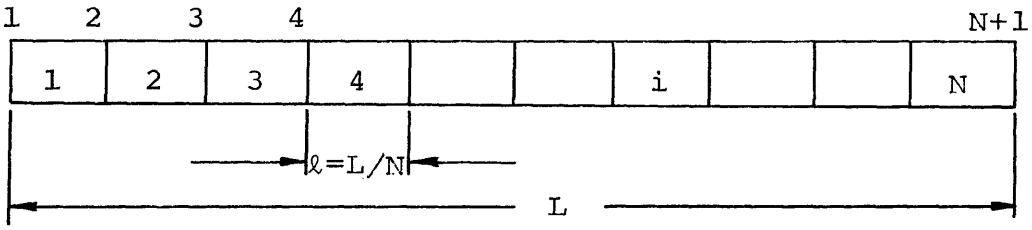


(a) Uniform Beam

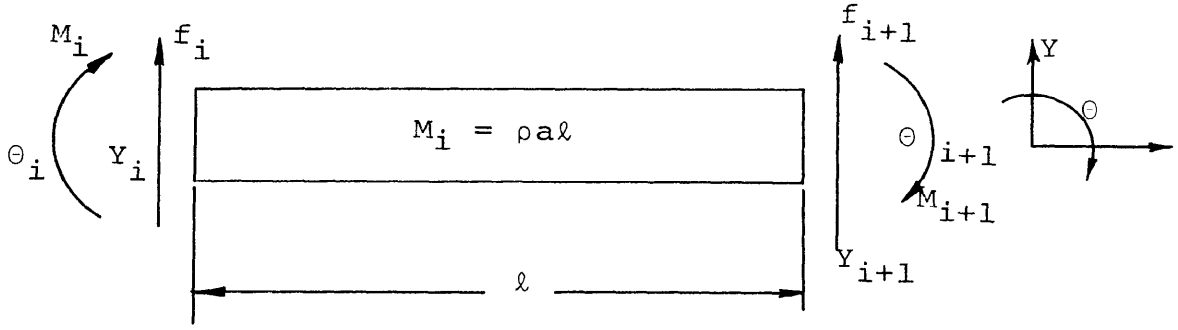


(b) Free Body Diagram of a Beam Segment

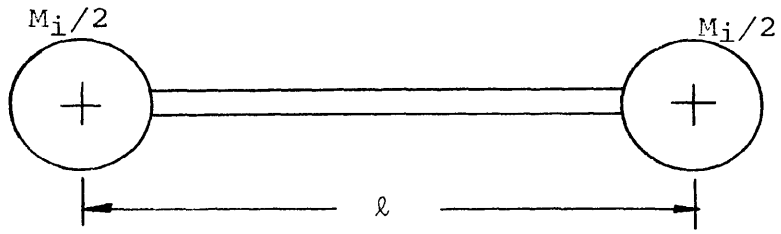


(c) Lumped Mass Model

Figure B.1 Lumped mass model for a uniform beam

The stiffness matrix for the simply supported beam is

$$\left[K\right] = 2EI/\ell^3 \left[\begin{array}{c|c} a & b \\ \hline c & d \end{array}\right] \qquad \begin{matrix}(2N\times 2N)\\ \text{matrix}\end{matrix} \qquad (B.3)$$

where

$$\left.\begin{aligned}
\left[a\right] &= \begin{bmatrix} 12 & -6 & 0 & 0\cdots\cdots \\ -6 & 12 & -6 & 0\cdots\cdots \\ 0 & -6 & 12 & -6\ \cdots\cdots \\ \cdot & \cdot & \cdot & \cdot \quad\quad \cdot \\ \cdot & \cdot & \cdot & \cdot\ -6 \quad 12 \end{bmatrix} && (N-1)\times(N-1) \\
\left[b\right] &= \begin{bmatrix} 3\ell & o & -3\ell & 0\ \cdots\cdots \\ 0 & 3\ell & 0 & -3\ell\cdots\cdots \\ \cdot & \cdot & \cdot & \cdot \quad\quad \cdot \quad\quad \cdot \\ \cdot & \cdot & \cdot & \cdot\ 3\ell \quad 0 \quad 3\ell \end{bmatrix} && (N-1)\times(N+1) \\
\left[c\right] &= \begin{bmatrix} 3\ell & 0 & 0 & \cdots\cdots \\ 0 & 3\ell & 0 & \cdots\cdots \\ -3\ell & 0 & 3\ell & \cdots\cdots \\ \cdot & \cdot & \cdot & \cdot \quad\quad \cdot \quad\quad \cdot \\ \cdot & \cdot & \cdot & \cdot \quad\quad \cdot \quad -3\ell \end{bmatrix} && (N+1)\times(N-1) \\
\left[d\right] &= \begin{bmatrix} 2\ell^2 & \ell^2 & 0 & 0 & \cdots\cdots \\ \ell^2 & 2\ell^2 & \ell^2 & 0 & \cdots\cdots \\ 0 & \ell^2 & 2\ell^2 & \ell^2 & 0\ \cdots\cdots \\ \cdot & \tilde{\cdot} & \cdot & \cdot \quad\quad \cdot & \cdot \quad\quad \cdot \\ \cdot & \cdot & \cdot & \cdot \quad\quad \cdot & \ell^2 \quad 2\ell^2 \end{bmatrix} && (N+1)\times(N+1)
\end{aligned}\right\} \qquad (B.4)$$

For a clamped beam the stiffness matrix is given by

$$\left[K\right] = 2EI/\ell^3 \left[\begin{array}{c|c} e & f \\ \hline g & h \end{array}\right] \qquad (2N-2)\times(2N-2) \qquad \text{(B.5)}$$

where

$$\left.\begin{aligned}
\left[e\right] &= \begin{bmatrix} 12 & -6 & 0 & 0 & \cdots & \cdot \\ -6 & 12 & -6 & 0 & \cdots & \cdot \\ 0 & -6 & 12 & -6 & \cdots & \cdot \\ \cdot & \cdot & \cdot & \cdot & & \\ \cdot & \cdot & \cdot & \cdot & -6 & 12 \end{bmatrix} && (N\times N) \\
\left[f\right] &= \begin{bmatrix} 0 & -3\ell & 0 & 0 & 0 & \cdots \\ 3\ell & 0 & -3\ell & 0 & 0 & \cdots \\ 0 & 3\ell & 0 & -3\ell & 0 & \cdots \\ \cdot & \cdot & \cdot & \cdot & \cdot & \cdot \\ \cdot & \cdot & \cdot & \cdot & 3\ell & 0 \end{bmatrix} && (N\times N) \\
\left[g\right] &= \begin{bmatrix} 0 & 3\ell & 0 & 0 & 0 & \cdots \\ -3\ell & 0 & 3\ell & 0 & 0 & \cdots \\ 0 & -3\ell & 0 & 3\ell & 0 & \cdots \\ \cdot & \cdot & \cdot & \cdot & \cdot & \cdot \\ \cdot & \cdot & \cdot & \cdot & -3\ell & 0 \end{bmatrix} && (N\times N) \\
\left[h\right] &= \begin{bmatrix} 4\ell^2 & \ell^2 & 0 & 0 & \cdots & \\ \ell^2 & 4\ell^2 & \ell^2 & 0 & \cdots & \\ 0 & \ell^2 & 4\ell^2 & \ell^2 & 0 & \cdots \\ \cdot & \cdot & \cdot & \cdot & \cdot & \cdot \\ \cdot & \cdot & \cdot & \cdot & \ell^2 & 4\ell^2 \end{bmatrix} && (N\times N)
\end{aligned}\right\} \qquad \text{(B.6)}$$

## B.2 THE EQUATION OF MOTION

The differential equations of motion for a multidegree of freedom system are given as

$$\left[M\right]\left\{\ddot{Y}\right\} + \left[K\right]\left\{Y\right\} = \left\{F\right\} \quad .$$

The governing homogeneous differential equations of motion for the lumped mass model of the Bernoulli-Euler beam can be put in the form

$$\left[\begin{array}{c|c} M & 0 \\ \hline 0 & J \end{array}\right]\left\{\begin{array}{c} \ddot{Y} \\ \hline \ddot{\Theta} \end{array}\right\} + \left[\begin{array}{c|c} K_{11} & K_{12} \\ \hline K_{21} & K_{22} \end{array}\right]\left\{\begin{array}{c} Y \\ \hline \Theta \end{array}\right\} = \left\{\begin{array}{c} 0 \\ \hline 0 \end{array}\right\} \quad .$$

Neglecting $J_i\Theta_i$ ($\ll M_iY_i$) for the lower modes, the rotation can be expressed as

$$\left\{\Theta\right\} = - \left[K_{22}\right]^{-1}\left[K_{21}\right]\left\{Y\right\} \quad .$$

Substituting the result into equations involving linear displacements gives

$$\left[M\right]\left\{\ddot{Y}\right\} + \left[\left[K_{11}\right] - \left(\left[K_{12}\right]\left[K_{22}\right]^{-1}\left[K_{21}\right]\right)\right]\left\{Y\right\} = \left\{0\right\}$$

which reduces to

$$\left[M\right]\left\{\ddot{Y}\right\} + \left[S\right]\left\{Y\right\} = \left\{0\right\} \qquad \text{(B.7)}$$

where

$$\left[S\right] = \left[K_{11}\right] - \left[K_{12}\right]\left[K_{22}\right]^{-1}\left[K_{21}\right] \quad .$$

With a sinusoidal base excitation the absolute displacement can be expressed in the form

$$\left\{Y\right\} = \left\{Y_r\right\} + \left\{\begin{matrix}1\\1\\1\end{matrix}\right\} h \, \mathrm{Sin}\Omega t$$

and with this substitution the equation of motion reduces to

$$\left[M\right]\left\{\ddot{Y}_r\right\} + \left[S\right]\left\{Y_r\right\} = \left\{M_i\right\} h\Omega^2 \, \mathrm{Sin}\Omega t \quad . \tag{B.8}$$

B.3 UNDAMPED HOMOGENEOUS SOLUTION

By substituting

$$\left\{Y\right\} = \left[M\right]^{-\frac{1}{2}}\left\{Z\right\} \tag{B.8a}$$

into Eq. (B.8) and premultiplying by $\left[M\right]^{-\frac{1}{2}}$

$$\left[M\right]^{-\frac{1}{2}}\left[M\right]\left[M\right]^{-\frac{1}{2}}\left\{\ddot{Z}\right\} + \left[M\right]^{-\frac{1}{2}}\left[S\right]\left[M\right]^{-\frac{1}{2}}\left\{Z\right\} = \left\{0\right\}$$

or

$$\left[I\right]\left\{\ddot{Z}\right\} + \left[H\right]\left\{Z\right\} = \left\{0\right\} \tag{B.8b}$$

where

$$\left[H\right] = \left[M\right]^{-\frac{1}{2}} \left[S\right] \left[M\right]^{-\frac{1}{2}} \quad .$$

Assuming a solution to Eq. (B.8b) in the form

$$\left\{Z\right\} = \left\{A\right\} e^{i\omega t} \tag{B.9}$$

the characteristic determinant becomes

$$\left| \left[H\right] - \left[I\right]\omega^2 \right| = 0 \quad .$$

The solution of this equation gives the eigenvalues, $\omega_i$, and these quantities together with Eq. (B.9) can be used to obtain the modal matrix $\left[A\right]$ (eigenvectors). These characteristic vectors, in the original coordinate system become

$$\left[A'\right] = \left[M\right]^{-\frac{1}{2}} \left[A\right] \quad .$$

The matrix $\left[A'\right]$ is normalized to give $\left[\Phi\right]$ such that product of $\left[\Phi\right]^T \left[M\right]\left[\Phi\right]$ is equal to $\bar{m}\left[I\right]$ ; $\bar{m}$ being the generalized mass which is a constant. If $\left[\Phi\right]$ and $\left[A\right]$ are related as

$$\left[\Phi\right] = \left[C_{ij}\right] \left[A\right] \tag{B.9a}$$

then the constants, $C_i$, can be obtained from the equation

$$C_i = \sqrt{\bar{m}/D_i} \tag{B.9b}$$

where

$$D_i = \left\{A_i'\right\}^T \left[M\right] \left\{A_i'\right\} \quad . \tag{B.10}$$

It can also be shown that $\left[\Phi\right]$ satisfies

$$\left[\Phi\right]^T \left[K\right] \left[\Phi\right] = \bar{m} \left[\omega_i^2\right] \quad . \tag{B.11}$$

## B.4 VISCOUSLY DAMPED DISCRETE SYSTEMS

It is assumed in the following derivation that the damping is due to the relative velocity only and that it is obtained by a linear combination of stiffness and mass matrices, i.e.,

$$\left[C\right] = C_1\left[M\right] + C_2\left[K\right] \tag{B.12}$$

where $C_1$ and $C_2$ are constants.

When damping is included the differential equation of motion with harmonic base excitation becomes

$$\left[M\right]\{Y_r\} + \left[C\right]\{Y_r\} + \left[K\right]\{Y_r\} = \{M_i\}\, h\Omega^2 \mathrm{Sin}\Omega t \ . \tag{B.13}$$

A transformation to principal coordinates can be effected by using

$$\left\{Y_r\right\} = \left[\Phi\right]\left\{p\right\} \tag{B.14}$$

where $\left[\Phi\right]$ is the modal matrix for the undamped system. Premultiplying Eq. (B.13) by $\left[\Phi\right]^T$ and substituting Eq. (B.14) gives

$$\left[\Phi\right]^T\left[M\right]\left[\Phi\right]\left\{\ddot{p}\right\} + \left[\Phi\right]^T\left[C\right]\left[\Phi\right]\left\{\dot{p}\right\} + \left[\Phi\right]^T\left[K\right]\left[\Phi\right]\left\{p\right\}$$
$$= \left[\Phi\right]^T\left\{M_i\right\} h\Omega^2 \, \mathrm{Sin}\Omega t$$

With the help of Eq. (B.12), Eq. (B.11) and Eq. (B.10) this equation reduces to

$$\bar{m}\left[I\right]\left\{\ddot{p}\right\} + \left[C_1\bar{m}\left[I\right] + C_2\bar{m}\left[\omega_1^2\right]\right]\left\{\dot{p}\right\} + \bar{m}\left[\omega_1^2\right]\left\{p\right\}$$
$$= \left[\Phi\right]^T\left\{M_i\right\} h\Omega^2 \, \mathrm{Sin}\Omega t \quad . \tag{B.15a}$$

The ith equation then becomes

$$\ddot{p}_i + 2\xi_i\omega_i\dot{p}_i + \omega_i^2 p_i = \frac{1}{\bar{m}} F_i \, \mathrm{Sin}\Omega t \tag{B.15b}$$

where $\xi_i$ = damping ratio for the ith principal mode

$\omega_i$ = ith natural frequency

and

$$2\xi_i\omega_i = C_1 + C_2\omega_i^2 \quad ,$$

$$\left\{F\right\} = \left[\Phi\right]^T \left\{M_i\right\} h\Omega^2 \quad .$$

Comparing Eq. (B.15b) with the equation of motion for a single degree of freedom system the solution can be developed as two parts, that of free and forced vibrations.

Case I Free Vibration

Refering to Eq. (B.15b)

$$\left\{F_i\right\} = 0$$

$$p_i(t) = e^{-\xi_i\omega_i t}\left( A_i \operatorname{Sin}\omega_{di}t + B_i \operatorname{Cos}\omega_{di}t \right)$$

where

$$\omega_{di} = \omega_i\sqrt{1 - \xi_i^2} \quad .$$

Based on these results, the solution to Eq. (B.15a) is

$$\left\{p(t)\right\} = \left[E\right]\left\{\left[\operatorname{Sin}D\right]\left\{A\right\} + \left[\operatorname{Cos}D\right]\left\{B\right\}\right\}$$

where

$$\left[E\right] = \operatorname{diag.}\left[e^{-\xi_i\omega_i t}\right]$$

$$\left[\operatorname{Sin}D\right] = \operatorname{diag.}\left[\operatorname{Sin}\omega_{di}t\right]$$

$$\left[\text{CosD}\right] = \text{diag.}\left[\text{Cos}\omega_{di}t\right]$$

and $\{A\}$ and $\{B\}$ are constants to be determined using the initial condition.

Case II Harmonic Base Excitation

In this case the ith uncoupled equation of motion is given by Eq. (B.15b). Applying a standard approach $p_i(t)$ can be expressed in the form

$$\left\{p_i(t)\right\} = \left\{(p_i(t))_H + (p_i(t))_P\right\}$$

i.e., the total solution consists of a homogeneous and a particular part.

The former is

$$\left\{p(t)\right\}_H = \left[E\right]\left\{\left[\text{SinD}\right]\left\{A\right\} + \left[\text{CosD}\right]\left\{B\right\}\right\} .$$

The particular solution is

$$p_i(t)_P = \frac{F_i}{\bar{m}} \frac{((\omega_i^2 - \Omega^2)\ \text{Sin}\Omega t - 2\xi_i\omega_i\Omega\ \text{Cos}\Omega t)}{(\omega_i^2 - \Omega^2)^2 + (2\xi_i\omega_i\Omega)^2} .$$

Hence

$$\left\{p_i(t)\right\}_P = \frac{1}{\bar{m}}\left[\sqrt{p_i^2 + Q_i^2}\right]^{-1}\left[\left[p_i\right]\text{Sin}\Omega t - \left[Q_i\right]\text{Cos}\Omega t\right]\left\{F\right\}$$

where

$$P_i = \omega_i^2 - \Omega^2$$

$$Q_i = 2\xi_i \omega_i \Omega \quad .$$

The total solution in the original coordinates

$$\left\{Y(t)\right\} = [\Phi][E]\left\{ [SIND]\left\{A\right\} + [COSD]\left\{B\right\}\right\}$$
$$+ \frac{1}{\bar{m}}[\Phi]\left[\widetilde{(P_i^2 + Q_i^2)}\right]^{-1}\left[\widetilde{P_i \; Sin\Omega t - Q_i \; Cos\Omega t}\right]\left\{F\right\}$$
$$+ \begin{Bmatrix} 1 \\ \vdots \\ 1 \end{Bmatrix} h \; Sin\Omega t \quad . \qquad (B.16)$$

If the initial conditions on the system are

$$\left\{Y_r(0)\right\} = \left\{Y_{r0}\right\} \qquad \text{and} \qquad \left\{\dot{Y}_r(0)\right\} = \left\{\dot{Y}_{r0}\right\}$$

then the condition on displacement gives

$$\left\{Y_{r0}\right\} = [\Phi]\left\{B_i\right\} + \frac{1}{\bar{m}}[\Phi]\left[\widetilde{(P_i^2 + Q_i^2)}\right]^{-1}\left[\widetilde{-Q_i}\right]\left\{F_i\right\} \quad .$$

Multiplying both sides by $[\Phi]^T[M]$ and using the normalization relation, the constants $B_i$ are given by

$$\left\{B_i\right\} = \frac{[\Phi]^T[M]}{\bar{m}}\left\{Y_{r0}\right\} + \frac{1}{\bar{m}}\left[\widetilde{(P_i^2 + Q_i^2)}\right]^{-1}\left[Q_i\right]\left\{F\right\} \quad .$$

If the initial displacements are zero, then

$$\left\{B_i\right\} = \frac{1}{\bar{m}}\left[\frac{Q_i}{P_i^2 + Q_i^2}\right]\left\{F\right\} \quad .$$

The initial condition on velocity gives

$$\left\{\dot{Y}_{ro}\right\} = \left[\Phi\right]\left\{\left(A_i\omega_{di} - \xi_i\omega_i B_i\right)\right\} + \frac{1}{\bar{m}}\left[\Phi\right]\left[\frac{\Omega P_i}{P_i^2 + Q_i^2}\right]\left\{F\right\} \quad .$$

Premultiplying both sides of this equation by $\left[\Phi\right]^T\left[M\right]$ results in

$$\left[\Phi\right]^T\left[M\right]\left\{\dot{Y}_{ro}\right\} = \bar{m}\left\{\left(A_i\omega_{di} - B_i\xi_i\omega_i\right)\right\} + \bar{m}\left[\frac{\Omega P_i}{P_i^2 + Q_i^2}\right]\left\{F\right\}$$

or

$$\left\{A_i\right\} = \frac{1}{\bar{m}}\left[\frac{1}{\omega_{di}}\right]\left[\Phi\right]^T\left[M\right]\left\{\dot{Y}_{ro}\right\} + \left\{\frac{\xi_i\omega_i}{\omega_{di}} B_i\right\}$$

$$- \frac{1}{\bar{m}}\left[\frac{1}{\omega_{di}}\right]\left[\frac{\Omega P_i}{P_i^2 + Q_i^2}\right]\left\{F\right\} \quad .$$

Again, if the initial velocities are zero, then

$$\left\{A_i\right\} = \left\{\frac{\xi_i\omega_i}{\omega_{di}} B_i\right\} - \frac{1}{\bar{m}}\left[\frac{1}{\omega_{di}}\right]\left[\frac{\Omega P_i}{P_i^2 + Q_i^2}\right]\left\{F\right\} \quad .$$

## B.5 RESPONSE DUE TO ARBITRARY IMPACT

For arbitrary impacts the following general assumptions are made

1. The time of impact is very small compared to the time period of vibration.
2. The impact is elastic and only the masses at the location of damper participate in conservation and transfer of momentum.
3. The beam as well as the particle do not change position during the impact.
4. The damper can be located at any of the node points.

The solution after and between impacts may be written as

$$\left\{Y(t)\right\} = [\Phi][E]\left\{\left[SIND\right]\left\{A_+\right\} + \left[COSD\right]\left\{B_+\right\}\right\} + \left\{1\right\} h\, Sin\Omega(t+t_1) + \frac{[\Phi]}{\bar{m}}\left[\frac{P_i\, Sin\Omega(t+t_1) - Q_i\, Cos\Omega(t+t_1)}{P_i^2 + Q_i^2}\right]\left\{F\right\} \qquad (B.17)$$

where $A_+$ and $B_+$ are to be determined from the initial conditions just after the impact.

Since the displacement during the impact remains unchanged, for an impact at time $t=t_1$, Eq. (B.16) becomes

$$Y(t_1) = [\Phi]\left\{e^{-\omega_i \xi_i t_1}(A_i Sin\omega_{di} t_1 + B_i Cos\omega_{di} t_1)\right\} + \left\{1\right\} h\, Sin\Omega t_1 + \frac{[\Phi]}{\bar{m}}\left[\frac{P_i\, Sin\Omega t_1 - Q_i\, Cos\Omega t_1}{P_i^2 + Q_i^2}\right]\left\{F\right\}$$

Equating these two results gives

$$B_{i+} = e^{-\omega_i \xi_i t_i} (A_i \, \mathrm{Sin}\omega_{di} t_1 + B_i \, \mathrm{Cos}\omega_{di} t_1) \quad .$$

For a damper particle of mass m and velocity v and symbols (+) and (-) as subscripts to denote a quantity after and before impact respectively, then from the definition of the coefficient of restitution

$$\dot{Y}_{d+} - v_+ = - e(\dot{Y}_{d-} - v_-)$$

or
$$\dot{Y}_{d+} - v = - e \, dv \qquad \text{(B.18)}$$

where $\dot{Y}_d$ = beam velocity at damper location

and $dv = Y_{d-} - v_-$ .

Since the motion of the system during impact must satisfy the momentum equation, then

$$m_d \dot{Y}_{d-} + mv_- = m_d \dot{Y}_{d+} + mv_+$$

or
$$\dot{Y}_{d+} + \frac{m}{m_d} v_+ = C_m \qquad \text{(B.19)}$$

where $C_m = Y_{d-} + \frac{m}{m_d} v_-$

and $m_d$ = mass at the damper location including the damper container.

Solving Eq. (B.18) and Eq. (B.19) gives

$$v = \frac{(C_m + e\ dv)}{(1 + m/m_d)}$$

and
$$Y_{d+} = \frac{(C_m + e\ dv)}{(1 + m/m_d)} - e\ dv \quad . \tag{B.20}$$

For all node points in the beam the velocity before and after impact remain the same except at the damper location. The velocity just after the impact at this node is given by Eq. (B.20). Differentiating Eq. (B.16) and setting $t=t_1$ gives the velocity before impact as follows

$$\begin{Bmatrix} \dot{Y}_i \end{Bmatrix} = \left[\Phi\right] \Big\{ e^{-\omega_i \xi_i t_1} (A_i \cos\omega_{di} t_1 - B_i \sin\omega_{di} t_1)\omega_{di} - \omega_i \xi_i\, e^{-\omega_i \xi_i t_1} (A_i \sin\omega_{di} t_1 + B_i \cos\omega_{di} t_1) \Big\} + \frac{1}{m} \left[\Phi\right] \left[ \frac{(P_i \cos\Omega t_1 + Q_i \sin\Omega t_1)\Omega}{P_i^2 + Q_i^2} \right] \{F_i\} + \begin{Bmatrix} 1 \\ 1 \\ \vdots \end{Bmatrix} h\Omega \cos\Omega t \quad .$$

Hence the beam velocity just after impact becomes

$$\begin{Bmatrix} \dot{Y}_i \end{Bmatrix}_+ = \begin{Bmatrix} \dot{Y}_1 \\ \dot{Y}_{d+} \\ \dot{Y}_{i-} \end{Bmatrix} \quad . \tag{B.21}$$

Differentiating Eq. (B.17) and setting t=0 gives

$$\left\{\dot{Y}\right\}_+ = \left[\Phi\right]\left\{A_{i+}\ \omega_{di} - \omega_i \xi_i\ B_{i+}\right\} + \frac{1}{\bar{m}}\left[\Phi\right]\left[\frac{(P_i\ \mathrm{Cos}\Omega t_1 + Q_i\ \mathrm{Sin}\Omega t_1)\Omega}{P_i^2 + Q_i^2}\right]\left\{F_i\right\} + \left\{\begin{matrix}1\\1\\\vdots\end{matrix}\right\} h\ \mathrm{Sin}\Omega t_1$$

which together with Eq. (B.21) yields

$$\left\{A_{i+}\right\} = \left[\omega_{di}\right]^{-1}\left\{\left\{\omega_i \xi_i B_{i+}\right\} - \frac{\left[\Phi\right]^T\left[M\right]}{\bar{m}}\left\{h\Omega \mathrm{Cos}\Omega t - \dot{Y}_{i+}\right\}\right\} - \frac{\left[\omega_{di}\right]^{-1}}{\bar{m}}\left[\frac{(P_i \mathrm{Cos}\Omega t + Q_i \mathrm{Sin}\Omega t)\Omega}{P_i^2 + Q_i^2}\right]\left\{F_i\right\} .$$

These are the new constants which enable the solution to be carried forward to the next impact.

# APPENDIX C

# EXPERIMENTAL EQUIPMENT AND SPECIMENS

## C.1 ELECTRODYNAMIC EXCITER

The MB Model C25H vibration exciter was used in this study. This unit is an air cooled, vibration exciter capable of producing sinusoidal mechanical vibrations over the frequency range of 5 - 2000 cycles per second. It has a force rating of 0 - 3500 pounds and a double amplitude, head displacement of 0.5 inch for continuous duty.

The exciter driving unit is equipped with an MB Model 252 Power Amplifier and MB Model N695 Oscillator having an automatic displacement, velocity and acceleration servo control, over a frequency range of 5 - 5000 HZ.

## C.2 RECORDING INSTRUMENT

### a. ACCELEROMETERS

The following were used:

| | | | | | |
|---|---|---|---|---|---|
| ENDEVCO Model 224C | S/N | VM93 | 11.6 | pc/g | 803PF |
| ENDEVCO Model 224C | S/N | VM94 | 11.7 | pc/g | 823PF |
| ENDEVCO Model 2221D | S/n | PA99 | 17.5 | pc/g | 892PF |

### b. CHARGE AMPLIFIER

Three ENDEVCO Model 2710B Solid State Charge Amplifiers were used to amplify the accelerometer signal.

### c. OSCILLOSCOPE

A Tektronix oscilloscope equiped with Type 3B3 time

base, Type 3C66 carrier amplifier (bridge balance), and Type 3A6 dual trace amplifier, was used. A Type C - 12 Polaroid Camera was also available with the oscilloscope.

d. DIGITAL COUNTER

Beckman Universal Timer Model No. 5230 was used.

e. LIGHT BEAM RECORDER

CEC Type 5-124 Recording Oscillograph with CEC Type 1-118 Carrier Amplifier was used to get the strain - time recordings.

f. STRAIN GAGES

All strain gages used were M ≡ M Type EA - 13 - 250BB-120, ¼", 120 ohms, G.F. = 2.07.

C.3 TEST SPECIMENS

a. BEAMS

Both clamped and simply supported beams were machined out of 1/8" thick mild steel plate and were 25 - ½" x 1½".

b. IMPACT DAMPERS

A pair of thick washers constituting the container for the damper particle was made of hardened steel. The collars attached to the clamped beam weighed 99gm. and those for the simply supported beam weighed 90.5 gm.

Three different damper particles of weights 17 gm., 44 gm. and 73 gm. were made of stainless steel.

c. END SUPPORTS

Hard steel rollers of 1/16 diameter were used to allow

axial motion of one end of the clamped beam. The simply supported end was designed with ¼" wide, .025" thick spring steel as the supporting element.